Effects of Day and Night Temperature on Rice Photosynthesis

University of Hohenheim



MSc. Candidate: Kristian Johnson

MATRIKEL # 679224

Institute of Agricultural Science in the Tropics (490)

Management of Crop Water Stress in the Tropics and Subtropics (490g)

Advisor: Prof. Dr. Folkard Asch

Second Reader: Prof. Dr. rer. nat. Andreas Fangmeier

Submitted on November 28th, 2018, Stuttgart, Germany

Abstract

With climate change, night temperatures are expected to increase faster than day temperatures. In several studies, high night temperatures have been reported to decrease the yield potential of rice. With rice being the primary staple for more than half of the world's population, projected yield decreases imply a major threat to food security. Nevertheless, physiological responses of rice plants to varying day and night temperatures are not fully understood and both positive and negative effects of high night temperatures have been described with regard to CO₂ assimilation and growth. Whereas respiratory losses have been shown to increase as a result of higher night temperatures, leaf conductance and net assimilation rates during the day were reported to be higher. It was hypothesized in this study that higher daytime net assimilation rates were potentially the result of a compensation mechanism in response to depleted carbohydrate pools within the leaf, associated with adjustments in regards to mesophyll conductance or reduction in photorespiration, or even if these adjustments are themselves direct response to higher night temperatures.

In the present study, four-week-old IR64 rice plants were exposed to different day and night temperatures for 12 days in a growth chamber experiment. The temperature treatments did not lead to any significant changes in morphology, except for the ratios indicating carbon allocation, specific leaf area and root to shoot ratio. Shifts in carbon allocation was also demonstrated by the increase in sucrose utilization or export as night temperature increased. However, there was no link found between the assimilation rate and the status of carbohydrates in the leaves. The assimilation rate and its component processes significantly responded to increases in day temperature, whereas mesophyll conductance showed no significant response either to day or night temperature. Photorespiration also responded solely to increases in day temperature. Further research is needed in rice in regards to the diurnal dynamics of sucrose transport and utilization, as well the interaction of the limited starch reserves to the assimilation rate.

Statutory Declaration

I, Kristian Philip Johnson, born on the 27 March 1990, matriculation number 679224, hereby declare that the attached Master's thesis has been independently prepared, solely with the support of the listed literature references, and that no information has been presented that has not been officially acknowledged.

Supervisors: Professor Dr. Folkard Asch, Prof. Dr. rer. nat. Andreas Fangmeier

Thesis Topic: Effects of day and night temperature on rice photosynthesis

Semester: 5

I declare, herewithin, that I have transferred the final digital text document (in a PDF format) to my mentoring supervisor and that the content and wording is entirely my own work. I am aware that the digital version of my document can and/or will be checked for plagiarism with the help of an analysis software program.

28, November, 2018 Stuttgart, Germany

Signature, Date:

Acknowledgements

My thanks and appreciation above all to Sabine Stürz, the voice of reason in times of confusion, and Marc Schmierer, a constant source for new ideas, for their untiring efforts to both understand and answer my never-ending cascade of questions...at all hours. Thanks to Alejandro Pieters for his expertise, computer/desk, and guidance in matters of photosynthesis, carbohydrates, SigmaPlot, and the lab. Many thanks Folkard Asch for his continuous support and advice throughout the experiment and beyond. My gratitude to Marc Cotter for the many times I rushed breathlessly into his office to announce yet another problem with the growth chambers, for which he would always calmly find a solution. Thanks to Julia Hartmann for her patience and understanding during spills and breaks in the lab, as well as her many accommodations to my last-minute requests for equipment, lab access, or liquid/gas N₂. My experiment was confusing, and the statistics even more so, my thanks to Filippo Capezzone for taking the time to answer my questions, and most importantly finding satisfactory solutions. Thanks to Jessica Lloyd for her insighful edits and moral support as a fellow basement-dweller. My time in the lab would not have been half the fun if it were not for Duy Hoang Vu.

For many months I was more or less a resident of the institute. I appreciate the forbearance of my colleagues, and in many cases the friendship, comradery, and 'encouragement' they gave each and every day, in particular from Benjamin Warth, Kevin Thellmann, and Pia Schneider.

Of course I couldn't have persevered without the support of my family. I may have been far from them through this experience, but they always made sure I knew of their unwavering faith in my decisions and their love.

The last, and most important thanks to Lucie Ducos for her love, support, and understanding for the late evenings and shortened weekends. Not to mention enthusiastically agreeing to move half a world away to Stuttgart, Germany so I could pursue this Masters program. Simply put, this thesis would not have been possible without her. Merci!

Contents

| | Abs | tract | i |
|---|-------|---|------|
| | State | utory Declaration | ii |
| | Ack | nowledgements | iii |
| | List | of Figures | vii |
| | List | of Tables | viii |
| 1 | Intro | oduction | 1 |
| | 1.1 | Status Quo | 1 |
| | 1.2 | Research Objectives and Hypothesis | 2 |
| 2 | Lite | rature Review | 2 |
| | 2.1 | Night Temperatures | 2 |
| | 2.2 | Rice and Global Climate Change | 3 |
| | 2.3 | Higher Night Temperature and Rice Growth | 4 |
| | 2.4 | Sink-Source Relationships | 5 |
| | 2.5 | Temperature and Respiration | 6 |
| | 2.6 | Temperature and Assimilation | 7 |
| | | 2.6.1 Mesophyll Conductance | 8 |
| | | 2.6.2 V_{cmax} and J_{max} | 9 |
| | | 2.6.3 Triose Phosphate Utilization | 10 |
| | | 2.6.4 Growth Temperature | 10 |
| | 2.7 | Respiration and Assimilation | 11 |
| | 2.8 | Modeling Photosynthesis | 12 |
| | | 2.8.1 Estimating Photosynthetic Parameters | 14 |
| | 2.9 | Photorespiration | 16 |
| | 2.10 | Photorespiration and Temperature | 17 |
| | 2.11 | Rice Plants | 17 |
| 3 | Mat | erials and Methods | 18 |
| | 3.1 | Experimental Design | 18 |
| | 3.2 | Growth Chambers | 20 |
| | | 3.2.1 Rice Cultivation | 22 |
| | 3.3 | Measurements | 23 |
| | | 3.3.1 A-C _i Curves | 23 |
| | | 3.3.2 Applying the Line-Fitting Model | 24 |
| | | 3.3.3 Photorespiration at $0\% O_2 \dots \dots \dots \dots \dots \dots$ | 25 |

| | | 3.3.4 R _d Measurements | 25 |
|----|--------|---|----------|
| | | 3.3.5 Temperature Curves | 26 |
| | | 3.3.6 Shading Treatment | 26 |
| | | 3.3.7 Assimilation Measurements at Ambient Conditions | 27 |
| | | 3.3.8 Chlorophyll and Carbohydrate Analysis | 27 |
| | | 3.3.9 Morphology | 29 |
| | | 3.3.10 Statistical Analysis | 29 |
| | | | |
| 4 | Res | | 30 |
| | 4.1 | Morphology | 30 |
| | 4.2 | Assimilation Measurements of Shaded and Unshaded Leaves | 31 |
| | 4.3 | A-C _i Curves and the ETR | 32 |
| | 4.4 | Estimated Photosynthetic Parameters | 34 |
| | | 4.4.1 V_{cmax} and J_{max} | 34 |
| | | 4.4.2 g_m and C_c | 35 |
| | | 4.4.3 C _{tr} | 38 |
| | 4.5 | Photorespiration | 39 |
| | 4.6 | Respiration Rate | 42 |
| | 4.7 | Temperature Curves | 42 |
| | 4.8 | Carbohydrates | 44 |
| | | 4.8.1 Sucrose | 44 |
| | | 4.8.2 Monosaccharides (Fructose & Glucose) | 45 |
| | 4.9 | Chlorophylls and Carotenoids | 46 |
| 5 | Dia | cussion | 48 |
| 3 | 5.1 | Morphology | 48 |
| | 5.2 | | 50 |
| | 5.2 | Photosynthesis and Respiration | 51 |
| | | Modeling Photosynthesis | |
| | 5.4 | Photorespiration | 55 50 |
| | 5.5 | Temperature Curves | 56 50 |
| | 5.6 | Sucrose and Monosaccharides | 58 |
| | 5.7 | Chlorophylls and Carotenoids | 60 |
| | 5.8 | Hypotheses | 61 |
| 6 | Con | nclusion | 62 |
| Re | eferei | nces | 63 |
| 7 | App | pendices | 72 |
| | 7.1 | Appendix 1 | 72 |
| | 7.2 | Appendix 2 | 73 |
| | | | |

| 7.3 | Appendix 3 | | | | | | | | | | | | | | | | | 74 |
|------|-------------|--|--|--|--|--|--|--|--|--|--|--|--|--|--|--|--|----|
| 7.4 | Appendix 4 | | | | | | | | | | | | | | | | | 74 |
| 7.5 | Appendix 5 | | | | | | | | | | | | | | | | | 75 |
| 7.6 | Appendix 6 | | | | | | | | | | | | | | | | | 76 |
| 7.7 | Appendix 7 | | | | | | | | | | | | | | | | | 76 |
| 7.8 | Appendix 8 | | | | | | | | | | | | | | | | | 77 |
| 7.9 | Appendix 9 | | | | | | | | | | | | | | | | | 78 |
| 7.10 | Appendix 10 | | | | | | | | | | | | | | | | | 79 |
| 7.11 | Appendix 11 | | | | | | | | | | | | | | | | | 79 |
| 7.12 | Appendix 12 | | | | | | | | | | | | | | | | | 80 |
| 7.13 | Appendix 13 | | | | | | | | | | | | | | | | | 80 |
| 7.14 | Appendix 14 | | | | | | | | | | | | | | | | | 81 |
| | | | | | | | | | | | | | | | | | | |

List of Figures

| 1 | The Rates and Limitations of Photosynthesis according to an A-C $_{i}$ Curve | 14 |
|----|--|----|
| 2 | Mean PAR of PSP1 | 21 |
| 3 | Mean PAR of PSP2 | 22 |
| 4 | Mean A-C $_i$ of L1 | 32 |
| 5 | Mean ETR- C _i of L1 | 33 |
| 6 | Mean Estimated g_m - C_i of L1 | 35 |
| 7 | Mean Estimated C_c - C_i of Leaf 1 | 36 |
| 8 | Mean A - C _c of L1 | 38 |
| 9 | Mean Photorespiration - C_i of L1 estimated by M2 \dots | 40 |
| 10 | Mean Temperature Curves of Leaf 1 | 43 |
| 11 | Appendix 1: Mean A-C _i of L2 | 72 |
| 12 | Appendix 2: Mean ETR- C _i of L2 | 73 |
| 13 | Appendix 4: Mean g_m - C_i of L2 | 74 |
| 14 | Appendix 4: Mean C_c - C_i of L2 | 75 |
| 15 | Appendix 5: Mean A - C _c of L2 | 75 |
| 16 | Appendix 8: Mean Photorespiration - C _i of L2 | 77 |
| 17 | Appendix 10: Mean Temperature Curves of Leaf 2 | 79 |

List of Tables

| 1 | Mean Temperatures in Growth Chamber PSP1 | 21 |
|----|---|----|
| 2 | Mean Temperatures in Growth Chamber PSP2 | 21 |
| 3 | Mean and S.E. of LA, Dry Mass, SLA, and RSR | 30 |
| 4 | Mean Assimilation Rate and S.E. of Shaded, Unshaded, and A-C _i at 450 ppm L1 | 31 |
| 5 | Mean and S.E. of J_{max} and V_{cmax} of L1 | 35 |
| 6 | Mean and S.E. of g_m and C_c at 450 ppm of L1 | 37 |
| 7 | Mean and S.E. C _{tr} of L1 | 39 |
| 8 | Mean and S.E. of Photorespiration measured by M1 of L1 | 39 |
| 9 | Mean and S.E. of Photorespiration measured by M2 at 300 and 450 ppm of L1 | 41 |
| 10 | Mean and S.E. of Respiration Rate of L1 | 42 |
| 11 | Mean and S.E. of Sucrose Concentrations at End of Day, Night, and Shading of | |
| | Leaf 1 | 45 |
| 12 | Mean and S.E. of Monosaccharide Concentrations at End of Day and Night of Leaf $\boldsymbol{1}$ | 46 |
| 13 | Mean and S.E. of SPAD of Leaf 1 | 46 |
| 14 | Mean and S.E. of <i>Ca</i> , <i>Cb</i> , and Total Chlorophyll Concentrations of Leaf 1 | 47 |
| 15 | Mean and S.E. Carotenoid Concentrations of Leaf 1 | 48 |
| 16 | Appendix 1: Mean and S.E. of Unshaded and A-C _i Curve Assimilation Rates of L2 | 73 |
| 17 | Appendix 3: Mean and S.E. of J_{max} and V_{cmax} of L2 | 74 |
| 18 | Appendix 6: Mean and S.E. of g_m and C_c at 450 ppm of L2 | 76 |
| 19 | Appendix 7: Mean and S.E. C _{tr} of L2 | 76 |
| 20 | Appendix 8: Mean and S.E. of Photorespiration according to M1 of L2 | 77 |
| 21 | Appendix 8: Mean and S.E. of Photorespiration according to M2 of L2 | 78 |
| 22 | Appendix 9: Mean and S.E. of Respiration of L2 | 78 |
| 23 | Appendix 11: Mean and S.E. of Sucrose Concentrations at End of Day and Night | |
| | of Leaf 2 | 79 |
| 24 | Appendix 12: Mean and S.E. of Monosaccharide Concentrations at End of Day | |
| | and Night of Leaf 2 | 80 |
| 25 | Appendix 13: Mean and S.E. Ca, Cb, and Total Chlorophyll Concentrations of Leaf 1 | 80 |
| 26 | Appendix 14: Mean and S.E. Carotenoid Concentrations of Leaf 1 | 81 |

List of Abbreviations

PSP1 Growth Chamber used for the Temperature Treatments

PSP2 Growth Chamber used for Germination and Early Vegetative Growth

HNT High Night Temperature
NT Night Temperature (°C)
DT Day Temperature (°C)

TR Temperature Treatment (D°C/N°C)

L1 The Youngest Developed Leaf on the Main Tiller
 L2 The Second Youngest Developed Leaf on the Main Tiller

LA Leaf Area (cm²)

SLA Specific Leaf Area (cm 2 g $^{-1}$)

RSR Root to Shoot Ratio

VPD Vapor Pressure Deficit (kPa)
Q₁₀ Temperature Coefficient

 $\begin{array}{ll} J_{max} & \text{Maximum Electron Transport Rate ($\mu mol \, e^- \, m^{-2} \, s^{-1}$)} \\ J_f & \text{Actual Electron Transport Rate ($\mu mol \, e^- \, m^{-2} \, s^{-1}$)} \\ V_{cmax} & \text{Maximum Carboxylation Rate ($\mu mol \, CO_2 \, m^{-2} \, s^{-1}$)} \end{array}$

 $\begin{array}{ll} \textbf{K}_{\textbf{O}} & \text{Michaelis-Menton Constant for Carboxylation (mmol mol}^{-1}) \\ \textbf{K}_{\textbf{C}} & \text{Michaelis-Menton Constant for Oxygenation (} \mu mol \, \text{mol}^{-1} \text{=} \text{ppm}) \end{array}$

 $\mathbf{g_m} \hspace{1cm} \text{Mesophyll Conductance } (\text{mol CO}_2 \, \text{m}^{-2} \, \text{s}^{-1})$

 $\begin{array}{ll} \textbf{C}_c & \text{CO}_2 \, \text{Concentration in the Chloroplast } (\mu\text{mol mol}^{-1}\text{=ppm}) \\ \textbf{C}_i & \text{Intercellular CO}_2 \, \text{Concentration } (\mu\text{mol mol}^{-1}\text{=ppm}) \\ \textbf{C}_a & \text{Ambient concentration of CO}_2 \, (\mu\text{mol mol}^{-1}\text{=ppm}) \\ \end{array}$

 $\begin{array}{ll} \textbf{C}_{tr} & \text{Transition C_c between Rubisco and RuBP-limited Photosynthesis $(\mu mol \, mol^{-1})$} \\ \textbf{A}_c & \text{Steady-State Photosynthesis Limited by Carboxylation $(\mu mol \, m^{-2} \, s^{-1})$} \\ \textbf{A}_j & \text{Steady-State Photosynthesis Limited by RuBP Regeneration $(\mu mol \, m^{-2} \, s^{-1})$} \\ \textbf{A}_n & \text{Steady-State Photosynthesis Limited by Triose Phosphates $(\mu mol \, m^{-2} \, s^{-1})$} \end{array}$

 R_d Respiration Rate During the Day (μ mol m $^{-2}$ s $^{-1}$)

 Γ^* Photocompensation Point

τ Leaf Absorption x Partitioning Factor between PII and PI (ppm)

 $m extbf{R}_{PR}$ Photorespiration (µmol m $^{-2}$ s $^{-1}$) FCB Farquhar-von Caemmerer-Berry Model

ROS Reactive Oxygen Species

 Φ_{PSII} Photochemical Yield of PSII (mol e⁻ mol⁻¹ photon)

α Leaf absorptance factorβ Photosystem partitioning factor

 I_{inc} Photosynthetically Active Photon Flux Density Incident on the Leaf

TPUTriose Phosphate Utilization (μ mol e- m-2 s-1)PPFDPhotosynthetic Photon Density (μ mol m-2 s-1)

 $\Phi_{ extbf{II}}$ The efficiency of Photosystem II $F_{ extbf{t}}$ Steady-state terminal fluorescence

F_m Maximal fluorescence

PAHBAH 4-hydroxybenzoic acid hydrazide

CaChlorophyll aCbChlorophyll b

 $\textbf{A}_{\textbf{max}} \hspace{1cm} \text{Maximum Assimilation Rate (μmol m$^{-2}$ s$^{-1}$)}$

1 Introduction

1.1 Status Quo

For more than half of the world, rice (*Oryza sativa*) is an indispensable crop (Seck et al., 2012). It comprises 20 % of the daily calorie intake of more than 3.5 billion people (ibid). As a staple depended on by so many for their daily caloric and, to a limited extent, protein intake, any threat to rice production could pose a significant risk to global food systems. In rice cultivation, the greatest limitation is temperature (De Datta, 1981). Projections of global climate change indicate there will not only be increases in average earth surface temperature over the next century (IPCC, 2014), but that night temperature in particular will increase at a greater rate than day temperature (Alexander et al., 2006). The area most affected, with more frequent hot temperature extremes will be the tropics and subtropics (IPCC, 2014). The majority of rice cultivation by area lies between the latitudes 40°N and 10°S, which is the subtropics and tropics (Aselmann & Crutzen, 1989). The effects of both shifts in temperature as well as increased CO₂ concentration generally on plant growth, and rice in particular is largely unclear (Cheng et al., 2009).

Current projections of changes in rice production are highly variable, depending on the model and the climate change scenario (Tao et al., 2008), and the effects of increased night temperature on rice growth are not fully understood, with responses that range from positive to negative, to none at all (Jing et al., 2016). Understanding the underlying mechanisms is essential for accurate projection of future performance, adaptation, in terms of production system and cultivar, as well as improvement through breeding (Ray et al., 2013). After all, current rice yields must not only be maintained, but continually improved on, by an estimated 3 % every year, to match rising demand as the global population increases (ibid).

Generally, when yield was related to field night temperatures, it was shown to decrease as night temperature increased (Peng et al., 2004). Photosynthesis was either unaffected (Peraudeau et al., 2015), or increased with higher night temperatures (Kanno et al., 2009). However, the respiration rate increased with night temperatures (Peraudeau et al., 2015), which led to greater depletion of carbohydrate reserves and chlorosis in mores susceptible varieties (Glaubitz et al., 2014).

Based on source-sink dynamics, the resulting increase in the sink, carbohydrate depletion from higher respiration, should influence the source, photosynthesis (Venkateswarlu & Visperas, 1987). In some plant species, such as cottonwood trees (*Populus deltoides*), it has been shown that low carbohydrate levels led to higher assimilation rates the following day (Turnbull et al., 2002). The mechanisms behind this improvement in assimilation rate was from greater performance in the individual components of photosynthesis, Rubisco performance, RuBP regeneration, and triose phosphate utilization (Turnbull et al., 2002).

1.2 Research Objectives and Hypothesis

This study was performed in growth chambers at the Hans-Ruthenberg-Institute (490) at the University of Hohenheim from the end of February to the beginning of July during 2018. The aim was to investigate the effect of temperature on rice photosynthesis, with emphasis on the effect of night temperature through a series of temperature treatments. One rice variety was tested, the international check and representative *indica* variety IR64, and was cultivated hydroponically over the course of six weeks.

The aim of the temperature treatments was to determine the following proposed research questions:

- What are the effects of day and night temperatures on rice photosynthesis?
- What are the underlying adjustments in photosynthesis, and can the changes in the component processes, such as mesophyll conductance and photorespiration be quantified?
- How are sucrose and monosaccharide concentrations affected by day and night temperature?
- Are the carbohydrate concentrations in the leaf and photosynthesis coupled? If so, how is the dynamic influenced by day and night temperatures?

From these research questions, the following hypotheses were formulated:

- 1. Higher night temperature leads to higher net assimilation rates.
 - This response is driven by lower photorespiration
 - Depleted carbohydrate reserves in the morning due to either increased respiration rate or export
 - Increased mesophyll conductance.

2 Literature Review

2.1 Night Temperatures

The Intergovernmental Panel on Climate Change (IPCC) 2014 climate change report projects Earth surface temperature increases, relative to levels in 1986-2005, are likely in the range of $0.3\,^{\circ}$ C to $0.7\,^{\circ}$ C for the period of 2016-2035. By the end of the 21st century (2081-2100), global surface temperatures relative to the levels in 1850-1900 are projected, with high confidence, to exceed $1.5\,^{\circ}$ C, and even likely to exceed $2\,^{\circ}$ C. Relative to levels in 1986-2005, and across the climate scenarios, the mean surface temperature increase could range from $0.3\,^{\circ}$ C to $4.8\,^{\circ}$ C over the

period of 2081-2100. Beyond any doubt is the increased frequency of hot temperature extremes, and fewer cold extremes (IPCC, 2014). The most extreme values within these projection ranges are expected to apply for the subtropics and tropics, which are also the primary latitudes for rice production (Stocker et al., 2013).

While useful in pointing out global trends, these projections provides little insight into temperature and precipitation extremes. This would require measurements taken daily, whereas analysis of climactic trends over the past few decades has mostly relied on changes between monthly and yearly temperature averages. To achieve this, a significantly higher level of detail is required (Jones & Moberg, 2003). This is problematic at a global level, at which data on much of Central and South America, Africa, and South Asia was severely lacking (Folland et al., 2001). Recent international collaborative efforts to accelerate digitalization of local weather records has gone someway in filling the gap on a daily level.

The result has been a more complete global climactic picture in terms of temperature and precipitation extremes. One of the main findings from the newly available data was that for over 70 % of global land area, a significant decrease in cold nights in proportion to warm nights was observed (Alexander et al., 2006). In more complete datasets, covering the Northern hemisphere at mid-latitudes, the 25-year period between 1979-2003 had warmer nights than all of the century previous (Alexander et al., 2006). In the Philippines, an increase of 1.13 °C over 25 years (1979-2003) was documented (Peng et al., 2004), and the night time temperature extremes increased by 0.18 °C every decade over 45 years (1950-1995) in Libya (Jones et al., 1999). Not only are nights becoming warmer, but at a faster rate than during the day (Sillmann et al., 2013). Based on multi-ensemble models, asymmetric warming of nights to day will likely continue (ibid). To explain this diurnal variation, night-time warming has been attributed to changes in the planetary boundary layer, soil moisture content, cloud cover, precipitation, and changing land use/land cover (Alward et al., 1999). It is often cited that an observed increase in global continental cloud cover over the past century is the primary driver behind higher minimum temperatures, trapping heat emitted from the surface (ibid). However, a conclusive link has yet to be found between any of the mentioned forcers and higher night temperatures, and one that could apply on a global scale (Davy et al., 2017). A multi-linear regression model to compare their effect on temperature trends, showed boundary layer depth to be the best predictor, but specifically in the boreal annual cycle, and not during the summer (ibid).

2.2 Rice and Global Climate Change

Rice (*Oryza sativa*) is the primary staple for more than half of the world (Seck et al., 2012). Over 3.5 billion people rely on rice to provide for more than 20 % of their daily calorie intake (ibid). The vast majority of rice producers and consumers (90 %) are concentrated in Asia, followed by Africa and North and South America (FAO, 2013). Rice is a versatile crop, cultivated in dry

and wet conditions, at low and high altitudes, in agro-climactic zones ranging from temperate to tropical (Seck et al., 2012). Most rice production, 75 %, is based on irrigated lowland systems (ibid), which can only be established in areas with specific physical requirements: high average temperatures, easy availability of water, and soils that limit percolation (FAO, 2013). The majority of rice cultivation by area lies between the latitudes 40°N and 10°S, which is roughly the tropics and subtropics (Aselmann & Crutzen, 1989). Temperature is the most limiting factor in rice cultivation (De Datta, 1981), and its critical limits are minimum temperatures of 12 °C to 20 °C and maximum temperatures from 34 °C to 38 °C (Yoshida, 1981). As a staple depended on by so many for their daily caloric and, to a limited extent, protein intake, any threat to rice production could pose a significant risk to global food systems. Current projections of changes in rice production are highly variable, depending on the model and the climate change scenario (Tao et al., 2008). However, higher CO₂ and temperatures are known to affect rice growth and yield, but the effects have yet to be fully quantified (Cheng et al., 2009). Understanding the underlying mechanisms is essential for accurate projection of future performance, adaptation, in terms of production system and cultivar, as well as improvement through breeding (Ray et al., 2013). After all, current rice yields must not only be maintained, but continually improved on, by an estimated 3 % every year, to match rising demand as the global population increases (ibid).

2.3 Higher Night Temperature and Rice Growth

The effect of night temperature on rice performance is not fully understood, despite indications it may have a negative impact (Jing et al., 2016). It was indirectly measured by comparing yield on an International Rice Research Institute (IRRI) farm to local weather conditions over the same 11 year period. There was a high correlation between mean minimum temperature and yield. With every 1 °C increase in night temperature, there was a 10 % decrease in yield (Peng et al., 2004). In a greenhouse experiment, hydroponically grown plants under natural light conditions were placed under two different temperature treatments after heading, 22 °C and 27 °C, and both at a constant day temperature of 27 °C. In the higher night temperature (HNT) treatment, the dry weight of panicles was reduced, although the biomass of other plant parts was higher, indicating a change in carbon allocation (Kanno & Makino, 2010). This was also observed in rice plants grown at night either under 32 °C, or at ambient night temperatures, 27 °C, and again at constant day temperatures, 32 °C. Rice plants grown under HNT had a 90 % decrease in yield and a decrease in spikelet fertility, even though photosynthetic rates were not affected (Mohammed & Tarpley, 2009). In an inverted temperature treatment, with night temperatures higher than day temperatures, HNT lowered rice grain quality, and changed protein expression in response to temperature stress during grain filling (Li et al., 2011).

Most studies have focused on the effect of HNT on *japonica* type and related rice varieties, and to a lesser extent on *indica* species, which are more commonly grown in the tropics (Peraudeau et

al., 2015). To compare HNT effects between the two cultivar groups, Peraudeau et al. (2014) grew *indica* and *japonica* variety rice plants in a greenhouse in Montpellier, France and on the field at IRRI in Los Baños, the Philippines. In the greenhouse, the diurnal temperatures were 29 °C during the day, and 21 °C in the night, whereas the HNT temperature treatments were 25 °C and 29 °C. In the field experiments, rings of thermal radiators were placed around sections of the field, to equally surround the rice varieties, and increased the night temperature by around 1 °C from ambient. In both field and greenhouse, plants grown in the HNT treatment showed increased respiration at night, without any subsequent increase in assimilation, as well as a decreased specific leaf area (SLA). In contrast to the *japonica* cultivars, *indica* did not show a decrease in yield as shown by Peng et al. (2004). In another effort to determine differences across rice cultivars in regards to HNT susceptibility, 12 cultivars, a mixture *indica* and *japonica*, were grown in growth chambers under the control, 28 °C day and 21 °C night, and a HNT treatment, 30 °C day and 28 °C night. The respiration rate was significantly increased at HNT, and in the case of more susceptible cultivars to HNT, chlorosis in the leaves was also observed, along with comparatively less carbohydrates stored in the leaves (Glaubitz et al., 2014).

2.4 Sink-Source Relationships

Over the course of the day, photosynthates, starch and sucrose, are generated from the assimilation of carbon from atmospheric CO₂, and steadily increase in concentration in the leaf (S. Farrar & Farrar, 1985). The photosynthates, mostly in the form of sucrose (Lemoine et al., 2013), are then exported to the rest of the plant via the phloem, and used to synthesize new leaves or other sink tissues such as roots, and reproductive structures (Mullen & Koller, 1988). The balance between production and utilization is described as 'photosynthate partitioning' or the 'sink-source relationship', in which the source, the leaf, harnesses solar energy to provide for the sink, non-photosynthesizing organs and processes, such as growth (Venkateswarlu & Visperas, 1987). The 'size' of either sink or source, refers to the degree of influence it plays within the sink-source relationship, and varies according to plant, development stage, as well as environment (ibid). This balance, constantly shifting according to internal and external conditions, requires exact coordination between carbon assimilation, as part of photosynthesis, its storage, and ultimate utilization in the plant (ibid).

Sucrose generated from assimilation during the day is either used immediately for growth and maintenance, or stored along with fructans, polymers of fructose, in the vacuole (Gordon et al., 1980) for later export and use during the night. In the commonly used model plant, *Arabidopsis thaliana*, a relationship has been shown between the amount of starch stored during the day and the length of night (Smith & Stitt, 2007). Not only is the degradation of starch during the night linear, but the rate of degradation is precisely timed use up most of the stored starch only by the end of the night (ibid).

In rice, the carbon compounds generated during photosynthesis are more often stored not as starch in the leaf blade, but sucrose $C_{12}H_{22}O_{11}$ (Ishimaru et al., 2007). In contrast, photosynthates are stored as starch in leaf sheaths and the culm, with the exception of the flag leaf sheath, which instead accumulates sucrose, glucose, and fructose (ibid). Although far less is known about monocots in regards to night mobilization of carbohydrate reserves, a study of barley leaves determined that light, temperature, and day length are still the drivers of carbohydrate storage and mobilization. Additionally, sucrose and starch synthesis rates after 10-11 hours of light exposure decreased, coinciding with a shift towards fructan synthesis, a reserve carbohydrate in some species. During the night, sucrose utilization was initially fast, and then slowed as reserves were depleted (Sicher et al., 1984). However, unlike monocots barley and wheat, rice does not produce fructans. Rice uses three times more sucrose at night than starch, mobilized at a more controlled rate, and its utilization rates are exponential, facilitated by sucrose transporters, mainly SUT2 (Mueller et al., 2018).

Growth in rice plants is highest during the day. In upland rice plants, leaf elongation rates were 15 % to 30 % higher during the day as compared to the night, but when night temperatures were higher than 27 °C, the elongation rate exceeded the rates during the day (Cutler et al., 1980). Rice's tendency for a higher growth rate based on temperature, and regardless of timing in day or night was also observed in other monocots, such as maize ($Zea\ mays$). In contrast to dicots, their leaf expansion rates were more dependent on temperature rather than circadian rhythm (Poire et al., 2010). Growth is not the only determinant of carbohydrate mobilization, plant development also plays a role, for example after the rice plant has reached heading, carbohydrates are remobilized to the panicles for grain filling (Ishimaru et al., 2007). Cell growth and elongation have a high Q_{10} , a unit-less factor representing the rate increase at a temperature increase of 10 °C, indicating the susceptibility of a biological or chemical system to changes in temperature. A high Q_{10} suggests a chemically rather than physically driven process (Went, 1953).

2.5 Temperature and Respiration

Respiration is the CO₂ evolving, aerobic, metabolic process in the mitochondria that releases the energy stored in the carbon compounds generated by photosynthesis (Taiz & Zeiger, 2002). It is best measured at night, to avoid the confounding exchanges of gas associated with assimilation and photorespiration. As much as 30 % to 70 % of the carbon gained through photosynthesis is evolved through respiration (Peterson & Zelitch, 1982). Although most often associated with the dark, it continually takes place, even if there are diurnal shifts in its function within the plant (C. P. Lee et al., 2010), indicated by a significant reorganization of the tricarboxylic acid cycle (TCA) (Nunes-Nesi et al., 2011). As expected for a process composed of a series of biochemical reactions, it is often cited to have a Q₁₀ of around 2 (Lambers, 1985). However, the response of respiration to temperature is best modeled by a combination of Arrhenhius kinetics

and Michaelis-Menton kinetics, due to its enzymatic steps (Kruse et al., 2011). This approach may still be too simplistic, as the sensitivity of respiration to temperature is not constant, and decreases approaching its temperature optimum and beyond, making it difficult to precisely model (Tjoelker et al., 2001).

The purpose of the products derived from respiration is not only for plant growth and maintenance, but also long-distance transport processes, such as phloem loading, nutrient uptake, and N assimilation (Lambers et al., 2008). The sensitivity of temperature on each of these component processes varies, for example maintenance is most sensitive to temperature (Will, 2000). As a result, when averaged to a whole plant level and at longer timespans, the Q_{10} of respiration is lower than the often used value of 2 (Frantz et al., 2004). The Q_{10} of respiration is also often overstated and can be attributed to the relatively short length of the temperature treatment, around 15-20 days in many published experiments (Perdomo et al., 2016). Over longer time periods, day respiration rates at increased temperatures approached rates at the original growth temperature (Atkin et al., 2006). The respiration Q_{10} also varies across species (Bunce, 2007). Respiration in the day (R_d) is thought to be less than respiration in dark due to suppression when the plant is exposed to light (Zou et al., 2011). Less is known about the effect of temperature on R_d , though in several *Plantago* species subjected to increased temperatures, R_d decreased (Atkin et al., 2006).

At HNT, rice respiration (at night) has been shown to increase, which corresponded with a decrease in yield, but with either no or little effect on biomass (Cheng et al., 2009; Glaubitz et al., 2014; Peraudeau et al., 2015). This phenomenon has been observed in other species as well, cottonwood trees (*Populus deltoides*) (Turnbull et al., 2002), lettuce (*Lactuca sativa*), tomato (*Solanum lycopersicum*), and soybean (*Glycine max*) (Frantz et al., 2004). Other than temperature, respiration rates have also been shown to be affected by N status (Tjoelker et al., 2008), canopy position (Griffin et al., 2002), and in some instances seen to correspond with carbohydrate availability (Ow et al., 2008).

2.6 Temperature and Assimilation

Assimilation is considered sensitive to temperature (Raschke, 1970), but due to the complexity and sheer number of interlinked systems involved, it is difficult to determine the overall acclimation potential of photosynthesis to changes in temperature (Baldry et al., 1966). Consequently, there is no one Q_{10} value, but for each component process of assimilation (ibid). Nevertheless, an estimation of effect from temperature change can be determined if assimilation (in a C_3 plant) is broken down into its component steps, in the sequence followed by atmospheric gases as they move from the stomatal cavity to the chloroplast, where CO_2 and O_2 then enters into the Calvin-Benson cycle (Yamasaki et al., 2002). Once inside the substomatal cavity, temperature may have greatest impact on the first step of the CO_2 molecule's journey, its solubilization. It decreases as

temperature increases, and at a faster rate in comparison to O_2 , present at higher concentrations in the atmosphere (Gevantman, 2000). Higher concentrations of solubilized O_2 increases the rate of photorespiration, decreasing the net assimilation rate (Ku & Edwards, 1978).

2.6.1 Mesophyll Conductance

The rate of passage of CO_2 as a gas and then a liquid through the mesophyll, comprised of intercellular air spaces, cell walls, and the liquid inside the cells, is represented by mesophyll conductance (g_m) (Flexas et al., 2008). It is both finite and variable, and plays a significant role in limiting photosynthesis (Niinemets et al., 2009). Short-term changes in g_m are suggested to be linked to shifts in protein activity, such as aquaporins (cooporins), maximum g_m values relate to leaf anatomical features (Niinemets et al., 2009). According to analysis of datasets across plant species, the most influential are leaf thickness and density, which relate on a smaller scale to cell wall thickness and chloroplast distribution (Tomás et al., 2013). CO_2 diffusion in thinner leaves is more dependent on aquaporins and carbonic anhydrases, whereas in thicker leaves it is cell wall conductance (Scafaro et al., 2011). Wild rice species (*Oryza meridionalis*, and *O. australiensis*) were determined by microscopy to have thicker cell walls than their domesticated relatives (*Oryza sativa*) (ibid). g_m (μm^{-2} s $^{-1}$ Pa $^{-1}$) was measured by isotope discrimination, and negatively correlated to cell wall thickness (ibid). Two g_m estimation methods, the variable J method and isotope discrimination, show that g_m , similar to stomatal conductance (g_s), responds to short-term shifts in C_i (Vrabl et al., 2009).

 CO_2 is fixed by Rubisco within the stroma of the chloroplast (Taiz & Zeiger, 2002). Therefore, assimilation should ideally be represented in relation to the concentration of CO_2 inside the chloroplast (C_c) because the original model describes Rubisco and electron transport activity from the level of carboxylation occurring in the storm of the chloroplast (T. D. Sharkey et al., 2007). The original model though assumed the concentration of CO_2 in the chloroplast was equivalent to the CO_2 concentration in the intercellular fraction (von Caemmerer & Evans, 2015). Many plant species are considered to have little difference between C_i and C_c , hence an A- C_c would be appropriate (ibid). However, the partial pressure of CO_2 can drop significantly as it moves from outside the leaf (C_a), through the intercellular space (C_i) and the through the chloroplast, particularly in thicker leaves (ibid). Thus, C_c is estimated with g_m (ibid). Their relationship can be described by the following equation:

$$C_c = C_i - \frac{A}{g_m}$$

As indicated in the above equation, an accurate determination of g_m is fundamental to the conversion of the A-C_i to an A-C_c curve, and ultimately the derivation of parameters V_{cmax} and J_{max} .

Based on measurements in tobacco leaves, g_m was observed to have a Q_{10} value of 2.2, and considering the Q_{10} for the diffusion of CO_2 in water is 1.25 (Tamimi et al., 1994), indicates g_m is a protein mediated process thought to be linked to either or a combination of carbonic anhydrases or aquaporins (C. J. Bernacchi et al., 2002). In the same experiment on tobacco plants, both variable and constant J methods were used to show that g_m increases exponentially with temperature until a peak of 35-37.5 °C, followed by a steep decline. In rice, g_m has been shown to exponentially increase until 40 °C (Scafaro et al., 2011). Although it increases in parallel with temperature, it does not match the similarly increasing capacity of 1,5-bisphosphate carboxylase/oxygenase (Rubisco), and as a result is considered a limitation at higher temperatures. However, g_m has been shown to vary widely across genus, species, and even cultivar, reflecting the diversity in strategy in regards to photosynthetic efficiency (Flexas et al., 2008; von Caemmerer & Evans, 2015). The cited results are not from direct measurements, it is not currently possible to directly measure g_m , and values are instead derived from a mechanistic model relying on certain assumptions, such as cell wall porosity and membrane permeability (von Caemmerer & Evans, 2015).

2.6.2 V_{cmax} and J_{max}

Once CO₂ has reached the chloroplast, the assimilation rate is also limited by the carboxylation of ribulose 1,5-bisphosphate (RuBP) by the enzyme Rubisco, and the regeneration of RuBP, which is dependent on the electron transport rate in the light reactions of photosynthesis and light intensity (G. Farquhar et al., 1980). According to the coordination hypothesis of photosynthetic of resource allocation, assimilation limited by the carboxylation rate of Rubisco (A_c) is equal to assimilation constrained by RuBP regeneration (A_i) (J.-L. Chen et al., 1993). Consequently, not only do the maximum rate of carboxylation, V_{cmax} , and electron transport, J_{max} , influence A_c , and A_i , but are themselves linked. For example, the ratio of J_{max} to V_{cmax} is consistently around 1.5 and 2 across species (Wullschleger, 1993). Coordination is necessary to avoid damage to the leaf and maintain energy efficiency (photostasis), as demonstrated in the scenario where V_{cmax} is limiting, and investment in J_{max} would not only be unused, but the generated reducing power would require dissipation to avoid photoinhibition (Krause et al., 2012). However, in light-limiting conditions, a higher J_{max} would increase photosynthesis. Within shorter timespans, decoupling is observed as the reducing power generated in electron transport is redistributed to other processes, such as N assimilation or the Mehler reaction (A. P. Walker et al., 2014). Also, increases in temperature decrease the specificity of Rubisco for CO₂ (Brooks & Farquhar, 1985). Modeled measurements of tobacco (Nicotiana tabacum) have shown that the Rubiscolimited phase of photosynthesis is little affected by temperatures above 20 °C (Sage & Kubien, 2007).

Without taking into account oxygenation, the carboxylation rate of Rubisco increases with temperature, as shown by the high Q_{10} of V_{cmax} (Hall & Keys, 1983). However, this is complicated by Rubisco activase, an enzymatic regulator of Rubisco, which has been shown to deactivate

Rubisco at temperatures lower than the theoretical range it can effectively function (Sage et al., 2008). Deactivation of Rubisco by Rubisco activase is thought to be in response to a shift from Rubisco limited photosynthesis to the other limitations to photosynthesis (von Caemmerer & Quick, 2000).

 J_{max} also increases with temperature (Niinemets et al., 1999), but decreases above 30 °C, the shape of the temperature curve depends on the species and growth conditions (Leuning, 2002). Over a longer period of exposure to increased temperatures, the electron transport chain acclimates through stabilization of the cell membrane by increasing production of the carotenoid zeaxanthin, reducing cell membrane and thylakoid fluidity (Havaux, 1998). The amount of components that comprise the electron transport chain, such as the cytochrome bf complex or overall thylakoid protein levels, also determine J_{max} (von Caemmerer, 2000). The difficulty in determining the effect of temperature on J_{max} and V_{cmax} lies in their coordination (J.-L. Chen et al., 1993), and the feedback limitations in response to external (light) and internal conditions (TPU) (T. D. Sharkey et al., 2007). Despite these complications the temperature dependence of V_{cmax} and linked J_{max} is commonly modeled with a modified Arrhenius equation (Leuning, 1997), which may be an oversimplification.

2.6.3 Triose Phosphate Utilization

Under CO_2 saturated conditions, triose phosphate utilization (TPU) becomes the largest limitation to photosynthesis (von Caemmerer, 2000). At this stage, when assimilation is plotted against the intercellular CO_2 fraction, the line forms a plateau (ibid). Modeled measurements of tobacco (C. Bernacchi et al., 2003) show TPU has a Q_{10} of around 2 (Sage & Kubien, 2007). Increasing temperature shifts TPU higher either through increased electron transport capacity, or improved inorganic phosphate regeneration capacity (ibid). Its temperature dependence is higher than RuBP regeneration, due to the high Q_{10} of starch and sucrose synthesis (Pollock & Lloyd, 1987).

2.6.4 Growth Temperature

At a larger spatial and temporal scale, short term increases in day temperature have been shown to directly increase assimilation (Turnbull et al., 2002). The response of assimilation to temperature is relative to the growth temperature and an inherent potential for acclimation, which varies across plant species (Berry & Björkman, 1980). There is scant research in regards to species-specific acclimation rates, and those available are not consistent in terms of time provided for acclimation to varying temperature, which can take several days before a steady state is achieved (Perdomo et al., 2016). There is also the risk measured upward shifts in optimum temperatures for photosynthesis are otherwise the result of stomatal conductance (Lin et al.,

2012). Vapor pressure deficit (VPD) can significantly affect measurement of the optimum temp of assimilation. For example, at higher VPD, stomata close, reducing C_i within the leaf, limiting assimilation, and misleading results (ibid).

The influence of growth temperature is supported by the maximum rates of photosynthesis, which was observed at lower temperatures in plants that were grown at lower temperatures (Berry & Björkman, 1980). This holds true for plant grown at higher temperatures (ibid). However, the optimum growth temperature is flexible, and through acclimation, can shift by one-third to one-half the number of degrees as the growth temperature (ibid). One factor behind temperature acclimation is a shift in the concentration of photosynthetic enzymes (Rubisco and cytochrome f), which were present at increased concentrations in spinach plants (*Spinacia oleracea*) grown at cooler temperatures to compensate for lower enzymatic activity from the lower temperatures (Yamori et al., 2005). Rice grown at D30 °C/N23 °C and shifted to D18 °C/N15 °C had reduced concentrations of components of photosystem II and chlorophyll was reduced. Sucrose synthase and cytosolic fructose bisphosphatases were increased, indicating reallocation towards inorganic phosphate regeneration (Makino et al., 1994). Several plant species switched to an increased temperature setting produce an isoform of Rubisco activase more stable in heat (Portis, 2003). Growth temperatures also correlate to the energy of activation for maximum carboxylase rates (Perdomo et al., 2015).

Acclimation has its limits, and temperatures beyond the inherent range of the plant species leads to stress, indicated by reduction in Rubisco, chlorophyll, and a steep decline in photosynthesis attributed to breakdown in the PS II apparatus (Berry & Björkman, 1980; (Yamasaki et al., 2002)).

2.7 Respiration and Assimilation

It is not clear from previous studies if there is a coupling between respiration and assimilation rates, even though respiration depends on the substrate supply of photosynthesis, and photosynthesis on the generated ATP and oxidation of excess redox equivalents (Bunce, 2007). In amaranth (*Amaranthus hypochondriacus*) and soybean plants exposed to HNT, respiration decreased due to apparent substrate limitation, corresponding to low assimilation rates during the day. However, after one night of acclimation, respiration rates rebounded regardless of the assimilation rate during the preceding day (ibid). Similarly, two alpine perennials, *Bistorta bistortoides* and *Campanula rotundifolia*, under low and high light conditions, accumulated fewer carbohydrates under low light, but the respiration rate was maintained in both species across both light treatments, indicating a lack of interaction between assimilation and respiration (McCutchan & Monson, 2001). The decoupling of assimilation and respiration, or the lack of response of the photosynthesis to the carbon status in the leaves, was observed in several species of tropical rainforest trees that were selectively girdled to prevent carbohydrate export through the phloem from the leaves.

Not only was the respiration rate unaffected, but there was no interaction between carbohydrate (glucose, fructose, and starch) levels within the leaves and photosynthesis rates (Asao & Ryan, 2015). However, in rice, increased photosynthesis from higher light intensities have been shown to lead to a marginally higher dark respiration Q_{10} (K.-h. Lee & Akita, 2000). Less is known about the link between $R_{\rm d}$ and assimilation rate (Atkin et al., 2006).

However, models at a canopy level at a timescale averaged across weeks, months, or years, show the coupling of respiration and photosynthesis rates (Dewar et al., 1998). Turnbull et al. (2002) in a greenhouse experiment on cottonwood trees (*Populus deltoides* Bartr.ex Marsh) demonstrated that at HNT there is a related increase in respiration in the case of higher assimilation. The 2-year-old cottonwood saplings were exposed to three temperature treatments combining day and night temperature increases over the course of three days: D25 °C/N15 °C, D28 °C/N20 °C, and D31 °C/N25 °C. The respiration rate increased by 77 % between the lowest and highest night temperatures, whereas the soluble sugars and starch concentrations in the leaves declined significantly with the increase in temperature by sunrise. The subsequent light saturated photosynthetic capacity increased by 38 % to 64 % at each night temperature increase respectively. The increase in assimilation was explained by significantly higher V_{cmax} and J_{max}, suggesting improvements in Rubisco's efficiency and the electron transport chain. It should be noted that differences in the gas-exchange process and availability and allocation of resources of herbaceous annuals and woody perennials have been observed (Wullschleger, 1993).

2.8 Modeling Photosynthesis

To understand changes in C₃ photosynthesis, the Farquhar-van Caemmerer-Berry (FCB) model is most often used (G. Farquhar et al., 1980). Despite modifications since its first formulation (Harley et al., 1992; Wullschleger, 1993), the model remains the most relevant framework for describing the biochemical reactions of photosynthesis. Fundamentally, photosynthesis is the reflection of the two most commonly observed steady states. In the first, photosynthetic rates can be predicted according to the unique characteristics of Rubisco, and assumes the substrate RuBP is not limiting (A_c) (von Caemmerer, 2000). This occurs at low concentrations of CO₂. In the second, photosynthetic rates are predicted assuming the limitation is the regeneration rate of RuBP, and is most often observed at higher concentrations of CO₂ (A_i) (ibid). Other factors that may play a role in this second steady state, are the light intensity and the activity of intermediate enzymatic steps in the Calvin-Benson cycle (ibid). Based on the changes to assimilation over different concentrations of CO_2 , other photosynthetic parameters can be estimated, such as J_{max} and V_{cmax} , given it is known if Rubisco or RuBP regeneration is limiting (T. D. Sharkey et al., 2007). In the third steady state, less often observed, the limitation stems not from the processes within the chloroplast, but rather the exchange of triose phosphates between cytoplasm and chloroplast (ibid). In this state assimilation does not respond to increasing CO₂ or for that matter O₂ (T. D. Sharkey, 1985). The model of the three described steady states of photosynthesis is based on the three following equations:

In the scenario of the first steady state, A is Rubisco limited and Eq.1 applies:

$$A_c = V_{cmax} \left(\frac{C_c - \Gamma^*}{C_c + K_c (1 + \frac{O}{K_o})} \right) - R_d \tag{1}$$

 V_{cmax} represents the maximum carboxylation rate, C_c , the CO_2 concentration in the chloroplast or at Rubisco, K_c , the Michaelis constant of Rubisco for CO_2 fixation, O, the partial pressure of O_2 in the chloroplast or at Rubisco, K_c the Michaelis constant of Rubisco for O_2 fixation, C_0 fixation rate during the day, and C_0 the concentration of CO_2 at which assimilation (CO_2 fixation) is matched by the CO_2 evolution from photorespiration and respiration. Plotted, a linear regression best applies, with C_0 as slope and day respiration, C_0 as the y-intercept (Long & Bernacchi, 2003).

The second steady state is limited by the regeneration of RuBP. The derivation of its equation is described in greater detail by von Caemmerer (2000), and the final result is shown by Eq. 2 below:

$$A_j = J \frac{C_c - \Gamma^*}{4C_c + 8\Gamma^*} - R_d \tag{2}$$

J refers to the electron transport rate at saturating light. As in Eq.1, Γ^* refers to the photocompensation point, and R_d , the respiration rate during the day. It is assumed that four electrons are required per carboxylation and oxygenation. Although, 4 and 8 are in fact conservative estimates, and reflect the electron transport rate through PSII and ultimately the production of NADPH.

The less commonly observed triose phosphate utilization limitation is modeled by Eq. 3 below:

$$A_p = 3TPU - R_d \tag{3}$$

Eq.3 mostly refers to the export/utilization of triose phosphates (TPU) from the chloroplast, but also reflects the export of carbon from the Benson-Calvin cycle, such as in photorespiration. In this scenario, assimilation doesn't change, and in fact sometimes is reduced at higher CO₂ concentrations (von Caemmerer, 2000).

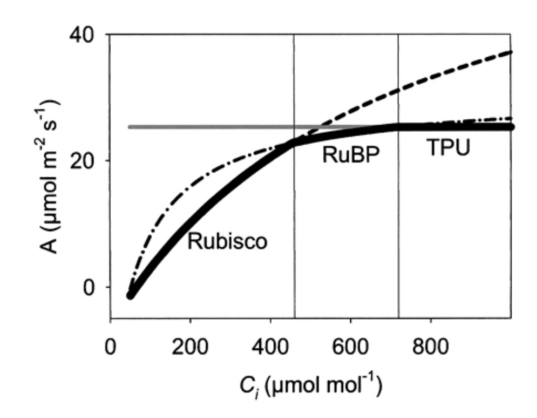


Figure 1: The rates of Photosynthesis depending on the limitations of Rubisco, RuBP, or TPU taken from Bernacchi & Long (2003). The actual photosynthetic rate (solid line) is the minimum of these three potential limitations.

The foundation for the above models is accurate information of the kinetic properties of Rubisco. Although assumed to be widely conserved among C_3 plants, they can vary widely between species (G. G. Tcherkez et al., 2006). The difficulty in the application of the FCB equations lies in determining the point in the response of assimilation to C_i at which the underlying photosynthetic processes are described by the equation (T. D. Sharkey et al., 2007). Several line-fitting methodologies have been proposed (Long & Bernacchi, 2003; Ethier & Livingston, 2004; (T. D. Sharkey et al., 2007)), though most suffer in terms of accuracy due to the difficulty of estimating g_m and therefore C_c an essential component of equations 1 and 2.

2.8.1 Estimating Photosynthetic Parameters

The mechanistic FCB model has become over the past 30 years the necessary starting point for any attempt at characterization of the biochemical relationships underlying net assimilation rate, as well as modeling the environmental and genetic influences on plant productivity (Gu et al., 2014). From the FCB model, parameters V_{cmax} , J_{max} , and g_m can be estimated from CO_2 response curves of net assimilation, A- C_i curves. To fit the model to experimental data and thereby derive the above photosynthetic parameters, several line-fitting models have been proposed (Ethier & Livingston, 2004; T. D. Sharkey et al., 2007; Dubois et al., 2007; Yin et al., 2011; Bellasio et al., 2016). However, these curve-fitting models make assumptions about g_m that could lead to significant underestimation of V_{cmax} and J, while simultaneously overestimating g_m (T.-W. Chen et al., 2015).

The foundation of the variable J method is the relationship between photosystem II fluorescence and the ETR, described by the equation $\Phi_{PSII} = \Delta F / F'_m = (F'_m - F_s) F'_m$. In the equation, F represents steady state fluorescence, and F_m the maximum fluorescence emitted during a saturating light pulse (Genty et al., 1989), such as that used in the multiphase flash (MPF) method used in

conjunction with the gas exchange analysis in this study (Loriaux et al., 2013). Both variable and constant J methods assume a leaf absorptance (α) of 0.84 and a partitioning factor (β) between PSII and PSI, often set to 0.5. α and β are laborious to measure, and are in most studies assumed. The product of α x β , τ is the fraction of photosynthetic photon density (PPFD) harvested by PSII (Yin et al., 2004). τ can then be used to determine the amount of irradiance was absorbed by the leaf and with Φ_{PSII} , from fluorescence measurements, can be used to calculate the actual electron transport rate (J_f) using the following equation:

$$J_f = \alpha * \beta * I_{inc} * \phi_{PSII} \tag{4}$$

The electron transport rate was measured at saturating light, meaning J_f is equivalent to J_{max} . Moualeu-Ngangue et al. (2016) fit the A-C_i and ϕ_{PSII} -C_i curves simultaneously by generating a guess value for τ , which is not influenced by CO_2 , from the above equation, thereby avoiding assuming or fitting a value for g_m . τ values were constrained between 0.225 and 0.59, as α values in literature were between 0.5-0.95 (Bauerle et al., 2004), and β values between 0.45-0.6 (A. Laisk & Loreto, 1996). Not having to fit g_m , allows for the dependence of g_m on C_i to be calculated, and in comparison with other models, such as the Dubois method, has a lower RMSE. Parameters from gas exchange and fluorescence measurements, net assimilation (A), C_i , PPFD (I_{inc}), and ϕ_{PSII} were the inputs for an optimization algorithm to minimize the distance between A_c and A_j to the measured A-C_i curve. The end result is a fitted curve based on the minimums of the three steady states of photosynthesis, A_c , A_j , and A_p and that resembles the sequence of measured data points. Separately plotted, A_c , A_j , and A_p resemble the Figure 1.

The optimization algorithm is an iterative process in which the inputs (A, C_i , I_{inc} , ϕ_{PSII}) are used to calculate g_m by the following modified equation (Harley et al., 1992):

$$g_m = \frac{A(\tau I_{inc} \Phi_{PSII} - 4(A + R_d))}{\tau I_{inc} \Phi_{PSII}(C_i + 2\Gamma^*)(A + R_d)}$$
(5)

The generated g_m value can convert the A-C_i to a A-C_c curve by the following equation:

$$C_c = C_i - \frac{A_c}{g_m} \tag{6}$$

 C_c was then used in the FCB equations for A_c and A_j along with guess values for V_{cmax} and J. Based on the sum of squares between the estimated A against the real A, the algorithm updates each estimated parameter (V_{cmax} , J_{max} , and τ) depending on the partial derivatives. This process continues until the convergence criteria have been met. The parameters that can be estimated by this photosynthetic model from the gas exchange and fluorescence measurements are J_{max} , V_{cmax} , g_m , C_c , photorespiration, K_O , K_C , the triose phosphate utilization rate (TPU), Γ^* , and the C_c concentration where the limitation to assimilation shifts from Rubisco to RuBP regeneration,

C_{ctr}. This was determined by the following equation:

$$C_{ctr} = \frac{\frac{K_c(1 + O/K_o)J}{4V_{cmax}} - 2\Gamma^*}{1 - \frac{J}{4V_{cmax}}}$$
(7)

2.9 Photorespiration

Rubisco is an equal opportunity enzyme that catalyses both the reaction between CO₂ and RuBP, and O₂ with RuBP (T. D. Sharkey, 1988). The product of the latter is one molecule of 3-phosphoglycerate (3-PGA) and one of 2-phosphoglycolate (2-PG), a toxin that inhibits enzymes within the Calvin-Benson cycle (Peterhansel et al., 2010). Photorespiration is the energy-intensive, CO₂ evolving pathway that metabolizes 2-PG. The CO₂ released is the product of the oxidation of glycine, one of the many steps in the photorespiratory pathway (Husic et al., 1987). It is considered the second most impactful process in the biogeosphere after photosynthesis itself. After all, in our current oxygen rich atmosphere it is a constantly occurring reaction in most land plants (Ludwig & Canvin, 1971). Under moderate conditions, the oxygenase reaction is thought to be responsible for a loss of 25 % of the carbon assimilated during photosynthesis (ibid). It does this as a competitive inhibitor of Rubisco, as well as diverting energy from carboxylation to oxygenation (T. Sharkey, 1986).

The photorespiratory rate is determined by the amount and kinetic properties of Rubisco, and the concentrations of its substrates, CO₂, O₂, and RuBP (Peterhänsel & Maurino, 2010). In drier and warmer climates, the stomata close to reduce water loss through transpiration, and the oxygenation rate increases further as the concentration of CO₂ decreases without constant gas exchange (ibid). At higher temperatures, the solubility of gases decrease, and CO₂ solubility decreases at a faster rate than O₂, increasing photorespiration rates (Ku & Edwards, 1978). The recovery of 2-PG and conversion to 3-PGA, ultimately regenerating RuBP, is itself a complex series of enzymatic steps over three organelles, chloroplast, peroxisome, and mitochondria, as well as the cytosol (Peterhansel et al., 2010). Intertwined are several other metabolic processes, such as nitrogen assimilation, respiration, and redox signaling (Bauwe et al., 2010). This energyintensive process serves as an alternative sink, competing with the Calvin-Benson cycle for the products of the light reaction, ATP and NADPH (von Caemmerer, 2000). This does not necessarily represent a wasteful diversion of energy resources. Under excess light, the photorespiratory pathway minimizes damage by protecting PSII. Consequently, it is considered essential for growth and photoprotection of C₃ plants under low CO₂ conditions (Takahashi & Badger, 2011). The high fluxes of photorespiratory intermediates between the various organelles is managed by a series of transporters, rather than passive diffusion (Peterhansel et al., 2010).

Photorespiration is difficult to directly measure because of the re-assimilation of evolved CO₂ produced during photorespiration, and the other CO₂ evolving process coinciding in time,

 R_d . If the kinetic properties of Rubisco are known, then photorespiration could be estimated (T. D. Sharkey, 1988), using a derivation of the FCB models (Busch, 2013), shown below:

$$R_{PR} = 0.5V_O = \frac{A + R_d}{\frac{C_C}{\Gamma^*} - 1} \tag{8}$$

Whereas assimilation and R_d can be measured through gas-exchange analysis, the difficulty is determining the values of C_c and Γ^* . C_c can not be determined without first estimating g_m . The relationship is modeled by the following equation (Pons et al., 2009):

$$C_c = C_i - \frac{A}{g_m} \tag{9}$$

 Γ^* is reliant on the accurate determination of Rubisco kinetics, which are species dependent. Depending on the species, values can be found in the literature based on *in vivo* studies on Rubisco (Makino et al., 1988; von Caemmerer, 2000; Perdomo et al., 2016)

2.10 Photorespiration and Temperature

Temperature increases VPD, and therefore the transpiration rate (Pallas et al., 1967). In response, the stomata close to reduce water loss, and as the CO₂ concentration decreases within the leaf the oxygenation rate increases (Kozaki & Takeba, 1996). Also, O₂ solubility decreases at a lower rate than CO₂ at increased temperatures (ibid). Rubisco's oxygenase activity increases, as the reaction, which requires a higher energy of activation, becomes less of a limitation as this threshold is more easily reached (ibid). Temperature increases correlate with light intensity, which leads to enhanced generation of NADH in the light reactions of photosynthesis, which may exceed the demands of the Calvin cycle and instead reduce O₂ to generate reactive oxygen species (ROS) (ibid). Therefore at increased temperatures, photorespiration becomes a necessary part of the acclimation process, its success depending on the efficiency of the conversion of 2-PG into 3-PGA for RuBP regeneration, and the prevention of PSII photoinhibition by detoxifying ROS (Zhang et al., 2013). In general, the solubility of gases decreases with temperature, but the solubility of CO₂ decreases more rapidly than O₂ (Gevantman, 2000), and Rubisco is less efficient at discriminating between the two (Brooks & Farquhar, 1985). Photorespiration as a result of the above combined mechanisms is highly sensitive to changes in temperature.

2.11 Rice Plants

One rice variety was grown and tested, the semi-dwarf, *indica* variety cultivar IR64. Released in 1985 in the Philippines, it is a high-yielding 'mega-variety' that matures quickly and has a

high resistance against blast, bacterial wilt, and brown planthoppers. Above all, it has a high cooking quality and a good taste. Due to these qualities it spread rapidly, and to such an extent that 20 years after its introduction it was still cultivated on over 10 million hectares (ha) (Mackill & Khush, 2018). Although mostly grown in Southeast Asia, it is also well-adapted to the Sahel regions in West Africa (M. E. De Vries et al., 2011). Its popularity has meant that it is commonly used as a representative indica variety in research and breeding programs (Mackill & Khush, 2018).

Grown in the Philippines, IR64 has an average height of 100 cm and its total growth duration is around 117 days (Khush, 2005). Unlike later improved varieties with fewer, but larger tillers and panicles, IR64 is high-tillering (Okami et al., 2015). It is considered a high-yielding variety, and during the dry season at IRRI headquarters at Los Bãnos, the Philippines, it yielded up to 8.76 and 8.28 t ha⁻¹ in 1996 and 1998 respectively (Peng et al., 2000). IR64 is susceptible to drought stress, a likely consequence of its shallow root system(Henry et al., 2011). It is also sensitive to high and low temperatures primarily during flowering (Coast et al., 2016). In experiments with HNT, IR64 has been shown to be somewhat tolerant (Glaubitz et al., 2014).

3 Materials and Methods

3.1 Experimental Design

The aim of the experiment is to determine the impact of changes in day and night temperatures on rice photosynthesis. Over the course of 34 days one rice variety (IR64) was germinated, and then transplanted into nutrient solution and grown within a growth chamber, programmed to a 12-hour diurnal cycle: day and night temperature 28 °C, 22 °C respectively. This is the optimal temperature range for rice growth (Krishnan et al., 2011). After four weeks, the rice plants, still in the vegetative stage, were transferred to a second growth chamber for the following temperature treatments (under the same environmental conditions) over the duration of 12 days:

- Day: 30 °C Night: 20 °C (Average: 25 °C)
- Day: 20 °C Night: 30 °C (Average: 25 °C)
- Day: 25 °C Night: 20 °C (Average: 22.5 °C)
- Day: 20 °C Night: 25 °C (Average: 22.5 °C)
- Day: 30 °C Night: 25 °C (Average: 27.5 °C)
- Day: 25 °C Night: 30 °C (Average: 27.5 °C)

Day and night temperatures in the treatments are in some cases necessarily inverted to avoid higher average overall temperature, and risk heat stress. Inversion allows for a wider range of night temperatures to be tested. They are also arranged so that not only can the individual effects of day or night temperatures be determined, but also the significance of the magnitude of difference between day and night temperatures.

The growth chambers can only accommodate 60 rice plants in 11 nutrient solution containers as well as one germination tray. As a result, germination, early growth, and treatments were staggered over time. Each treatment had 30 plants with at least two extra if replacements were needed. The same growth chambers were consistently used, either for germination and initial growth or the temperature treatments. Before the onset of the temperature treatment, five plants were randomly selected, and several growth parameters measured: tiller number, length of the main tiller, leaf area (LA), and root, leaf, and sheath biomass after drying in the oven at 60 °C to 80 °C for at least 48 hrs. In the second week of measurement, a series of gas exchange measurements were conducted on the youngest (L1) and second youngest developed leaf (L2) on the main tiller within the growth chamber. This was achieved by fixing the measuring head of the infra-red gas analyzer to a tripod inside the growth chamber, with the tubes connecting to the IRGA running through an outlet in the growth chamber sidewall. Thereby maintaining consistent growth conditions on a plant level during measurement. All gas exchange measurements were conducted throughout the day, but staying within the range of 30 min after the programmed start of day and the end of day. Photosynthesis is more stable during the day in a controlled environment, such as a climate chamber than in the field (Hennessey & Field, 1991). Temperature curve measurements were done outside of the growth chamber in the event the dew point was significantly lower than the temperature in PSP1, otherwise the temperature was temporarily lowered.

On the first day of the second week of the temperature treatment, four randomly selected rice plants were selected and an A-C_i curve, a method to characterize photosynthesis, was measured on L2. The development of the leaf was determined by the appearance of leaf 0, and to a lesser extent the presence of auricle, ligule, and collar. After each complete C_a series for the A-C_i curve was completed, assimilation at 0.002 % O2 was recorded, followed by a respiration measurement after a 30 min. dark adaption period. A-C_i curves for L1 of another four randomly selected plants were conducted on the second day. Temperature curves, used to determine the temperature optima for assimilation, were measured from L2 of four randomly selected rice plants. After temperature treatments in the evening of the third day, the shading treatment on L1 started, and 10 plants were randomly selected. A baseline SPAD was first established for all shaded leaves in case of leaf degeneration, and then the leaves were covered in aluminum foil. On the fourth day, a temperature curve was measured from L1. In the evening, leaf samples for carbohydrate analysis were taken at three leaf levels (when possible) from each of five randomly selected rice plants just before the end of day (j 20:00), for maximum levels of photosynthates. The morning of the fifth and last day of measurement, five rice plants were randomly selected and leaf samples for carbohydrate analysis at three leaf levels were taken before the beginning of day (¡8:00). Five of the of the shaded plants were randomly selected and samples were taken at three leaf levels for carbohydrate analysis. The assimilation rate of L1 of the remaining shaded plants was measured after around 30 minutes, or until the point assimilation became stable. Of the remaining 7 plants, five were randomly selected and the assimilation rates at three leaf levels measured. Afterwards, growth parameters of the same five plants were measured: tiller number, length of the main tiller, leaf area, and root, leaf, and sheath biomass after drying in the oven at 60 °C to 80 °C for at least 48 hrs.

3.2 Growth Chambers

The experiment was carried out in growth chambers at the Hans-Ruthenberg Institut at the University of Hohenheim, Stuttgart, Germany from February-July, 2018. Two Percival Scientific Plant (PSP) Growth Chambers (Percival Scientific, U.S.A.) (Model E-75L1C8) were used for germination and growth of the rice plants. Plant active radiation (PAR) was provided by high output fluorescent lights. Humidity (rh%) and temperature (°C), as well as the CO₂ concentration (ppm) were monitored and controlled using the proprietary Intellus controller system, linked to a 2005 model WMA-4 CO₂ Gas Analyzer (PP Systems, U.S.A). The growth chambers could be programmed to mimic a diurnal rhythm, in the case of this experiment, 12 hrs of day and night, to match typical tropical light conditions and preferable for indica variety IR64. The lights were on from 8:00 to 20:00. The dimensions of the interior of the growth chamber is 142 cm wide, 73 cm deep, and a height of 146 cm. The rack was set in both growth chambers to a height of 63 cm from the interior chamber floor. Humidity and CO₂ levels were programmed to remain constant at 75 % relative humidity, and at a CO_2 concentration of 450 ppm. The CO_2 concentration, temperature, and humidity were monitored, adjusted, and recorded by the PSP growth chambers at minute step. Over the entire period of the experiment, the CO₂ concentration in the treatment growth chamber (PSP1) was an average 460 ± 89 ppm, and in the nursery growth chamber (PSP2) an average 463 ± 78 ppm. This could not be otherwise verified beyond the WMA-4 Gas Analyzer system, which uses an infrared measurement technique. Whereas temperature and humidity were also monitored and recorded by TGP-4500 Tinytag temperature and humidity loggers (Gemini Data Loggers Ltd, U.K.) that were placed on the rack among the rice plants for more precise estimates of conditions at plant level. During the experiment period, the average relative humidity (RH) was 74.8 ± 5.0 % in PSP1, and 75.4 ± 5.0 % in PSP2. The temperature regime was consistent in PSP2, used for germination and early growth, whereas PSP1 was modified to fit the temperature treatment.

Table 1: Mean Temperatures with Standard Deviation during the Temperature Treatments in Growth Chamber PSP1

| Date | Day | Night |
|-----------------|----------------|----------|
| (D.M.Y) | (°C) | (°C) |
| 12.2.18-25.6.18 | 28.2 ± 1.7 | 22.3±1.2 |

Table 2: Mean Temperatures with Standard Deviation during the Temperature Treatments in Growth Chamber PSP2

| Date | Treatment | Day | Night |
|-----------------|-----------------|----------------|------------------|
| (D.M.Y) | (Day°C/Night°C) | (°C) | (°C) |
| 2.4.18-13.4.18 | 20/30 | 21.1±2.3 | 29.3±2.3 |
| 16.4.18-27.4.18 | 30/25 | 29.2 ± 1.1 | 26.3 ± 2.0 |
| 30.4.18-11.5.18 | 25/30 | 25.5 ± 1.2 | 29.3 ± 2.8 |
| 14.5.18-25.5.18 | 30/20 | 30.0 ± 1.8 | 20.3 ± 1.3 |
| 28.5.18-8.6.18 | 25/20 | 25.3 ± 1.8 | $20.8 {\pm} 1.7$ |
| 11.6.18-22.6.18 | 20/25 | 20.5 ± 1.3 | $24.8 {\pm} 0.9$ |
| 25.6.18-6.7.18 | 25/20 | 24.4 ± 1.3 | 20.1 ± 0.7 |

As shown in Figures 2 and 3, light conditions were variable within both growth chambers. PAR levels measured at canopy level of rice plants at the end of the temperature treatments were in the range of $1000\,\mu\text{mol}\,\text{m}^{-2}\,\text{s}^{-1}$ to $1400\,\mu\text{mol}\,\text{m}^{-2}\,\text{s}^{-1}$. The PAR at the perimeters of the growth chambers were lower than at the center. Light conditions were homogenized on a plant level by rotating the rice plants twice a week. Every week, PAR was measured with a Meteon Irradiance Reader (Kipp & Zonen, Netherlands) in an empty growth chamber from the height of a nutrient solution container which the rice plants were grown in.

PSP1

| 429 (+/-)29 | 541 (+/-)39 | 537 (+/-) 47 | 420 (+/-)39 |
|--|-------------------------------------|---|-------------------------------------|
| mol m ⁻² s ⁻¹ | mol m ⁻² s ⁻¹ | mol m ⁻² s ⁻¹ | mol m ⁻² s ⁻¹ |
| 586 (+/-) 46 mol m ⁻² s ⁻¹ | | 573 (+/-)49 mol m ⁻² s ⁻¹ | |
| 433 (+/-)38 | 556 (+/-)53 | 555 (+/-) 67 | 434.8 (+/-)54 |
| mol m ⁻² s ⁻¹ | mol m ⁻² s ⁻¹ | mol m ⁻² s ⁻¹ | mol m ⁻² s ⁻¹ |

Front of Growth Chamber

Figure 2: Mean PAR (μ mol m $^{-2}$ s $^{-1}$) of PSP1 with Standard Deviation

PSP₂

| 433 (+/-) 37 | 561 (+/-)33 | 554 (+/-) 27 | 432 (+/-)24 |
|--|-------------------------------------|--|-------------------------------------|
| mol m ⁻² s ⁻¹ | mol m ⁻² s ⁻¹ | mol m ⁻² s ⁻¹ | mol m ⁻² s ⁻¹ |
| 570 (+/-) 67 mol m ⁻² s ⁻¹ | | 584 (+/-)34 mol m ⁻² s ⁻¹ | |
| 422 (+/-)55 | 534 (+/-)151 | 565 (+/-)68 | 427 (+/-)28 |
| mol m ⁻² s ⁻¹ | mol m ⁻² s ⁻¹ | mol m ⁻² s ⁻¹ | mol m ⁻² s ⁻¹ |

Front of Growth Chamber

Figure 3: Mean PAR (μ mol m⁻² s⁻¹) of PSP2 with Standard Deviation

3.2.1 Rice Cultivation

IR64 seeds were germinated on a moistened filter paper in a shaded container in a growth chamber kept at a constant diurnal cycle of 22 °C at night and 28 °C for four weeks. Approximately 8 days after germination, 36 of the most vigorous seedlings were selected and placed in packed sand in a seed tray with the drainage holes covered by filter paper to prevent the sand falling out, and suspended initially in tap water. At the development of the second true leaf, around 3 days later, the tap water was replaced with 50% Yoshida's original nutrient solution: NH₄NO₃; NaH₂PO₄ · 2 H₂₀; K₂SO₄ CaCl₂ · 2 H₂₀; MgSO₄ · 7 H₂O; C₆H₈O₇; FeCl₃ · 6 H₂O; MnCl₂ · 4 H₂O; $ZnSO_4 \cdot H_2O$; $CuSO_4 \cdot 5 H_2O$; $(NH_4)_6Mo_7O_{24} \cdot 4 H_2O$; H_3BO_3 and adjusted from an initial pH of around 2 to a pH of 5.5 with NaOH application (Cock, Yoshida, & Forno, 1976). Over time, the prepared nutrient solution's pH drifts upwards, and HCl is added to return it to pH 5.5. The pH was measured with a SD 300 pH meter (Aqualytic[®], Germany). After 5 days, and before the roots extended outside of the seed tray, the rice seedlings were removed from the sand. To avoid root damage, they were flooded in warm water and carefully separated from the seed tray, sand, and filter paper. Thirty-two of the most vigorous seedlings were again selected, set in foam collars, and placed in a 1 liter plastic container covered in aluminum, filled with 100% Yoshida original solution. Every 7 days the nutrient solution was replaced. To preserve homogeneity in light conditions, the rice plants were rotated 2 times a week within their row as well as cycled as a row within the growth chamber. Due to the staggered timing of each treatment due to time and space constraints, each treatment group could only occupy one side of PSP2. Four weeks after germination, the rice plants were moved to PSP1 for the 2 week long temperature treatment. During the temperature treatment the containers containing nutrient solution were refilled daily with fresh nutrient solution to avoid nutrient or drought stress. However, this was only a factor during the second week of treatment, when the rice plants had grown to the point their roots occupied most of the container's volume.

3.3 Measurements

3.3.1 A-C_i Curves

Photosynthesis can be characterized by measuring the response of assimilation (μ mol m⁻² s⁻¹) to the concentration of CO_2 in the intercellular space (C_i) . Parameters V_{cmax} , J_{max} , and V_{TPU} can be estimated from the A-C_i curve. In practice, the initial slope of the A-C_i curve refers to the Rubisco limited phase, and the curve the RuBP regeneration limited phase (Long & Bernacchi, 2003). Gas exchange and fluorescence measurements were taken with a Walz GFS-3000 portable infra-red gas analyzer (IRGA) with a measuring head equipped with blue and red emitting diodes (Heinz Walz GmbH, Germany). The intercellular CO₂ fraction (C_i) was determined from a series of calculations developed by Caemmerer and Farquhar (1981), which rely on the infra-red measurement of the differential mole fraction of H₂O and CO₂ (von Caemmerer & Farquhar, 1981). The GFS-3000 IRGA measuring head is also equipped with pulse amplitude modulated fluorometry (PAM), using the saturation pulse method, which provide insight into the flux of excitation energy being directed into photochemical pathways. Chlorophyll fluorescence analysis indicates the source of the limitation to assimilation at each gas exchange data point. For example, the series of points showing increasing photosynthetic electron transport as the CO₂ concentration increases, Rubisco is the limitation, whereas little change despite increasing CO₂ concentration suggests a RuBP-regeneration limitation. The final and frequently unobserved TPU limitation is marked by a decrease in electron transport as the CO₂ concentration increases. Fluorescence data can also be used to for determining g_m (T. D. Sharkey et al., 2007).

The protocol used for the A-C_i was based on Ainsworth et al. (2002) and Moualeu-Ngangue et al. (2016). The first step is establishing and recording steady state photosynthesis at the growth CO₂ concentration, around 450 ppm, and saturating light conditions. Based on light-curves and the maximum PAR measured at canopy level within the growth chamber, $1300 \,\mu\text{mol}\,\text{m}^{-2}\,\text{s}^{-1}$ was chosen. Steady state assimilation means no systematic decrease or increase is observed over 5 minutes. Once reached and the assimilation, Ci, and fluorescence recorded, the ambient CO2 concentration was progressively decreased to 350, 250, 200, 150, 100, and finally 50 ppm. To avoid deactivation of Rubisco, measurements should be taken quickly at lower C_a levels. C_a was then returned to ambient levels, and after the original assimilation rate had been restored, the Ca was increased to 600, 900, 1200, and finally 1500 ppm. All A-C_i measurements were conducted at constant relative humidity, 50 %, whereas the VPD varied according to the cuvette temperature, which was set to the ambient temperature in the growth chamber. The IR64 leaves were not wide enough to fully fill the $4\,\mathrm{cm}^{-2}$ cuvette. As a result, leaf area in the cuvette was determined through the combination of a cellphone image taken through the glass window of the cuvette of each leaf used in gas exchange measurements, and ImageJ software (National Institutes of Health, U.S.A.) (Schneider et al., 2012).

The leakage of CO₂ through the foam seal of the cuvette was measured after each treatment run,

due to the distorting physical presence of the rice leaf as well as the compression of the foam over measurements. From inside the growth chambers, gas exchange was recorded at each C_a point used for the A- C_i curve with a non-photosynthesizing freeze-dried rice leaf in the cuvette to mimic the rice leaves. A derived polynomial regression representing CO_2 leakage to cuvette CO_2 concentrations was applied to each C_a used in the gas-exchange measurements. This process was repeated for each treatment run to take into account the potentially changing nature of the foam of the cuvette over time, and is reflected within all calculated parameters to avoid bias (Flexas et al., 2007).

3.3.2 Applying the Line-Fitting Model

In this study, the line-fitting model developed by Moualeu-Ngangue et al. (2016) was used to estimate V_{cmax} , J_{max} , C_c , an adapted value for K_c , K_o and Γ^* . The TPU limitation was not estimated because it was not an area of focus, and the root mean square error was reduced through its omission.

Moualeu-Ngangue et al. (2016) used cucumber (*Cucumis sativus*) in their photosynthetic model. It is well-documented that Rubisco kinetics vary according to the species (Prins et al., 2016), differences that can bias model parameterization. Therefore, the model was adapted to rice by inputting the measured kinetic parameters, chloroplastic CO2 photocompensation point (Γ), and Michaelis-Menton constants, K_O and K_C , of rice Rubisco *in vitro*, according to the *in vitro* measurements of Perdomo et al., (2016). In addition, the model estimated the photosynthetic parameters at leaf temperature during measurement. The temperature dependency of rubisco kinetics (K_C , K_O , and Γ^* was modified using an Arrhenius function according to Medlyn et al. (2002), as shown in the three following equations:

$$K_C = 300exp\left(\frac{79430(T_k - 298)}{(298RT_k)}\right) \tag{10}$$

$$K_O = 471 exp\left(\frac{36380(T_k - 298)}{(298.15RT_k)}\right) \tag{11}$$

$$\Gamma^* = 42.75 exp\left(\frac{37830(T_k - 298)}{(298.15RT_k)}\right)$$
 (12)

 T_k represents the leaf temperature in Kelvin and R is the universal gas constant (8.314 J mol⁻¹ K⁻¹).

Therefore all estimates reflect the conditions within the leaf at the time of measurement. The line-fitting model of Moualeu-Ngangue et al. (2016) was provided in the form of a Microsoft Excel spreadsheet, but was later converted to Python language code to manage the larger datasets generated by the measurements and parameterize the model for rice. Based on a comparison of residuals from the modeled data, the optimization algorithm chosen was the Nelder-Mead

method, rather than the Levenberg-Marquardt algorithm suggested by Moualeu-Ngangue et al. (2016).

3.3.3 Photorespiration at $0\% O_2$

 O_2 is a competitive substrate for Rubisco that results in glycolate, a toxin, after reacting with RuBP, which must then be removed through a complex and energy-intensive process, ultimately inhibiting photosynthesis. One of the byproducts of this pathway is CO_2 , hence the name **photorespiration**. In theory, if O_2 is removed, photosynthesis could proceed unhindered, at least in regards to the Rubisco limitation. To achieve this, assimilation would be measured at only 2 % O_2 , rather than the ambient 21 %, and photorespiration could be quantified by comparing the increased photosynthetic rate to its counterpart at ambient conditions (Biosciences, n.d.). Low O_2 conditions were created by replacing ambient air with pneumatic connector in the Walz IRGA for drawing outside air into the system, was connected to a container filled with distilled water and an air stone linked to a N_2 pressurized gas tank. The air stone diffused the N_2 in the distilled water, preventing damage to the IRGA from the pressurized stream of N_2 coming directly from the tank, and humidified it. The pressurized N_2 gas, with a 0% humidity, it is otherwise too dry for the IRGA to measure. The high purity of the N_2 gas can lead to anoxic conditions within the cuvette, disrupting respiration among other processes. Therefore, measurement had to be done quickly to prevent damage to the leaf.

3.3.4 R_d Measurements

Modeling photosynthesis requires knowledge of both CO₂ O₂ fluxes, and photorespiration and respiration are the processes determining the CO₂ flux. Respiration during the day is difficult to measure, as CO_2 is also evolved by photorespiration and at a much higher rate, half that of the carboxylation rate. Consequently, it is mostly measured indirectly via either the Kok (Kok, 1948) or Laisk (A. K. Laisk, 1977) method. The Kok method estimates R_d from an assimilation to light curve at decreasing levels of light to extrapolate assimilation at zero light. The Laisk method estimates R_d from A/C_i curves at different light intensities (G. Tcherkez et al., 2017). Initially, the day respiration rate was based on short light response curves according to the Yin method, a modification of the Kok method. Similar to the Kok method, it requires measurement of assimilation at lower light intensities, but plots it against the photosystem II electron transport efficiency from fluorescence measurements (Yin et al., 2011). This was abandoned after the first treatment run due to the concern that the source of the observed Kok effect was not of the suppression of respiration by assimilation, and is instead related to g_m (G. D. Farquhar & Busch, 2017). As a result, day respiration was assumed to be equivalent to respiration at dark, and measured accordingly. The light source, on the same leaves the A-C_i curve was measured from, was turned off in the sealed cuvette, and the gas exchange measurement taken after at least 30

minutes until theoretical dark adoption, demonstrated to be similar to rates after 7 hrs. in the dark (Griffin & Turnbull, 2012). Although measured in the dark, it still reflects conditions in the day, such as in surrounding protein and substrate concentrations that may affect the respiration rate (O'Leary et al., 2017).

3.3.5 Temperature Curves

Acclimation of photosynthesis to changes in temperature was measured on the youngest and second youngest developed leaf of the rice plants in each temperature treatment. The protocol of the temperature curve was loosely based on Turnbull et al. (2002). Although in his experiment, cottonwood trees were used and the temperature range narrower (6 °C. Steady-state assimilation was measured in response to leaf temperature, determined inside the cuvette of the IRGA measuring head by a thermocouple in direct contact with the underside of the leaf. The leaf temperature was manipulated by the cuvette temperature, starting at 18 °C and ending at 36 °C, with an interval between each measurement point of 3 °C. This range was chosen because it covers the typical temperature range of the low-lying tropics. Assimilation was measured at a saturating PPFD, 2000 μ mol m⁻² s⁻¹, and ambient CO₂ concentration, 450 ppm. Temperature acclimation of photosynthesis can be confounded by shifts in stomatal conductance. This was avoided by adjusting the relative humidity (rh%) relative to the increase in temperature, maintaining humidity within the range of 40 % to 50 %.

3.3.6 Shading Treatment

The aim of the shading treatment, which occurred within the temperature treatment, was to effectively starve the leaf through shading, and observe the subsequent assimilation rate after reexposure to light. This was achieved by covering the youngest developed leaves of 10 randomly selected plants in aluminum foil to prevent any exposure to light for around 40 hours. Before the covering the leaf, SPAD was measured with SPAD-502 Plus chlorophyll meter (Konica Minolta, Japan) and averaged across five different points along the leaf. SPAD is a quick, non-destructive method used to estimate leaf chlorophyll content, which also can reflect leaf N content levels (Xiong et al., 2015). A baseline measurement was needed to later determine if the photosynthetic apparatus, as indicated by chlorophyll and chloroplast content, of the shaded leaf had degraded. The aluminum foil was removed on one plant at a time and the shaded leaf promptly placed in the IRGA cuvette. The assimilation rate was measured by the Walz-3000 IRGA at ambient light conditions observed at leaf level, $1300\,\mu\text{mol}\,\text{m}^{-2}\,\text{s}^{-1}$ after steady state photosynthesis was observed, generally after 15-20 min exposure to ambient light conditions (Maxwell & Johnson, 2000).

3.3.7 Assimilation Measurements at Ambient Conditions

On the final day of the temperature treatments, the assimilation rates of the remaining rice plants were measured in the growth chamber with the IRGA under ambient conditions (450 ppm, PPFD $1300\,\mu\text{mol}\,\text{m}^{-2}\,\text{s}^{-1}$), the relative humidity inside the cuvette was 50%. All leaves on the main tiller were measured, though not all plants had a third youngest developed leaf (L3). The point assimilation measurements were recorded once steady-state photosynthesis had been achieved. As in all gas-exchange measurements, the area of the leaf in the cuvette was measured through the combination of cellphone image and ImageJ software. The determined leakage amount was also taken into account.

In the analysis, they were differentiated from the measurements taken at an ambient C_a as part of the A- C_i curve measurement sequence, due to the potential effect on Calvin cycle intermediate pools from a reduction in ambient CO_2 (Long & Bernacchi, 2003). Therefore, although measured under ambient conditions they were not representative of the assimilation rate of the rice plants during the temperature treatment.

3.3.8 Chlorophyll and Carbohydrate Analysis

Rice plant leaves store their photosynthates primarily in the form of sucrose (a disaccharide composed of glucose and fructose), rather than starch. Photosynthates are also transported via the phloem in the form of sucrose, as it less reactive than glucose. Therefore sucrose levels not only reflect photosynthesis, but photosynthate export from the leaf. Glucose and fructose levels were also taken into account in accordance with the findings of Glaubitz et. al (2014), who showed increasing levels in some cultivars of rice in response to HNT. Chlorophylls and carotenoids were tested to determine the effect of day and night temperatures on the light harvesting complex. They also serve as indicators of nutrient status within the plant. Their concentrations do not change within the span of one night, which was later statistically confirmed. Therefore, the samples taken from the end of day and end of night were combined to make a sample population of 10 rice plants. However, samples from the shaded plants were excluded even if SPAD measurements of the leaves before and after the shading treatment, showed no significant difference.

Sampling and Extraction Leaf samples (2.5 cm x the width of the leaf, typically 0.7 mm to 0.9 mm) were taken from randomly selected rice plants at three leaf levels at the end of day, at the beginning of day, and from leaves shaded over 48 hours. Each sampling group consisted of five plants. The samples for the end and beginning of day started to be taken around 30-40 min before 8:00 or 20:00, so that they would reflect either the highest (after 12h of assimilation) or lowest (after 12h respiration) concentrations of sucrose in the leaf. After determining the width

and length of the leaf, two samples were taken just above half of the length of the leaf. They were then promptly placed in a labelled aluminum envelope and in a container of liquid nitrogen (-196 °C). Afterwards, they were transferred to a refrigerator maintained at -80 °C.

Chlorophyll and Carotenoids Leaf contents were exhaustively extracted by heating at 70 °C for 30 min. the leaf samples in a solvent with a known extinction coefficient, 96 % ethanol. The bleached remainder was stored in the refrigerator for possible starch analysis at a later point. The extract solution was diluted by 50 % with 96 % ethanol. Using the Lambert-Beer law linearly linking absorptance with concentration, chlorophyll a, b and total carotenoid concentrations were calculated from the absorbance at $A_{470 \text{ nm}}$, $A_{649 \text{ nm}}$, and $A_{665 \text{ nm}}$ (Lichtenthaler & Wellburn, 1983). The absorbance of the extract pipetted into a flat-bottomed microplate (Merck, Darmstadt, Germany) without the lid was measured by a spectrophotometer, Tecan infinite 200Pro (Tecan Trading AG, Switzerland).

Monosaccharides and Disaccharides The leaf extract used for chlorophyll and carotenoid absorbance measurements was also used to determine the leaf sucrose ($C_{12}H_{22}O_{11}$ concentration. Anthrone reagent ($C_{14}H_{10}O$) was dissolved in 13.8M H_2SO_4 , mixed with the leaf extract, and heated at 40 °C for 20 min. The prepared anthrone reagent should be used within 12 hrs. (Yemm & Willis, 1954). Varying concentrations (0-1,000 μ M) of sucrose standards were reacted with the anthrone reagent for a calibration curve. They were measured within the same measurement runs as the samples to reflect measurement conditions. The reaction of the anthrone reagent with sucrose created a turquoise solution that fades in intensity over time. Its optical density was measured with the Tecan infinite 200Pro at A_{620nm} (Yemm & Willis, 1954). The sucrose concentrations in leaf extract from leaves sampled at end of day were too high and did not within the calibration curve. They were diluted by 80 % with 96 % ethanol, whereas end of night and shaded leaf samples were diluted by 66 %.

Glucose and fructose were measured from the leaf extract also used in the above described procedures. Reducing sugars (glucose and fructose) react with acid hydrazides to form intensely yellow anions. For this procedure p-hydroxybenzoic acid hydrazide (PAHBAH) was used. It was first dissolved in 0.5M HCl and then mixed with 0.5M NaOH. Once the 50% diluted leaf extract was added, the solution was heated at $100\,^{\circ}$ C for 10 min. Varying concentrations of glucose standards (0-500 μ M) were simultaneously prepared for the calibration curve to reflect measurement conditions. The reaction of PAHBAH and reducing sugars, produces a yellow solution that fades in intensity over time. All samples were diluted by $50\,\%$ with $96\,\%$ ethanol. Its optical density was measured with the Tecan infinite 200Pro at A_{410nm} (Lever, 1972).

3.3.9 Morphology

Before and after the temperature treatment, five plants were randomly selected and tiller number, plant height, leaf area (LA), and leaf, sheath, and root dry mass. A tiller was defined as having at least two leaves. Plant height was considered the distance from the culm to the tip of the longest, developed leaf on the main tiller. The leaf area was determined by a LI-3000C scanning head fed by the LI-3050C Transparent Belt Conveyer Accessory (LI-COR, U.S.A.). Rice plant leaf, stem, and root dry mass was weighed on an electric balance after being placed in a drying oven set at 60 °C to 80 °C in a labeled paper bag for at least 48 hrs.

3.3.10 Statistical Analysis

All statistical analyses were performed with SAS software, Version 9.4 of the SAS system for Windows (2014), copyright SAS Institute Inc. (Cary, NC, U.S.A.). The SAS procedure Proc MIXED was used because errors were assumed to be correlated, and due to the structure of the temperature treatments it was also necessary to fit means as well as covariances. Within the model the random variable was considered the treatment run. The mixed model was then used to perform Type III tests of the fixed effects, in this case the temperature treatments and their component night and day temperatures, on growth parameters, assimilation, the model outputs, and non-structural carbohydrate concentrations. Other possible fixed effects were also tested, such as the magnitude of difference between day and night temperature, as well as the average overall temperature. Due to the constraint of space within the growth chambers, coupled with the immersive nature of a temperature treatment, only one true replication (D25 °C/N20 °C) was possible. The 'chamber effect' derived from the comparison between the one replicated temperature treatment was assumed to be consistent for the rest of the temperature treatments. Confounding effects, such as the potential impact of varying conditions over time in PSP2 on early growth, were taken into account by using measurements before the temperature treatment as covariates.

Apart from figures 1-3, figures were produced using SigmaPlot (Systat Software, San Jose, CA, U.S.A.). The means and standard error presented in the tables and text are the predicted marginal means (referred to as 'LS-means' in SAS) rather than arithmetic means, and reflect the covariates and applied statistical model. Figures 2 and 3 show the standard deviation, whereas the following figures show the arithmetic means with error bars representing the standard error of the mean.

4 Results

4.1 Morphology

The morphology of the rice plants was characterized at the beginning of the temperature treatment from five randomly selected plants, and at the end from five randomly selected plants. The measured parameters comprised of plant height, leaf area (LA), and tiller number. After drying, leaf, sheath, and root dry masses were also determined, and ratios, specific leaf area (SLA) and the root dry mass to shoot dry mass (RSR).

As seen in Table 3 there was large variation in LA, but it was not significant in relation to day (DT), night temperature (NT), or their combined effects, represented by the temperature treatments (TR). The marginal means according to NT were in the range of 436.16 ± 55.93 cm² at 25 °C, and 454.75 ± 61.96 cm² at 30 °C. The magnitude between DT and NT was not significant, though the highest LA was in TR D30 °C/N20 °C. Rice plant height, tiller number, dry mass, and all of its constituents (leaf, sheath, and root mass) were unaffected by DT, NT or by TR. The marginal means according to NT were 6.80 ± 0.77 g at 20 °C and 7.05 ± 0.97 g at 30 °C. Whereas the range of marginal means according to DT, were 7.16 \pm 0.98 g at 20 °C and 6.64 \pm 0.86 g at 30 °C. The RSR was significant in regards to TR (p=<0.001). The greatest RSR was in TR D25 °C/N30 °C, and the least in TR D30 °C/N20 °C. The marginal means of RSR based on NT, were 0.40 ± 0.01 at 20 °C, and at 30 °C, 0.46 ± 0.01 . Based on DT, they were 0.45 ± 0.01 at 20 °C, and 0.40 ± 0.01 at 30 °C. The SLA was also significantly influenced by TR (p=<0.001), but not DT or NT. The marginal mean related to NT was 21.22 ± 0.50 cm² g⁻¹ at 20 °C, and 23.58 ± 0.57 cm² g⁻¹ at 30 °C. In regards to DT, the marginal mean of SLA was $21.29 \pm 0.56 \, \text{cm}^2 \, \text{g}^{-1}$ at $20 \, ^{\circ}\text{C}$, and $23.85 \pm 0.56 \, \text{cm}^2 \, \text{g}^{-1}$ at 30 °C. In Table 3, the marginal means in relation to the TRs show that TR D25 °C/N30 °C had the greatest SLA, and TR D25 °C/N20 °C the least.

Table 3: Mean and S.E. of LA, Dry Mass, SLA, and RSR (n=5) by Temperature Treatment, measured at the end of the temperature treatment

| Treatment | L | A | Dry I | Mass | RS | SR | SL | ιA | |
|-----------------|--------------------|-------|-------|------|------|------|--------------------|-----------------|--|
| | Mean | S.E. | Mean | S.E. | Mean | S.E. | Mean | S.E. | |
| (Day°C/Night°C) | (cm ²) | | (g) | | | | (cm ² g | ⁻¹) | |
| 20/25 | 420.97 | 98.17 | 7.43 | 1.49 | 0.47 | 0.02 | 21.49 | 0.39 | |
| 20/30 | 420.33 | 98.41 | 7.01 | 1.50 | 0.47 | 0.02 | 22.19 | 0.39 | |
| 25/20 | 382.49 | 69.39 | 6.67 | 1.06 | 0.42 | 0.01 | 20.53 | 0.27 | |
| 25/30 | 437.80 | 98.18 | 7.36 | 1.49 | 0.48 | 0.02 | 23.54 | 0.40 | |
| 30/20 | 513.27 | 98.30 | 6.68 | 1.06 | 0.36 | 0.02 | 23.12 | 0.38 | |
| 30/25 | 431.64 | 99.51 | 6.31 | 1.51 | 0.42 | 0.02 | 23.27 | 0.39 | |

4.2 Assimilation Measurements of Shaded and Unshaded Leaves

Single point assimilation measurements under ambient conditions across leaf levels on the main tiller were taken at the end of the TRs. The assimilation rates of L1 are shown in Table 4. There was a significant (p=<0.05) increase in assimilation rates to DT. At a DT of 20 °C, the marginal mean was $17.59 \pm 1.05 \, \mu \text{mol m}^{-2} \, \text{s}^{-1}$ and $22.19 \pm 1.08 \, \mu \text{mol m}^{-2} \, \text{s}^{-1}$ at $30 \, ^{\circ}\text{C}$, though this was $0.72 \pm 1.45 \, \mu \text{mol m}^{-2} \, \text{s}^{-1}$ lower than the assimilation rate at $25 \, ^{\circ}\text{C}$. Assimilation rates did not significantly respond to NT. The marginal means in regards to NT ranged from $20.81 \pm 0.96 \, \mu \text{mol m}^{-2} \, \text{s}^{-1}$ at $20 \, ^{\circ}\text{C}$ to $19.55 \pm 0.96 \, \mu \text{mol m}^{-2} \, \text{s}^{-1}$ at $30 \, ^{\circ}\text{C}$. However, assimilation rates were significantly different according to TR (p=<0.001). The highest assimilation rates were measured in TR D30 $\, ^{\circ}\text{C}$ /N20 $\, ^{\circ}\text{C}$, and the lowest in its inverse, TR D20 $\, ^{\circ}\text{C}$ /N30 $\, ^{\circ}\text{C}$.

While found to be significant in L1, DT was not significant in L2 (see Appendix 1), which was also the case for NT and TR. The assimilation rates in L1 and L2 were compared against each other, and their response to the TRs was not significantly different (p=0.96), though the assimilation rates in L1 were significantly higher than those of L2. Not only were the assimilation rates of either leaf not significantly related of each other (p=0.40).

Table 4: Mean Assimilation Rate and S.E. of Shaded, Unshaded, and A- C_i at 450 L1 (n=5) by Temperature Treatment

| Treatment | Unshaded Leaves Shaded Leaves | | Unshaded Leaves Shaded Leaves A- | | Leaves Shaded Leaves | | Unshaded Leaves Shaded Leaves A-C _i Cu | | Curve | |
|-----------------|--|------|--|------|-----------------------------|------|---|--|-------|--|
| | Mean | S.E. | Mean | S.E. | Mean | S.E. | | | | |
| (Day°C/Night°C) | $(\mu \text{mol m}^{-2} \text{s}^{-1})$ | | $(\mu \text{mol m}^{-2} \text{s}^{-1})$ | | $(\mu mol m^{-2} s^{-1})$ | | | | | |
| 20/25 | 19.74 | 1.06 | 17.98 | 1.41 | 17.95 | 1.67 | | | | |
| 20/30 | 15.41 | 1.16 | 19.25 | 1.41 | 15.83 | 1.67 | | | | |
| 25/20 | 22.42 | 0.82 | 21.97 | 1.00 | 17.74 | 1.18 | | | | |
| 25/30 | 22.39 | 1.16 | 18.67 | 1.41 | 18.90 | 1.67 | | | | |
| 30/20 | 22.94 | 1.16 | 21.12 | 1.41 | 22.60 | 1.67 | | | | |
| 30/25 | 22.79 | 1.16 | 19.39 | 1.41 | 21.75 | 1.67 | | | | |

The shading treatment involved covering L1 in aluminum foil for around 40 hrs, and then measuring the assimilation rate once steady state photosynthesis had been reached after exposure to light. NT, DT, and TR were not found to be significant. The range of marginal means in regards to NT were $21.54 \pm 0.91 \, \mu \text{mol m}^{-2} \, \text{s}^{-1}$ at $20 \, ^{\circ}\text{C}$, and $19.01 \pm 1.01 \, \mu \text{mol m}^{-2} \, \text{s}^{-1}$ at $30 \, ^{\circ}\text{C}$. Based on DT, there was little change in assimilation rate marginal means, with the largest difference between $20 \, ^{\circ}\text{C}$ and $25 \, ^{\circ}\text{C}$, of $0.45 \pm 1.48 \, \mu \text{mol m}^{-2} \, \text{s}^{-1}$.

There was no significant relationship between assimilation rates of unshaded and shaded leaves in relation to the TR. However, the difference between them in relation to the TRs was significant (p=<0.05). In TR D20 °C/N30 °C, the assimilation rate of the shaded leaves was

 $3.84\pm1.59\,\mu\text{mol}\,\text{m}^{-2}\,\text{s}^{-1}$ greater than the assimilation rate of the unshaded leaves. Whereas in TR D25 °C/N30 °C, the assimilation rates of the unshaded leaves was $3.72\pm1.59\,\mu\text{mol}\,\text{m}^{-2}\,\text{s}^{-1}$ greater than the assimilation rate of the shaded leaves. At lower DTs and NTs, the unshaded leaves had higher assimilation rates, but as they increased (25 °C and 30 °C), the assimilation rates of the unshaded leaves were consistently higher.

4.3 A-C_i Curves and the ETR

Models of assimilation assume it to be the result of the the cumulative limitations of its three biochemical states, each with its own distinctive behavior in response to changes in CO_2 concentration, which is reflected by the shape of the A-C_i curve. To accurately describe photosynthesis, the FCB model needs to be fitted to the measured points represented by the A-C_i curve.

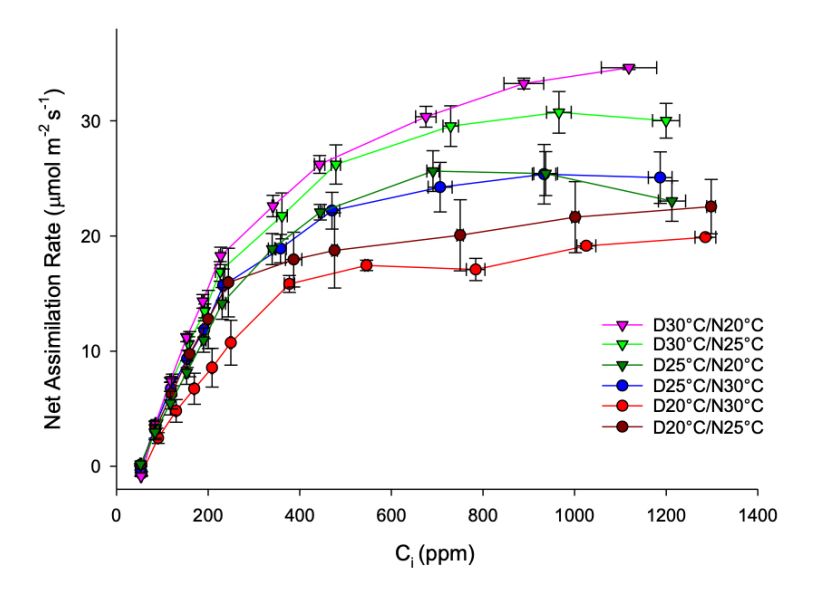


Figure 4: Mean A- C_i Curves of Leaf 1 (n=4) by Temperature Treatment, the error bars represent the standard error of the mean

The shape of the mean A-C_i curves by TR in Figure 4 show the response of photosynthesis to CO₂ (C_i) and temperature. As such, and supporting the results of the assimilation measurements in the unshaded leaves at the end of the TRs, the A-C_i curve responds primarily to DT. This is shown by the curves of the TRs with the highest DTs, TR D30 °C/N20 °C, with a maximum assimilation rate of $34.61 \pm 0.16 \, \mu \text{mol m}^{-2} \, \text{s}^{-1}$ at a C_i of $1118.83 \pm 60.41 \, \text{ppm}$, and D30 °C/N 25 °C, which had a maximum assimilation rate of $30.73 \pm 1.80 \, \mu \text{mol m}^{-2} \, \text{s}^{-1}$ at a C_i $1199.88 \pm 29.50 \, \text{ppm}$. These were in contrast with the curves of the TRs with the lowest DTs, TRs D20 °C/N30 °C,

which had a maximum assimilation rate of $19.88\pm0.07\,\mu\text{mol}\,\text{m}^{-2}\,\text{s}^{-1}$ at a C_i 1285.85 ± 22.71 ppm and D20 °C/N25 °C, which had a maximum assimilation rate of $22.54\pm2.35\,\mu\text{mol}\,\text{m}^{-2}\,\text{s}^{-1}$ at a C_i 1298.25 ± 14.22 ppm. The effect of NT was shown by comparing TRs D20 °C/N30 °C to D20 °C/N25 °C, and TRs D30 °C/N20 °C to D30 °C/N25 °C. The A- C_i curves of L2 mirror the trends in L1 (see Appendix 1).

Although recorded in a different context and on different days, the assimilation rates measured at ambient CO_2 concentrations (450 ppm) were taken from the A- C_i curve measurements, and compared to the assimilation rates of the unshaded leaves. Not only were the assimilation rates not significantly different from each other (p=0.88), but the measurements from the A- C_i curve were also exclusively significantly influenced by DT (p=<0.05).

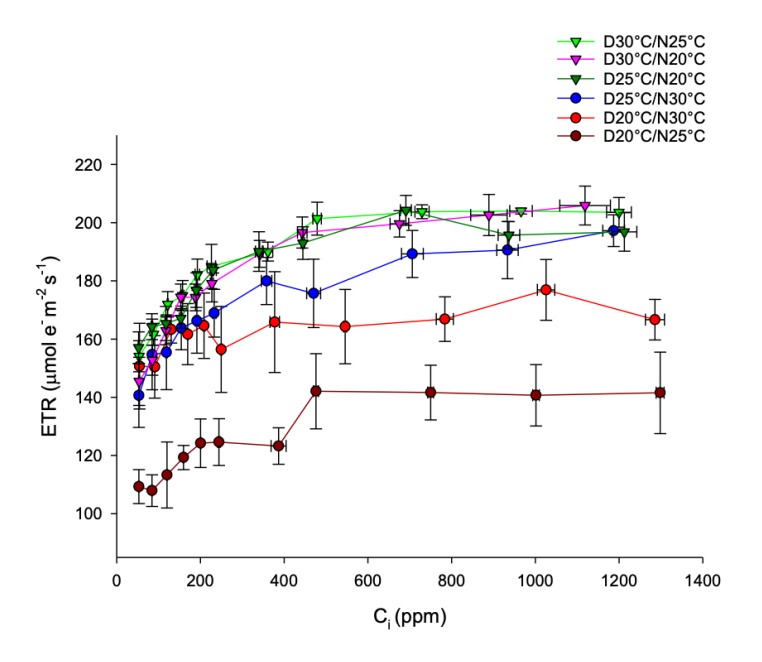


Figure 5: Mean ETR- C_i with SD of Leaf 1 (n=4) by Temperature Treatment, the error bars represent the standard error of the mean

The electron transport rate (ETR) was estimated based on measurements of the fluorescence of PSII (YII) during steady-state photosynthesis. Fluorescence provides further insight into photosynthesis, by representing the demand of energy of the dark to the light photo-reactions.

In Figure 5, the response of ETR to C_i according to TR is shown. The shape and grouping of the lines reflect the influence of DT. Although nearly all of the TRs <200 ppm C_i increased at a similar rate, with the exception of the consistently lower ETR rate of TR D20 °C/N25 °C, they separated as the C_i increased. The highest ETR was consistently observed in TRs D30 °C/N20 °C, which had a maximum ETR of $205.87 \pm 6.67 \, \mu \text{mol} \, \text{e}^{\text{-}} \, \text{m}^{-2} \, \text{s}^{-1}$ at a C_i of $1118.83 \pm 60.41 \, \text{ppm}$, and D30 °C/N25 °C, which had a maximum ETR of $203.97 \pm 0.98 \, \mu \text{mol} \, \text{e}^{\text{-}} \, \text{m}^{-2} \, \text{s}^{-1}$ at a C_i of

965.87 \pm 26.82 ppm. The TRs with the lowest ETR also had the lowest DTs, TR D20 °C/N25 °C, which had a maximum ETR of 142.07 \pm 12.92 μ mol e⁻ m⁻² s⁻¹ at a C_i of 475.85 \pm 20.80 ppm, and TR D20 °C/N30 °C, which had a maximum ETR of 176.89 \pm 10.43 μ mol e⁻ m⁻² s⁻¹ at a C_i of 1025.71 \pm 70.55 ppm. NT did not have a clear effect on ETR, but had an effect on ETR as shown by comparing TRs D20 °C/N25 °C and D20 °C/N30 °C.

4.4 Estimated Photosynthetic Parameters

4.4.1 V_{cmax} and J_{max}

The combination of fluorescence and assimilation measurements across concentrations of CO_2 , allow for the estimation of photosynthetic parameters V_{cmax} and J_{max} using the model of Moualeu-Ngangue et al. (2016) adapted to rice.

 J_{max} in L1 was significantly influenced by DT (p=<0.01) and TR (p=<0.05), but not NT. The increase in J_{max} from increasing DT was shown in the marginal means, at 20 °C the mean J_{max} was 157.59 \pm 14.52 μ mol e⁻ m⁻² s⁻¹ and at 30 °C, it was 240.81 μ mol e⁻ m⁻² s⁻¹. The effect of TR is shown in Table 5, emphasizing the influence of DT, with the highest J_{max} in the TRs D30 °C/N25 °C and D30 °C/N20 °C, whereas the lowest J_{max} was in TRs D20 °C/N25 °C, and D20 °C/N30 °C.

The effect of NT, DT, and TR were insignificant. The marginal means of V_{cmax} according to DT ranged from $145.14\pm11.65\,\mu\text{mol}\,CO_2\,m^{-2}\,s^{-1}$ at $20\,^{\circ}\text{C}$, $156.69\pm10.39\,\mu\text{mol}\,CO_2\,m^{-2}\,s^{-1}$ at $25\,^{\circ}\text{C}$, and $165.10\pm11.65\,\mu\text{mol}\,CO_2\,m^{-2}\,s^{-1}$ at $30\,^{\circ}\text{C}$. V_{cmax} marginal means by TR are shown in Table 5, with the greatest V_{cmax} found in D30 $^{\circ}\text{C}/N25\,^{\circ}\text{C}$.

 J_{max} responded more strongly to DT than V_{cmax} , and the gap between them significantly widened (p=<0.001) as the DT increased. When their interdependence was analyzed, J_{max} and V_{cmax} significantly predicted each other (p=<0.001).

In contrast, in L2 (see Appendix 3), J_{max} did not significantly respond to DT, though it still was affected by the TR (p=<0.05), and increased with the average temperature. Changes in V_{cmax} were similarly insignificant. As in L1, there was a significant relationship between J_{max} and V_{cmax} (p=<0.001), meaning an increase in either parameter predicted an increase in the other.

| Table 5: Mean and S.E. of J_{max} and V_{cmax} | _{ix} of L1(n=4) by Temperature Treatment |
|--|---|
|--|---|

| Treatment | $J_{	ext{max}}$ | | V_{cmax} | |
|-----------------|---|-------|---|-------|
| | Mean | S.E. | Mean | S.E. |
| (Day°C/Night°C) | $(\mu \text{mol } e^- \text{m}^{-2} \text{s}^{-1})$ | | $(\mu \text{mol CO}_2 \text{m}^{-2} \text{s}^{-1})$ | |
| 20/25 | 153.28 | 19.22 | 146.38 | 15.32 |
| 20/30 | 163.80 | 19.22 | 141.01 | 15.32 |
| 25/20 | 208.02 | 13.59 | 161.41 | 10.83 |
| 25/30 | 213.33 | 19.22 | 145.21 | 15.32 |
| 30/20 | 237.80 | 19.22 | 164.32 | 15.32 |
| 30/25 | 238.73 | 19.22 | 173.68 | 15.32 |

4.4.2 g_m and C_c

 g_m was calculated by Eq.7, and is based on parameters derived from the combination of A- C_i curves and fluorescence measurements.

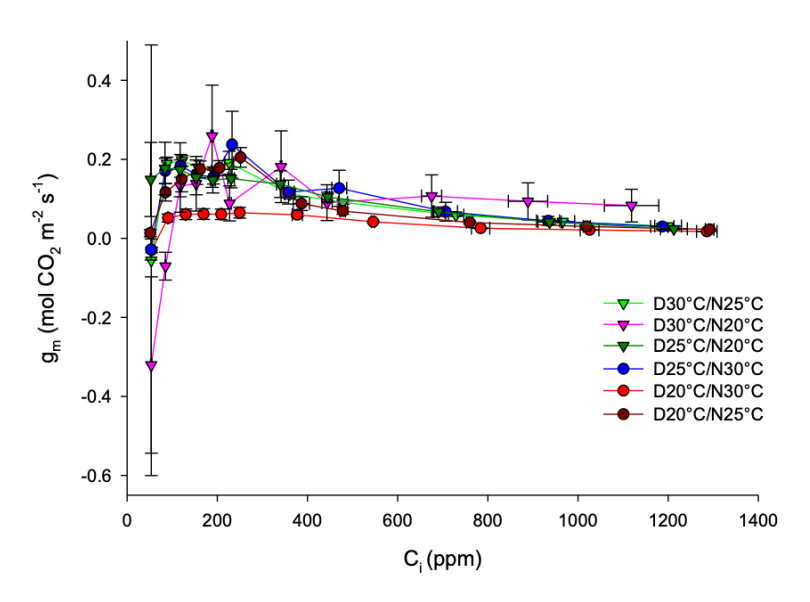


Figure 6: Mean Estimated g_m -C-subscripti of L1 (n=4) by Temperature Treatment, the error bars represent the standard error of the mean

The gas flux representing mesophyll conductance in L1 was between 1.50 mol CO_2 m $^{-2}$ s $^{-1}$ to -1.88 mol CO_2 m $^{-2}$ s $^{-1}$ as C_i increases. Figure 6 shows the response of g_m to changes in C_i and temperature. At the lowest C_i concentrations, g_m describes mostly a negative flux, but rapidly increases with C_i to a range between 0 mol CO_2 m $^{-2}$ s $^{-1}$ to 0.4 mol CO_2 m $^{-2}$ s $^{-1}$, followed by a

slight decline at the higher C_i concentrations. The greatest conductance was estimated in TRs with the highest DTs, such as TR D30 °C/N20 °C, which had a maximum mean g_m according to the measurement C_a of $0.26 \pm 0.23 \, \text{mol} \, \text{CO}_2 \, \text{m}^{-2} \, \text{s}^{-1}$ at a C_i of $188.23 \pm 2.51 \, \text{ppm}$, and TR D30 °C/N25 °C, which had a g_m of $0.19 \pm 0.03 \, \text{mol} \, \text{CO}_2 \, \text{m}^{-2} \, \text{s}^{-1}$ at a C_i of $225.93 \pm 10.06 \, \text{ppm}$. In contrast, lower DT corresponded with lower g_m , as seen in TR D30 °C/N20 °C, which had a maximum mean g_m according to the measurement C_a of $0.06 \pm 0.02 \, \text{mol} \, \text{CO}_2 \, \text{m}^{-2} \, \text{s}^{-1}$ at a C_i of $249.46 \pm 2.55 \, \text{ppm}$.

The trends observed in L1 are also found in L2, though the greatest g_m was observed in TR D30 °C/N25 °C.

Under ambient conditions, g_m did not have a significant response to changes in DT, NT, or TR. The range of marginal means of g_m related to DT, were from 0.09 ± 0.04 mol CO_2 m⁻² s⁻¹ at 20 °C to 0.13 ± 0.04 mol CO_2 m⁻² s⁻¹ at 30 °C. The marginal means of g_m according to NT were 0.16 ± 0.04 mol CO_2 m⁻² s⁻¹ at 20 °C, and 0.09 ± 0.04 mol CO_2 m⁻² s⁻¹ at 30 °C. According to the marginal means of g_m to TR, presented in Table 6, g_m was highest in TR D30 °C/N20 °C.

The relationship between g_m and assimilation rates was analyzed by comparing g_m at ambient C_a , 450 ppm, to the assimilation rates of the unshaded leaves at the end of the TRs, as well as the assimilation rates measured at a C_a of 450 ppm within the A- C_i curve measurements. In L1, g_m did not significantly relate to either group of assimilation rates. However, in L2 the assimilation rates from the A- C_i measurements were significantly related to g_m (p=<0.001), with an estimated slope of 110.02 \pm 14.27, 95% CI [80.25, 139.78].

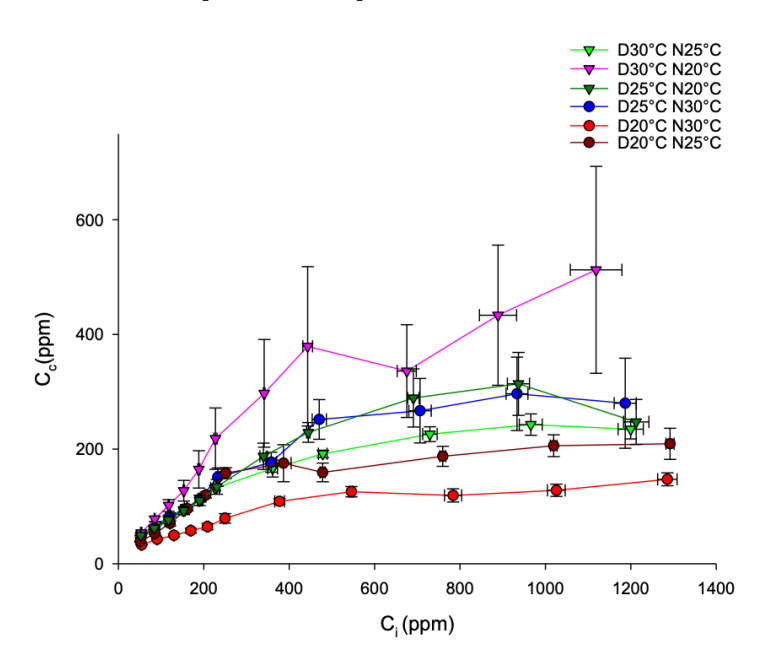


Figure 7: Mean Estimated C_c - C_i (n=4) by Temperature Treatment, the error bars represent the standard error of the mean

 C_c was estimated based on the assimilation rate, C_i , and g_m by Eq. 9, and is shown in relation to C_i in Figure 7. Generally, C_c increased with C_i , but stabilized after reaching a temperature determined inflection C_i , the TRs D20 °C/N30 °C and D20 °C/N25 °C plateaued at a lower C_i than TR D30 °C/N20 °C, which continued to increase past the tested C_i concentration range. As in g_m , higher DT was linked with higher C_c values, reflected by TR D30 °C/N20 °C, which had a maximum mean C_c value according to the measurement C_a of 512.63 \pm 18.81 ppm at a C_i of 1118.84 \pm 60.41 ppm. By contrast, the maximum mean C_c according to the measurement C_a for TR D20 °C/N30 °C was 147.20 \pm 22.31 ppm at a C_i of 1285.85 \pm 22.21 ppm.

Table 6: Mean and S.E. of g_m and C_c at 450 ppm of L1(n=4) by Temperature Treatment

| Treatment | g_{m} | | | C_c |
|-----------------|---|------|--------|-------|
| | Mean | S.E. | Mean | S.E. |
| (Day°C/Night°C) | $(\text{mol CO}_2 \text{m}^{-2} \text{s}^{-1})$ | | (ppm) | |
| 20/25 | 0.09 | 0.06 | 175.34 | 56.85 |
| 20/30 | 0.06 | 0.06 | 108.76 | 56.85 |
| 25/20 | 0.17 | 0.04 | 227.49 | 40.20 |
| 25/30 | 0.12 | 0.06 | 177.04 | 56.85 |
| 30/20 | 0.18 | 0.06 | 297.13 | 56.85 |
| 30/25 | 0.11 | 0.06 | 166.03 | 56.85 |

 C_c did not significantly respond to DT, NT, or TR in L1 or L2. The range of marginal means corresponding to DT, were from 170.08 \pm 46.23 ppm at 20 °C to 214.31 \pm 46.23 ppm at 30 °C. The marginal means of C_c to NT, ranged from 245.79 \pm 41.26 ppm at 20 °C to 155.19 \pm 46.23 ppm at 30 °C. The TR with the highest observed marginal mean C_c , was D30 °C/N20 °C.

Estimated C_c was also compared to assimilation rates in the unshaded leaves at the end of the TR, as well as the assimilation rates measured during the measurement of the A-C-subscripti curve. C_c was found to be significantly related (p=<0.05) to the assimilation rates extracted from the A- C_i curve at 450 ppm in L1 and L2, and the strength of the interaction was estimated to be 0.02 \pm 0.01, 95% CI [0.06, 0.11].

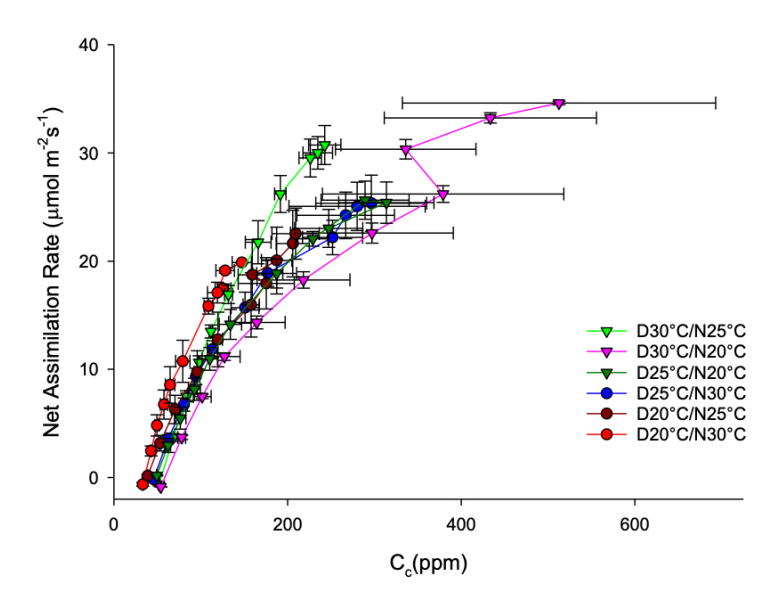


Figure 8: Mean A - C_i of L1 (n=4) by Temperature Treatment, the error bars represent the standard error of the mean

The FCB model describes photosynthetic behavior in response to C_c , not C_i . In Figure 8, the assimilation rate was plotted against C_c , and depicts a more linear relationship between C_c and assimilation rate than C_i to assimilation rate (A- C_i curve). Higher DT, represented by TRs D30 °C/N20 °C and D30 °C/N25 °C, had higher assimilation rates and consequently higher C_c , and as a result extended beyond the other TRs along both axes. This was also evident in L2 (see Appendix 5).

4.4.3 C_{tr}

The transition point in between photosynthesis limitations in terms of C_c can be determined from Eq. 7, which identifies the start and end of Rubisco limiting and RuBP regeneration limiting phases. Statistical analysis of the calculated C_{tr} per A- C_i curve, shows the transition point significantly increases with DT in L1 (p=<0.001) and TR (p=<0.001). The greatest difference in C_{tr} in the marginal means relating to the DTs, was between 25 °C, with a C_{tr} of 92.41 \pm 11.24 μ mol mol⁻¹, and at 30 °C, with a C_{tr} of 172.37 \pm 12.59 μ mol mol⁻¹. The marginal means according to TR in Table 7 show that the magnitude of difference between DT and NT influence C_{tr} , with the highest C_{tr} value in TR D30 °C/N20 °C, and the lowest, TR D20 °C/N25 °C.

In L2, DT (p=<0.001), NT (p=<0.05), and the TR (p=<0.05) were significant (see Appendix 7). Analysis of the marginal means show it increased with DT, but not necessarily with NT, except in the context of DT, reflected by the significant differences by TR.

Table 7: Mean and S.E. C_{tr} of L1(n=4) by Temperature Treatment

| Treatment | C_{tr} | |
|-----------------|----------------------------------|-------|
| (Day°C/Night°C) | Mean $(\mu \text{mol mol}^{-1})$ | S.E. |
| 20/25 | 23.28 | 12.73 |
| 20/30 | 34.98 | 12.73 |
| 25/20 | 86.93 | 9.00 |
| 25/30 | 117.51 | 12.73 |
| 30/20 | 181.04 | 12.73 |
| 30/25 | 148.03 | 12.73 |

4.5 Photorespiration

Photorespiration can not be directly measured due to competing CO_2 evolving processes during the day, such as respiration, and is instead estimated. In this study, it was done in two ways, the first (M1) by calculating the difference in assimilation rate at 21% and 0% O_2 , achieved by replacing O_2 with N_2 at a C_a considered limiting to Rubisco carboxylation, 300 ppm. The marginal means by TR are shown in Table 8. From the A-Csubscripti curve, the assimilation rate and C_c , combined with respiration rate and photocompensation point can be used to calculate photorespiration in Eq.5 (M2). Using M2 photorespiration can be plotted to C_i , as shown in Figure 9.

Table 8: Mean and S.E. of Photorespiration measured by M1 of L1(n=4) by Temperature Treatment

| Treatment | Photorespiration | | | |
|-----------------|-------------------|-----------------|--|--|
| | Mean | S.E. | | |
| (Day°C/Night°C) | $(\mu mol CO_2 n$ | $n^{-2} s^{-1}$ | | |
| 20/25 | 3.83 | 0.70 | | |
| 20/30 | 5.29 | 0.70 | | |
| 25/20 | 5.82 | 0.49 | | |
| 25/30 | 7.53 | 0.70 | | |
| 30/20 | 10.07 | 0.70 | | |
| 30/25 | 9.14 | 0.70 | | |

In M1, photorespiration in L1 was significantly influenced by DT (p=<0.001), and TR (p=<0.001), but not NT. According to DT, the marginal mean of the photorespiratory rate at 20 °C was $4.41 \pm 0.53 \, \mu$ mol CO₂ m⁻² s⁻¹, and $10.15 \pm 0.53 \, \mu$ mol CO₂ m⁻² s⁻¹ at 30 °C. The greatest increase in photorespiration was $3.93 \pm 0.72 \, \mu$ mol CO₂ m⁻² s⁻¹, between 25 °C and 30 °C. In Table 8, the

influence of DT, and to a limited extent NT, is reflected in the marginal means for TR. The magnitude between DT and NT, coupled with a high DT, resulted in the highest photorespiratory rate in TR D30 $^{\circ}$ C/N20 $^{\circ}$ C, compared to D30 $^{\circ}$ C/N25 $^{\circ}$ C. TR D20 $^{\circ}$ C/N30 $^{\circ}$ C had a higher photorespiratory rate to D20 $^{\circ}$ C/N25 $^{\circ}$ C.

In L2, only the DT was significant (p=<0.01) (see Appendix 8).

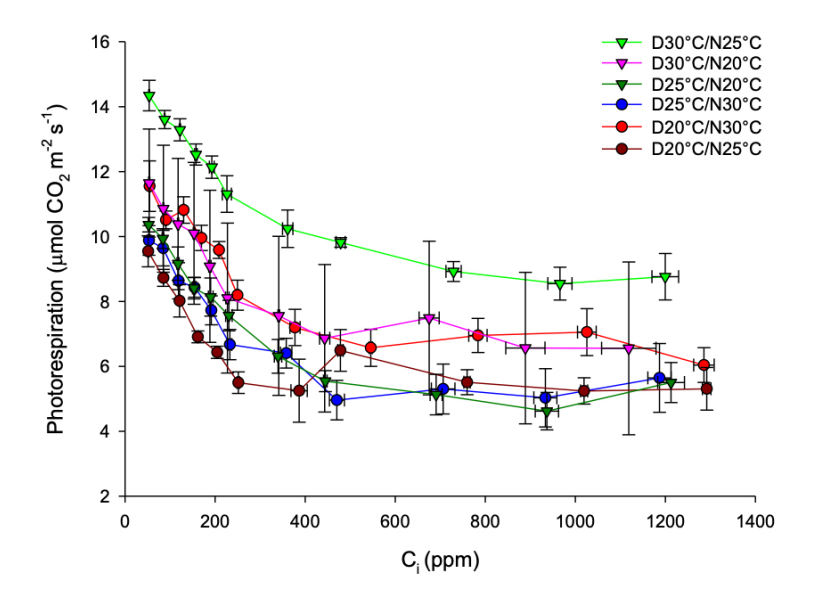


Figure 9: Mean Photorespiration - C_i with Standard Error Bars of L1 (n=4) by Temperature Treatment estimated by M1, the error bars represent the standard error of the mean

The photorespiratory rate decreased with the increase in C_i concentrations across TRs, clearly shown in Figure 9. The mean photorespiratory rate of the TRs was $11.23\pm0.80\,\mu\text{mol}\,CO_2\,m^{-2}\,s^{-1}$ at a C_a of 50 ppm, and $6.30\pm0.64\,\mu\text{mol}\,CO_2\,m^{-2}\,s^{-1}$ at a C_a of 1500 ppm. At higher C_i levels, the effect of DT became more apparent, in TR D30 °C/N25 °C, the mean photorespiratory rate at the greatest measured C_a , 1500 ppm was $8.76\pm0.71\,\mu\text{mol}\,CO_2\,m^{-2}\,s^{-1}$, whereas in TR D20 °C/N25 °C, the mean photorespiratory rate was $5.31\pm0.71\,\mu\text{mol}\,CO_2\,m^{-2}\,s^{-1}$.

| Table 9: Mean and S.E. of Photorespiration measured by M2 at 300 and 450 ppm of L1(n=4) by | 7 |
|--|---|
| Temperature Treatment | |

| Treatment | Photorespiration at 300 ppm | | Photorespiration at | 450 ppm |
|-----------------|---|------|--------------------------------|---------|
| | Mean S.E. | | Mean | S.E. |
| (Day°C/Night°C) | $(\mu \text{mol CO}_2 \text{m}^{-2} \text{s}^{-1})$ | | $(\mu mol CO_2 m^{-2} s^{-1})$ | |
| 20/25 | 5.50 | 0.99 | 5.25 | 1.43 |
| 20/30 | 8.19 | 0.99 | 7.20 | 1.43 |
| 25/20 | 8.18 | 0.70 | 5.30 | 1.01 |
| 25/30 | 6.67 | 0.99 | 6.41 | 1.43 |
| 30/20 | 8.11 | 0.99 | 7.56 | 1.43 |
| 30/25 | 11.31 | 0.99 | 10.24 | 1.43 |

The analysis of the photorespiratory rate using M2 at a C_a of 300 ppm of L1 showed a significant response to DT (p=<0.001) and TR (p=<0.05), but not TR. The marginal means in regards to DT, increased from $6.67 \pm 1.79 \, \mu \text{mol} \, \text{CO}_2 \, \text{m}^{-2} \, \text{s}^{-1}$ at $20 \, ^{\circ}\text{C}$ to $9.79 \pm 1.79 \, \mu \text{mol} \, \text{CO}_2 \, \text{m}^{-2} \, \text{s}^{-1}$ at $30 \, ^{\circ}\text{C}$. The marginal means by NT, ranged from $7.76 \pm 1.59 \, \mu \text{mol} \, \text{CO}_2 \, \text{m}^{-2} \, \text{s}^{-1}$ at $20 \, ^{\circ}\text{C}$ to $8.28 \pm 1.78 \, \mu \text{mol} \, \text{CO}_2 \, \text{m}^{-2} \, \text{s}^{-1}$ at $30 \, ^{\circ}\text{C}$. According to Table 9, the highest photorespiratory rate by TR was TR D30 $\, ^{\circ}\text{C}$ /N25 $\, ^{\circ}\text{C}$, and the lowest in TR D20 $\, ^{\circ}\text{C}$ /N25 $\, ^{\circ}\text{C}$. In L2, photorespiration responded significantly to DT (p=<0.01), and TR (p=<0.05) (see Appendix 8), but not NT.

Photorespiration estimated using M2 was also analyzed at a C_a of 450 ppm (Table 9) and significantly increased with DT (p=<0.05) in L1 and L2, but was not affected by shifts in NT, or the TR. The marginal mean at 20 °C, $5.65 \pm 1.13 \, \mu mol \, CO_2 \, m^{-2} \, s^{-1}$, increased to $9.35 \pm 1.13 \, \mu mol \, CO_2 \, m^{-2} \, s^{-1}$ at 30 °C. The photorespiratory rate was then compared to the assimilation rates measured of the unshaded leaves at ambient conditions at the end of the TR, as well as the assimilation rates at a C-subscripta of 450 measured as part of the A-C_i curve. It had an insignificant relationship with both groups of assimilation measurements in L1. In L2, photorespiration significantly influenced the assimilation rate from the A-C_i curve (p=<0.05). The relationship was also negative, shown by an estimate of its effect, $-0.63 \pm 0.30 \, 95\%$ CI [-1.25, -0.01].

M1 and M2 are based on different methodologies, and were compared to determine if they comparably described photorespiration in its response to DT, NT, and TR. Their estimates of photorespiratory rates at 300 ppm were found to be not significantly related in L1, but were significant (p=<0.05) in L2, and although varied between TRs, they reflected the same response of photorespiration to DT, as shown by an estimate of its effect, 0.45 \pm 0.21 95% CI [0.03, 0.88]. Despite no significant differences (p=0.75) in regards to their response to the TRs, photorespiration in L1 was not significantly predictive of photorespiration in L2.

4.6 Respiration Rate

 R_d was assumed to be equivalent to respiration rates measured without light. Based on statistical analysis of L1, there was no significant response to NT, DT, or TR. The marginal means of respiration according to DT was $0.89 \pm 0.22 \, \mu mol \, CO_2 \, m^{-2} \, s^{-1}$ at $20 \, ^{\circ} C$, and $0.94 \pm 0.22 \, \mu mol \, CO_2 \, m^{-2} \, s^{-1}$ at $30 \, ^{\circ} C$. In relation to NT, the marginal mean was $0.97 \pm 0.22 \, \mu mol \, CO_2 \, m^{-2} \, s^{-1}$ at $20 \, ^{\circ} C$ and $0.82 \pm 0.22 \, \mu mol \, CO_2 \, m^{-2} \, s^{-1}$ at $30 \, ^{\circ} C$. The marginal means by TR are shown in Table 10, with the highest respiration rate observed in TR D30 $^{\circ} C/N20 \, ^{\circ} C$, and the least in its inverse.

Respiration rates in L2 were similarly unaffected by changes in temperature (see Appendix 9).

Table 10: Mean and S.E. of Respiration Rate of L1(n=4) by Temperature Treatment, measured during the day

| Treatment | Respiration Rate | | | |
|-----------------|-------------------------|-----------------|--|--|
| | Mean | S.E. | | |
| (Day°C/Night°C) | (µmol CO ₂ n | $n^{-2} s^{-1}$ | | |
| 20/25 | 1.01 | 0.36 | | |
| 20/30 | 0.71 | 0.36 | | |
| 25/20 | 0.94 | 0.25 | | |
| 25/30 | 0.94 | 0.36 | | |
| 30/20 | 1.07 | 0.36 | | |
| 30/25 | 0.92 | 0.36 | | |

4.7 Temperature Curves

The ability of the rice plants to adapt photosynthesis to temperature was tested by measuring leaf assimilation at ambient CO_2 and saturating light at temperatures starting at $18\,^{\circ}C$ up to $36\,^{\circ}C$, at $3\,^{\circ}C$ intervals.

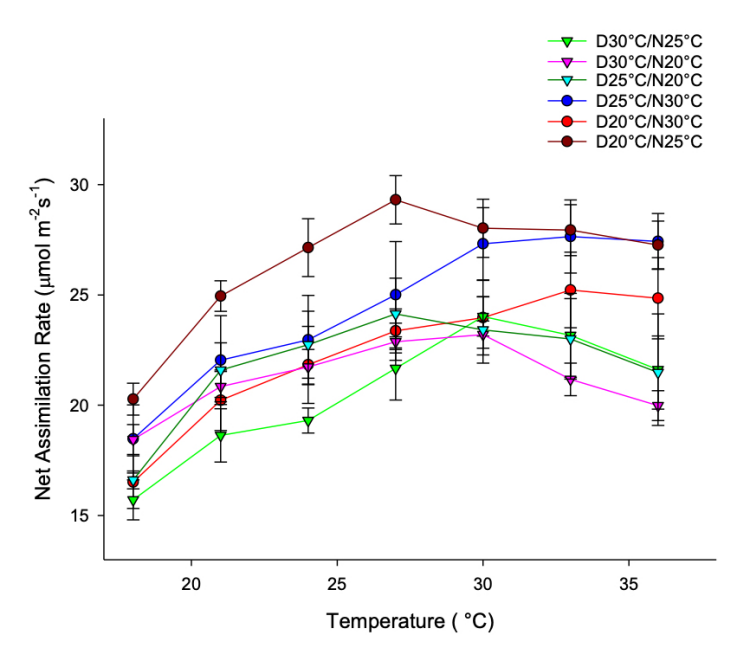


Figure 10: Mean Temperature Curves of Leaf 1 (n=4) by Temperature Treatment, the error bars represent the standard error of the mean

The resulting shape of the leaf assimilation response to temperature seen in Figure 10 is a curve, as assimilation increases with temperature, reaching a maximum, followed by a rapid decline, not fully visible within the tested temperature range. For all TR, the lowest assimilation rates were at 18 °C, and quickly separated according to TR. Rice plants grown in higher NTs than DTs were able to maintain their assimilation rates at NTs in comparison to rice plants under TRs with higher DTs to NTs. The maximum assimilation rate (A_{max}) in plants grown under higher NTs to DTs also shifted towards higher temperatures. Based on assimilation rate means, TR D25 °C/N30 °C had an A_{max} of 27.65 \pm 1.68 µmol m $^{-2}$ s $^{-1}$, measured at 33 °C, TR D20 °C/N25 °C had a A_{max} of 29.31 \pm 1.14 µmol m $^{-2}$ s $^{-1}$ at 27 °C, and the A_{max} of TR D20 °C/N30 °C was 25.23 \pm 1.71 µmol m $^{-2}$ s $^{-1}$ at 33 °C. Whereas TR D30 °C/N25 °C had an A_{max} of 24.02 \pm 0.89 µmol m $^{-2}$ s $^{-1}$ at 30 °C, 25.41 \pm 3.27 µmol m $^{-2}$ s $^{-1}$ at 24 °C in TR D30 °C/N20 °C, and 24.14 \pm 1.61 µmol m $^{-2}$ s $^{-1}$ at 27 °C in TR D25 °C/N20 °C. The mean A_{max} of plants grown at higher NT to DT was 27.40 \pm 1.03 µmol m $^{-2}$ s $^{-1}$, whereas in TRs with higher DTs to NTs, the mean A_{max} was 23.79 \pm 0.26 µmol m $^{-2}$ s $^{-1}$.

An analysis comparing the quadratic regressions of the assimilation rate according to TR, showed the difference between regressions were not significant in response to the TR in both L1 and L2.

4.8 Carbohydrates

4.8.1 Sucrose

Sucrose concentrations at the end of day were significantly higher than at the end of night in L1 (p=<0.001), reflected in the marginal means presented in Table 11. This also applied to L2 (see Appendix 11). On their own, sucrose concentrations at end of day, and at end of night were not independently affected by DT or NT. However, when sucrose concentrations at the end of day were taken into account as a covariate by the statistical model, higher NT led to significantly lower sucrose concentrations at end of night (p=<0.05). This is shown by the decrease in the marginal means of sucrose concentration relating to NT, at 20 °C, the sucrose concentration was 2.09 ± 0.18 mmol cm⁻², at 25 °C, it was 1.55 ± 0.20 mmol cm⁻², and at 30 °C, it was 1.00 ± 0.20 mmol cm⁻². The marginal means of sucrose concentrations measured in the leaf at the end of day were 4.02 ± 0.84 mmol cm⁻² at 20 °C, and 2.97 ± 0.84 mmol cm⁻². As seen in Table 11, the highest sucrose concentration at the end of day by TR was in D20 °C/N25 °C, and the lowest in TR D25 °C/N30 °C. More predictably considering the significance of NT, the highest sucrose concentrations at the end of night were found in TR D30 °C/N20 °C, and the lowest in TR D25 °C/N30 °C.

A similar trend was also observed in L2, but to a lesser, and non-significant extent (p=0.09) (see Appendix 10).

The main processes behind the difference between sucrose levels in the leaves at the end of day and end of night is export to sink tissues, a component of respiration. However, there was no interaction between sucrose concentrations and respiration rates. Export is also reflected by the RSR, which when compared with the sucrose concentrations in the leaves at the end of night and were found to significantly and strongly positively related (p=0.0370), with the strength of the effect of RSR to the concentration of sucrose at the end of night estimated to be -4.19 ± 0.19 in L1, 95% CI [-8.10, -0.27].

The link between RSR and sucrose concentrations in the leaves at the end of night were found to be insignificant in L2.

| Table 11: Mean and S.E. of Sucrose Concentrations at End of Day, Night, and Shading of Leaf 1 |
|---|
| (n=5) by Temperature Treatment |

| Treatment | End of Day | | End of | End of Night | | Treatment |
|-----------------|-----------------------|----------------|-----------------------|----------------|----------|-----------|
| | Mean | S.E. | Mean | S.E. | Mean | S.E. |
| (Day°C/Night°C) | (mmol cm ⁻ | ²) | (mmol cm ⁻ | ²) | (mmol cm | -2) |
| 20/25 | 3.61 | 1.38 | 1.72 | 0.34 | 0.90 | 0.50 |
| 20/30 | 4.19 | 1.38 | 1.03 | 0.34 | 0.55 | 0.50 |
| 25/20 | 3.41 | 0.97 | 2.01 | 0.24 | 1.40 | 0.36 |
| 25/30 | 2.61 | 1.38 | 1.02 | 0.34 | 0.25 | 0.50 |
| 30/20 | 2.91 | 1.38 | 2.10 | 0.34 | 0.99 | 0.50 |
| 30/25 | 3.14 | 1.38 | 1.42 | 0.34 | 0.99 | 0.50 |

The aim of the shading treatment was to deplete carbohydrate reserves in the leaf. The sucrose concentrations in shaded leaves were not significantly affected by DT or NT, and they were not significantly similar (p=0.44) to sucrose concentrations in leaves measured at the end of night. The average difference across TRs between the shaded leaves and the leaves sampled at end of night was 0.71 ± 0.48 mmol cm $^{-2}$. The marginal means relating sucrose concentration in the shaded leaves to NT were 1.26 ± 0.29 mmol cm $^{-2}$ at 20 °C and 0.33 ± 0.33 mmol cm $^{-2}$ at 30 °C. This is reflected in the the marginal means relating to TR in Table 11, with the lowest concentrations in TRs D25 °C/N30 °C and D20 °C/N30 °C, which also shows the effect of average temperature.

Sucrose levels at the end of day were compared to the assimilation rates in the unshaded leaves in L1 (Table 11) and L2 (see Appendix 11), but they were not significantly related (p=0.35). The sucrose levels in the shaded leaves were compared to the assimilation rates measured in the shaded leaves after exposure to light, but it was not significant.

4.8.2 Monosaccharides (Fructose & Glucose)

In contrast to sucrose concentrations, monosaccharide levels were significantly higher (p=<0.001) at the end of day compared to end of morning both in L1, displayed in Table 12, and L2 (see Appendix 12). Higher NT decreased monosaccharide concentrations at the end of night (p=<0.001) and also led to increased monosaccharide concentrations at the end of day (p=<0.05). Despite a general trend of decreasing monosaccharide concentrations as NT increased, the highest monosaccharide concentration in relation to NT, $0.93 \pm 0.05 \,\mathrm{mmol\,cm^{-2}}$, was measured at 25 °C. The highest monosaccharide concentrations in relation to DT, were at 25 °C, $1.13 \pm 0.05 \,\mathrm{mmol\,cm^{-2}}$.

Table 12: Mean and S.E. of Monosaccharide Concentrations at End of Day and Night of Leaf 1 (n=5) by Temperature Treatment

| Treatment | End of Day | | End of Night | |
|------------------|-------------------------------|------|-------------------------------|------|
| (Day°C/Night°C) | Mean (mmol cm ⁻²) | S.E. | Mean (mmol cm ⁻²) | S.E. |
| (Day C/Nigiti C) | (IIIIIIOI CIII) | | (IIIIIIOI CIII) | |
| 20/25 | 1.07 | 0.07 | 0.88 | 0.05 |
| 20/30 | 0.81 | 0.07 | 0.60 | 0.05 |
| 25/20 | 0.84 | 0.05 | 0.78 | 0.04 |
| 25/30 | 0.77 | 0.07 | 0.59 | 0.05 |
| 30/20 | 0.78 | 0.07 | 0.77 | 0.05 |
| 30/25 | 1.18 | 0.07 | 0.95 | 0.05 |

The relationship between monosaccharides, sucrose, and the assimilation rates of the unshaded and the shaded leaves, in relation to the TRs was analyzed. There was no significant relationship to sucrose levels or assimilation rates.

4.9 Chlorophylls and Carotenoids

If calibrated, SPAD could directly reflect chlorophyll concentrations in the leaf, but also serve as a reflection of plant nutrition. In this case, it serves as a useful complement to the absorbance measurements, and shows the trends in chlorophyll concentration in the shaded leaves. The NT (p=0.0003), DT (p=< 0.0001), and TR (p=< 0.0001) were significant. In terms of NT, the SPAD values decreased from 43.25 \pm 0.63 at 20 °C, to 39.06 \pm 0.71 at 30 °C, whereas they increased with DT, from 36.86 \pm 0.71 at 20 °C, to 44.13 \pm 0.71 at 30 °C. Therefore, the highest DT and lowest NT, should result in the highest SPAD, which is seen in Table 13 for TR D30 °C/N20 °C.

Table 13: Mean and S.E. of SPAD of Leaf 1 (n=5) by Temperature Treatment from the rice plants used for the Shading Treatment

| Treatment | SPA | AD |
|-----------------|-------|------|
| | Mean | S.E. |
| (Day°C/Night°C) | | |
| 20/25 | 36.70 | 0.90 |
| 20/30 | 34.30 | 0.90 |
| 25/20 | 44.01 | 0.64 |
| 25/30 | 40.60 | 0.90 |
| 30/20 | 46.98 | 0.90 |
| 30/25 | 43.14 | 0.90 |

Ca and Cb and carotenoid concentrations were measured in leaves sampled at the end of day, end of night, and shaded leaves. Ca concentrations responded significantly to TR (p=0.001), DT (p=<0.01), and NT (p=<0.05) in L1. Ca decreased in response to NT as shown by the marginal means relating to NT, at 20 °C the Ca concentration was $18.84 \pm 1.16 \,\mu g \, cm^{-2}$, and at 30 °C it was $15.86 \pm 1.30 \,\mu g \, cm^{-2}$. Whereas Ca concentration increased with DT, the marginal mean was $14.23 \pm 1.30 \,\mu g \, cm^{-2}$ at 20 °C, increasing to $20.16 \pm 1.30 \,\mu g \, cm^{-2}$ at 30 °C. The combination of these two trends was reflected in Table 14, with the highest Ca concentration marginal mean based on TR, TR D30 °C/N20 °C, and the lowest TR D20 °C/N25 °C. The trends and significance were also observed in L2 (see Appendix 13).

Table 14: Mean and S.E. of *Ca*, *Cb*, and Total Chlorophyll Concentrations of Leaf 1 (n=10) by Temperature Treatment, measured from plants sampled both at the end of day and end of night

| Treatment | Ca | Ca | | Cb | | ophylls |
|-----------------|--------------------|------|--------------------|------|--------------------|---------|
| | Mean | S.E. | Mean | S.E. | Mean | S.E. |
| (Day°C/Night°C) | $(\mu g cm^{-2})$ | | $(\mu g cm^{-2})$ | | $(\mu g cm^{-2})$ | |
| 20/25 | 12.13 | 1.89 | 4.38 | 0.46 | 16.51 | 2.35 |
| 20/30 | 13.49 | 1.89 | 4.86 | 0.46 | 18.35 | 2.35 |
| 25/20 | 16.12 | 1.33 | 5.80 | 0.33 | 21.93 | 1.66 |
| 25/30 | 14.07 | 1.89 | 5.50 | 0.46 | 19.57 | 2.35 |
| 30/20 | 23.64 | 1.89 | 9.00 | 0.46 | 32.64 | 2.35 |
| 30/25 | 16.81 | 1.89 | 6.40 | 0.46 | 23.22 | 2.35 |

Cb concentrations in L1 and L2 were influenced by TR (p=<0.001), DT (p=<0.001) and NT(p=<0.01). Cb concentration decreased as NT increased, but the lowest marginal mean in relation to NT was at 25 °C, with a Cb concentration of $4.93 \pm 0.49 \,\mu\mathrm{g}\,\mathrm{cm}^{-2}$. The trend in relation to DT is clearer, as the Cb concentration marginal means regarding DT increased from $4.62 \pm 0.69 \,\mu\mathrm{g}\,\mathrm{cm}^{-2}$ at 20 °C to $7.70 \pm 0.69 \,\mu\mathrm{g}\,\mathrm{cm}^{-2}$ at 30 °C. In Table 14, the combination of these two responses is shown, resulting in the highest Cb concentration marginal mean in TR D30 °C/N20 °C, and the lowest in D20 °C/N25 °C. The trends and significance in L1 were also present in L2 (see Appendix 13)

Total chlorophyll concentrations (Ca + Cb) in L1, shown in Table 14, and L2 (see Appendix 13) reflected the trends of its constituent parts, significantly decreasing as NT increased (p=<0.05), and increasing with DT (p=<0.001), but did not significantly respond to TR.

Carotenoid concentrations were influenced by DT (p=<0.05), NT (p=<0.01), and the TR (p=<0.01). Carotenoid concentrations decreased as NT increased, the marginal means in relation to NT fell from $3.21 \pm 0.15 \,\mu \mathrm{g} \,\mathrm{cm}^{-2}$ at $20 \,^{\circ}\mathrm{C}$ to $2.51 \pm 0.17 \,\mu \mathrm{g} \,\mathrm{cm}^{-2}$ at $30 \,^{\circ}\mathrm{C}$. However, with a marginal mean of $2.07 \pm 0.17 \,\mu \mathrm{g} \,\mathrm{cm}^{-2}$, the carotenoid concentration was lower at $25 \,^{\circ}\mathrm{C}$ than at $30 \,^{\circ}\mathrm{C}$. When taking into account DT, the carotenoid marginal mean increased from $2.66 \pm 0.17 \,\mu \mathrm{g} \,\mathrm{cm}^{-2}$

at 20 °C to $3.02\pm0.17\,\mu g\,cm^{-2}$ at 30 °C, but there was again a dip at 25 °C. Despite the trends individually observed according to DT and NT, the lowest carotenoid concentration marginal mean according to TR shown in Table 15 was measured in TR D20 °C/N25 °C, but the highest carotenoid concentration was in accordance with the above trends, and was observed in D30 °C/N20 °C.

DT, NT, and TR were similarly significant in L2 (see Appendix 14).

Table 15: Mean and S.E. Carotenoid Concentrations of Leaf 1 (n=10) by Temperature Treatment, measured from plants sampled both at the end of day and end of night

| Treatment | Carotenoids | |
|-----------------|--------------------------------|------|
| (Day°C/Night°C) | Mean (μg cm ⁻²) | S.E. |
| 20/25 | 2.17 | 0.30 |
| 20/30 | 2.53 | 0.30 |
| 25/20 | 2.70 | 0.21 |
| 25/30 | 2.05 | 0.30 |
| 30/20 | 3.67 | 0.30 |
| 30/25 | 2.47 | 0.30 |

5 Discussion

5.1 Morphology

Overall, few significant morphological changes were observed in the rice plants at the end of the TRs. Across all measured parameters, DT and NT individually had no significant effect on plant morphology. However, shifts in carbon partitioning, reflected by specific leaf area (SLA) and root to shoot ratio (RSR), significantly responded to the TRs. These differences are shown by the marginal means according to TR in Table 3.

Compared individually, the components of RSR (leaf, sheath, and root dry mass) were not significantly different, though when viewed on a whole plant basis, suggest a shift towards root growth as NT increased. The TR with the greatest RSR, D20 $^{\circ}$ C/N25 $^{\circ}$ C, also has the highest NT, and the other TR with a NT of 30 $^{\circ}$ C, with an RSR value 0.01 less. Whereas higher DT shifts the RSR more towards increases in aboveground dry mass, indicated by the lowest RSR, measured in TR D30 $^{\circ}$ C/N20 $^{\circ}$ C.

RSR reflects the biomass allocation between roots and shoots, and is influenced by a variety of factors, such as deficits in water or inorganic nutrients, light and CO₂ concentration, defoliation and pruning (J. B. Wilson, 1988). The partitioning of sucrose may also play a deciding role in

determining the RSR, therefore making RSR an indicator of source-to-sink sucrose transport as part of a broader response to environmental conditions (J. Farrar, 1996). Considering that fresh nutrient solution (Yoshida's original solution) was added to the rice plants regularly to prevent drought or nutrient stress, shifts in RSR should not reflect growth limitations resulting from nutrient or water availability. Other possible stresses, such as light and CO₂ concentrations are similarly unlikely, as the measured PAR in the growth chambers was sufficient for growth, plants were rotated throughout the chamber to mitigate the measured unevenness in light conditions, and there were no visible indications of light stress. CO2 concentrations were monitored and maintained within the growth chamber on a minute to minute basis. Considering the consistent response of RSR to HNT over time and treatment runs, it should instead be regarded as an indicator of shifts in the movement of sucrose from the leaves to the roots. The interaction with TR was significant, and the highest RSR values were in TRs with the highest NTs, and in particular those with higher NT to DT. This suggests increased sucrose export from source to sink tissues in response to HNT. In future studies, further investigation of sucrose transporter activity throughout the diurnal cycle could provide greater insight into sucrose export. It should be noted that in this study the roots and leaves were effectively maintained at the same temperature, which does not reflect field (paddy) conditions, where the roots are often warmer than the leaves during the night due to the water layer in a paddy system (Maruyama et al., 2017).

The effect of TR on SLA was significant, although its component parts (LA and leaf dry mass), when individually analyzed were not. Analysis of the differences between TRs in regards to SLA, displayed in Table 3, suggest the average temperature as well as NT influenced SLA. The greatest SLA was measured in TR D25 °C/N30 °C, and the lowest in D20 °C/N25 °C. SLA, like RSR, is an indicator of resource allocation within the plant, relating leaf dry matter content to leaf thickness, and both respond to environmental factors, such as the availability of nutrients and light (P. J. Wilson et al., 1999). The link between temperature and SLA is not clear in literature, and has been shown to vary widely depending on the species (Rosbakh et al., 2015). A 4°C increase in growth temperature led to an increase in SLA through increases in LA in Bellis perennis and Dactylis glomerata (Gunn & Farrar, 1999). In japonica rice varieties, the response to a constant DT of 27 °C, and increasing NT, 17 °C, 22 °C, and 27 °C showed an increase in total LA, and consequently a higher SLA (Kanno et al., 2009). In this experiment, differences in SLA could in part be attributed to measurement error. Rice leaves roll shortly after being separated from the tiller, reducing LA during measurement. Otherwise, self-shading by other leaves on the same or surrounding plants can reduce SLA, along with slight variations in leaf age at the time of sampling. As the TR was only for 12 days, significant changes in leaf structure may not be apparent. Changes in SLA in response to temperature would be clearer over a longer treatment time.

The variable morphological response of rice to changes in DT and NT is shown by the mixed results found in available literature, in which the effect of HNT ranges from negative to positive,

or none at all (Jing et al., 2016). In *indica* rice varieties, Yoshida et al. (1981) and Cheng et al. (2009) observed reduction in plant height, tiller number and total biomass. Cheng et al., (2010) found that *japonica* varieties grown at 27 °C had the greatest LA, tiller number, and biomass. Peraudeau et al. (2014) did not see any significant effect on biomass at maturity either in the field or in the greenhouse across *indica*, *japonica*, and *aus* type varieties.

Apart from temperature, relative humidity during the day and night influence rice morphology. In this study, the relative humidity was maintained at an unnatural constant 75 % during the day and night. In a rice paddy, the relative humidity is often higher at night than during the day because a greater volume of water moisture can be held in warmer air, and as the air cools at night, leads to an increase in relative humidity. In *japonica* varieties, high night relative humidity (90 %) led to increases in the LER, height, leaf blade length, root number, total root length, and dry matter production. These effects were amplified even further if the relative humidity during the day was also high (Hirai et al., 2000). Some of the morphological changes attributable to diurnal shifts in temperature are a response to relative humidity, and by keeping the relative humidity diurnally constant, expected morphological changes described in the literature were not observed.

The statistical model used to determine significance assumes the 'chamber effect' is accurately represented by the differences between the only true TR replication, D25 °C/N20 °C. However, in one of the runs of this TR, the plants showed symptoms of a nutrient deficiency days after being transplanted into nutrient solution, and subsequently were slower to develop in comparison to other treatment runs. As a result, the differences with its replicate may lead to an overestimation of the 'chamber effect'. The area of greatest deviance was morphology because the plants developed more slowly. Consequently, the larger 'chamber effect' could statistically mask some otherwise potentially significant differences.

5.2 Photosynthesis and Respiration

The point assimilation measurements of the unshaded leaves at ambient conditions were significantly influenced by the ambient temperature at which they were measured, which was the DT of the TR. The marginal mean of the assimilation rate increased from $17.59 \pm 1.05 \, \mu \text{mol m}^{-2} \, \text{s}^{-1}$ at $20\,^{\circ}\text{C}$ to $22.19 \pm 1.08 \, \mu \text{mol m}^{-2} \, \text{s}^{-1}$ at $30\,^{\circ}\text{C}$. NT had an insignificant influence on the assimilation rate. In literature, HNT was found to increase assimilation rates, as seen in cottonwood trees according to Turnbull et al., (2002) and rice according to Kanno et al., (2009). It was also found to have no effect, as shown by Peraudeau et al., (2015) in several varieties of rice, and Frantz et al., (2004) did not find significant changes in assimilation rate in lettuce, tomato, and soybean in relation to HNT.

The shaded leaf assimilation rates were not significantly affected by DT, NT, or TR, and were only significantly different from the assimilation rates of the unshaded leaves in their lack of response

to DT across TRs. This contradicts the link between the size of the sink affecting the assimilation rate shown by Turnbull et al., (2002). It is possible that more time than the 30-40 min given until steady state photosynthesis had been achieved was needed for photosynthesis to respond to the carbohydrate depletion in the leaf. Consequently, assimilation measurements should be taken not only directly after shading, but a day after. The age of the leaf was not a factor, as assimilation rates taken under ambient conditions during the A- C_i measurements earlier in the week were significantly similar to assimilation measurements at the end of the TR five days later.

The assimilation rates measured in this study were comparable to those measured of several rice varieties in the greenhouse (20 μ mol m⁻² s⁻¹ to 25 μ mol m⁻² s⁻¹ by Peraudeau et al., (2015), but not the field. The ratio between the assimilation and respiration rate, the average of which was 0.93 \pm 0.06 μ mol m⁻² s⁻¹, was around 10-20, which was as described by Björkman, (1981).

The respiration rate did not significantly respond to DT, NT, or TR. Regardless, respiration rates suggested a response to DT, considering in Table 10, the lowest marginal mean according to TR was in TR D20 °C/N30 °C, and the highest in D30 °C/N20 °C. Mitochondrial respiration is considered to be a thermal dependent process, often cited in literature with a Q₁₀ of 2 (Lambers, 1985). Although in theory representative of rates at night, respiration was measured during the day, and is reflective of daytime dynamics in the plant (Griffin & Turnbull, 2012). Respiration is composed of growth, maintenance and export components, and each has a different temperature sensitivity. For example, growth is considered unresponsive to temperature (F. P. De Vries et al., 1974), whereas maintenance respiration is dependent on temperature (McCree, 1974). Therefore, depending on the predominant process in the leaf at the time of measurement, respiration values will vary. The Yin method used by Moualeu-Ngangue et al. (2016) to measure respiration in the day (R_d) was not used due to theoretical concerns (G. D. Farquhar & Busch, 2017). Comparison before the experiment (unpublished data) indicated the method used in this study produced respiration values significantly larger than those generated by the Yin method. This was observed when both methods were used on rice plants in TR D30 °C/N20 °C, but on different TR runs. According to the Yin method, mean respiration was $0.40 \pm 0.05 \,\mu\text{mol}\,\text{m}^{-1}\,\text{s}^{-1}$, whereas the CO₂ flux measured from a darkened leaf was $1.07 \pm 0.36 \,\mu\text{mol}\,\text{m}^{-1}\,\text{s}^{-1}$. This raises questions as to the best method for R_d measurements.

5.3 Modeling Photosynthesis

Assimilation involves multiple and interlinked biochemical, and enzymatic steps, and as a result should increase with temperature. This is shown by the A- C_i curve of L1 (Fig.3) and L2 (see Appendix 1), in which the higher DTs led to higher assimilation rates throughout the sequence of C_i concentrations, though to varying extents depending on the position on the curve, and therefore according to the photosynthetic limitation. To more accurately quantify the response to temperature, assimilation needs to broken down into its component processes, which can be

identified based on the role their limitations play on the behavior of assimilation rate in response to C_i . The accurate grouping of the points along the A- C_i curve to each dominant component process is achieved by modeling assimilation. The model used in this study was a line-fitting algorithm from Moualeu-Ngangue et al. (2016) that applies the equations of the FCB model to the A- C_i curve (T. D. Sharkey et al., 2007).

The outputs were values for τ , representing leaf absorptance and photosystem partitioning, V_{cmax} , representing the maximum carboxylation rates of Rubisco, and J_{max} , representing the maximum rate of electron transport, C_{tr} , the transition point between Rubisco and RuBP limited photosynthesis, along with derived values at each measurement point for g_m , C_c , and photorespiration.

 V_{cmax} did not significantly respond to the TRs, despite increases in its marginal means in relation to DT, whereas J_{max} significantly increased with DT. The NT did not have a significant influence, though the marginal means by TR in Table 5 suggest increasing NT led to higher J_{max} values, such as the difference between TRs D20 °C/N25 °C and D25 °C/N30 °C. Whereas the marginal means by TR in Table 5 suggest the inverse for V_{cmax} , as shown by the difference between D25 °C/N20 °C and D20 °C/N25 °C. In cottonwood trees, Turnbull et al. (2006) reported significant increases in V_{cmax} to DT, but the largest response was when DT and NT were both increased. Whereas shifts in J_{max} were only observed when DT and NT were increased together. Not only is the model plant very different from rice, but the line-fitting model used was also different. It is not clear from literature how NT affects mechanisms related either to V_{cmax} or J_{max} , though it could relate to indirect changes in the balance of Calvin-Benson intermediates.

After analysis of 109 species, Wullschleger et al. (1993) found V_{cmax} and J_{max} are consistently linked, often in the ratio of 1-2, which agrees with the hypothesis of photosynthetic of resource allocation (J.-L. Chen et al., 1993). In this study, the estimates of V_{cmax} and J_{mx} ratio had a mean of 1.29 \pm 0.19, and their interaction across TRs was statistically significant. V_{cmax} and J_{max} are both considered dependent on temperature (Leuning, 2002). The lack of significant response in V_{cmax} to DT was in spite of its high Q_{10} value reported in literature (Hall & Keys, 1983). This could be explained by reduced Rubisco activation related to the ETR (Eichelmann et al., 2009), the slope in the temperature response of V_{cmax} within the tested temperature range (Archontoulis et al., 2011), or it could not have a basis in physiology, and is rather intrinsic to the design of the model. Most improvement in carboxylation is below 20 °C, whereas at higher temperatures increased carboxylation is offset by increased potential for oxygenation from 20 °C to 30 °C (Sage & Kubien, 2007). Within the model, the assumptions that underpin the calculation of g_m , along with the catalytic constants of Rubisco, could create significant biases that are reflected in the model's output (B. Walker et al., 2013).

The effect of temperature on both parameters was in part addressed through the adaptation of the catalytic constants of Rubisco kinetics, K_O and K_C , and the photorespiratory compensation point, Γ^* to temperature with a modified Arrhenius equation (Medlyn et al., 2002). The adapted

values should produce an accurate reflection of photosynthesis under measurement conditions. The line-fitting model of Moualeu-Ngangue et al. (2016) fits the FCB equations for the different steady states by guesses of V_{cmax} and J_{max} to fit C_c (based on the calculation of g_m), and for V_{cmax} , the modified K_O , K_C , Γ^* values as well as the R_d . Values for K_O , K_C , Γ^* were taken from the in vitro studies by Perdomo et al. (2016) using O. sativa L. cv. Bomba, a japonica, and could vary with the Rubisco kinetics of the *indica* variety used in this study, IR64. This was possibly indicated by the difference between the K_O and K_C values measured by Makino et al (1988), which were based on measurements of Oryza sativa L. cv. Gui zhao No.2, an indica variety. The difference is more likely attributable to differences in methodology. In particular, the model used has a high sensitivity to Γ^* values, which are reported to vary between and within species. Regardless, it is debatable whether Rubisco kinetics determined in vitro even accurately describe the behavior of Rubisco under physiological conditions. Either due to extraction or differences in assay conditions compared to the chloroplast stroma, Rubisco may have been degraded or inactivated (Perdomo et al., 2016). However, the values of K_0 , K_c and specificity of Rubisco ($S_{c/o}$), would remain unchanged, and in vivo measurements require mutants, the creation of which is beyond the technical capabilities of most laboratories (ibid). Considering their importance to the accuracy of estimates of V_{max} and J_{max} , the catalytic constants and photocompensation point should be specific at the cultivar, or even plant level. This is too expensive and laborious (ibid), and instead of in vivo determinations of Rubisco kinetics, co-estimation by the used model could be considered (Moualeu-Ngangue et al., 2016).

Other than Rubisco's catalytic constants and the photocompensation point, an accurate estimate of g_m is fundamental for the fitting of the FCB models. For example, V_{max} is more sensitive to shifts in g_m than J_{max}, based on analysis of A-C_i measurements across nearly 130 C₃ plant species (Sun et al., 2014). The general trend of g_m in response to changes in C_i can be observed in Figure 6 and are consistent with literature, in particular its decline as C_i increases (Flexas et al., 2007; Moualeu-Ngangue et al., 2016). The negative values observed at low C_i can be explained by the movement of CO₂ along the concentration gradient, in this case from the chloroplast to the sub-stomatal cavity or leaf exterior. Lower g_m at higher C_i could also be a response to concentration gradient, as CO₂ passively diffuses to the chloroplast without the need for enzymatic steps to speed up its pathway. The range of mean gm values across TRs were lower at ambient conditions (450 ppm) compared to other published mean g_m estimates for IR64, but at $400~\rm ppm$, $(0.3~\rm mol\,m^{-1}\,s^{-1})$ (Ouyang et al., 2017). g_m has been shown to have a high Q₁₀, 2.2 in tobacco leaves (Tamimi et al., 1994). In this study, it had no significant response to DT, NT, or TR, the marginal means by TR at a C_a of 450 ppm in Table 6, indicate increased conductance corresponding to increased DT and the inverse to NT, with the highest g_m in TR D30 °C/N25 °C.

Figure 6 displays the variability of g_m as it reacts to the CO₂ concentration and temperature, higher at lower concentrations, and slightly decreases, followed by a plateau at higher CO₂

concentrations. Therefore, its responsiveness to temperature may be best compared at lower C_i levels, though in this study, the focus was on photosynthetic performance at ambient conditions (450 ppm). Several estimated values for g_m in L1 in TR D30 °C/N20 °C were not only biochemically unlikely (at low C_i levels, around 50 ppm) but disparate, indicated by the large error bars in Figure 6 representing the standard error of the mean, indicating possible limitations of the curve-fitting model when handling higher assimilation rates. In future studies, g_m estimation should be complemented with an alternative method, such as the Variable J method, or isotope discrimination.

The C_c is directly related to g_m via Eq. 6, and the slope of each line suggests the influence of g_m . On comparison between Figure 6 and Figure 7, in both there is rapid increase at lower C_i concentrations, followed by a decline. The inflection point of each line's plateau shifted higher depending on the DT, which also corresponded with the assimilation rate. This was supported by the significance of the relationship between g_m and assimilation to the TRs in L2, and the significance of C_c to assimilation in both L1 and L2. The relationship between assimilation and C_c was again demonstrated in Figure 8. Higher assimilation rates, in response to increased temperature, requires greater CO_2 concentrations at the site of carboxylation, at least initially, until the limitation becomes RuBP regeneration or TPU, which could not be identified in the results of this study, though would be if lower temperatures had been used (Sage & Kubien, 2007).

The estimation of g_m within the model, calculated by Eq.7, depends on accurate fluorescence, assimilation, and respiration measurements, as well as Γ^* and a guess value, within given constraints, of τ , the product of the partitioning fraction between the two photosystems (β) and the amount of incoming light absorbed by the photosystems (α). The constraints of guess value of τ are potentially problematic, for example the values for leaf absorptance are based on values measured from lichens and red maple trees (*Acer rubrum*) (Bauerle et al., 2004). Other than with an integrating sphere under identical light conditions as the assimilation rate was measured under (Long & Bernacchi, 2003), leaf light absorption can be related to leaf chlorophyll content (Moualeu-Ngangue et al., 2016). If determined for each leaf, only β needs to be estimated, leading to a more accurate fit of the FCB equations. An external quantum sensor in combination with leaf fluorescence can also be used, based on the relationship between leaf transmittance and the blue and red LED absorptance measured by an integrating sphere and a spectroradiometer (LICOR, 2018).

The Yin method used by Moualeu-Ngangue et al. (2016) to measure R_d was not used due to theoretical concerns (G. D. Farquhar & Busch, 2017), and was instead based on gas exchange measurements during the day from the leaf after 30 min in the darkened conditions. However, the model was not parameterized for such a large difference in R_d , and could have led to led to skewed results. Another source of significant error was the fluorescence measurements, which could be linked to the location of the PAM-Fluorometer, which is placed externally, measuring

through a potentially smeared or dirty glass pane in the cuvette. Leakage from the cuvette during gas exchange measurements was taken into account. The photosynthetic response to changes in CO_2 is not consistent or predictable, and the A-C_i curve datasets are often noisy. This is due to the small sample sizes, and the time intensive nature of the gas-exchange measurements, leading to the outsize influence of outliers, but also the unpredictable behavior of a complex, interlinked process. According to the model's average sensitivity index of the estimated photosynthesis rate to each photosynthetic parameter, τ and R_d , followed by the assumed values of K_c and Γ^* , have the greatest influence on the estimated values respectively (Moualeu-Ngangue et al., 2016).

When the estimates of steady states A_c and A_j are plotted, C_{tr} is the point of intersection between them. Therefore, its shifts are according to either an increase in the slope of A_c , described by V_{cmax} , or a decrease in the slope of A_j , described by J_{max} . Therefore, C_{tr} represents the relationship between V_{cmax} and J_{max} The increased susceptibility of J_{max} to DT, represents a shift in the slope of A_j , hence why the C_{tr} values were highest in the TRs with the highest DTs.

5.4 Photorespiration

Photorespiration was estimated by two methods, in the first method (M1), assimilation was measured as the difference in assimilation at 21 % O_2 at an assumed limiting CO_2 concentration, 300 ppm and 0 % O_2 . M2 was based on the use of the derived g_m values from the model into Eq. 8. The analysis of M1 indicated that photorespiration responded significantly to increased DTs, though not to NTs, except in relation with DT, in the context of the TR. The results of M2 also significantly responded to increases in DT. When compared under ambient conditions, the photorespiratory rate estimated by M2 was significantly related to the assimilation rate extracted from the A- C_i curve, from which it was also derived. Although the effect of NT was insignificant, based on the marginal means in Table 8 and Table 9 (for L2 see Appendix 8), as well as the marginal means independently relating to NT, suggested HNT resulted in higher photorespiratory rates during the day. The response of the photorespiratory rate to temperature is supported in literature (Bauwe et al., 2010), as the solubility of CO_2 decreases in relation to O_2 in water (Gevantman, 2000), and the specificity of Rubisco also decreases (Brooks & Farquhar, 1985), and accordingly should increase with temperature.

Although M1 was a point measurement taken at one C_a , it served as a useful reflection of the reaction of photorespiration to the TRs. However, Sharkey et al. (1988) argue that switching to a low O_2 environment ignores the other component limitations of photosynthesis. If the limitation is RuBP regeneration or triose phosphate utilization, upon switching to a lower O_2 , unhindered assimilation, formerly limited by Rubisco, will not be observed. This was theoretically avoided by measuring the baseline assimilation rate at a CO_2 concentration at which Rubisco defined photosynthetic behavior. A complicating factor is the purity of the N_2 gas, which was 99.998 %

pure by volume. Thus the leaves were under anoxic conditions, which could have had unintended effects, such as disrupting the dominant consumer of O_2 , respiration (Rawyler et al., 2002). The assimilation rate after exposure to N_2 was observed to rapidly rise, briefly stabilize, at which point the measurement was taken, and was directly followed by a rapid reduction in assimilation rate. M2, as it relies on both directly measured parameters (R_d and A), assumed values (Γ^*), and estimated (g_m) shares the same areas of concern as those stated for the estimation of V_{cmax} and J_{max} . The values generated by both methods were compared in relation to the TRs and were found to be significantly similar in L2.

The advantage of M1 is its reliance on measurements rather than estimated parameters. It depends on choosing a C_a at which photosynthesis is exclusively limited by Rubisco, and the C_a used is in the range considered by Sharkey et al. (2007) to be the transition point between Rubisco and a RuBP limitation. It is difficult to accurately discern a range consistently within one limitation versus the other, this can only be achieved after the fact by estimating the transition point based on the C_c . Consequently, there is always the risk measurements of photorespiration made in M1 could also reflect a RuBP limitation, or at lower temperatures a TPU limitation, leading to an underestimation of photorespiratory rates. Regardless, in this study at least in L2, M1 and M2 similarly described the effect of temperature on photorespiratory rates.

In future, N_2 gas with lower purity should be used to avoid damage to the leaf. Although not ideal, according to Sharkey et al. (1988), not only is measuring assimilation under low O_2 conditions a useful complement to modeled photorespiration, but it can be used to determine the sensitivity of assimilation to O_2 and CO_2 variation. O_2 sensitivity is defined as $(A_{21} - A_2)/A_2$, where A_{21} refers to assimilation measured at 21 % O_2 , and A_2 assimilation measured at 2 % O_2 (Sage et al., 1987). If the sensitivity is near the modeled sensitivity, RuBP regeneration is limiting, in contrast a TPU limitation shows a value near zero or is even negative (ibid).

5.5 Temperature Curves

The temperature curves in L1 suggest adaptation of photosynthesis by the rice plant to HNT, despite the insignificant difference between the polynomial regressions of the curves. In Figure 10, the higher NT to DT TRs led to higher A_{max} values at higher temperatures in comparison to the higher DT to NT treatments. Increased range and resilience of photosynthesis to higher temperatures was also observed in cottonwood trees by Turnbull et al. (2002). This could indicate an effect on photosynthesis from HNT, though on further review, an increase in night temperature did not consistently increase A_{max} , or extend the range of photosynthesis, as shown by treatment D20 °C/N30 °C.

Although all measurements were taken at the point photosynthesis had achieved stability, instantaneous temperature acclimation does not signify acclimation capacity over a longer timespan (Yamori et al., 2005). In C_3 plants, acclimation to heat involves a decline in photorespiration and

 R_d , increased ETR, and the synthesis of a heat stable Rubisco activase (Sage & Kubien, 2007). Whereas acclimation to cold was not likely observed within the tested temperature range (18 °C to 36 °C. The proposed acclimations to heat when applied to the TRs partially match the results of the other measurements. The TR with the highest assimilation rate across temperatures, TR D20 °C/N25 °C, had the lowest measured ETR according to Figure 10 and the among the highest respiration rates (Table 10), but TR D20 °C/N25 °C had the lowest photorespiratory rate according to M1 (Table 8) and M2 (Table 9). However, ETR, respiration, or photorespiration can not be directly compared because they are measured at different temperatures. In future they should either be measured at 25 °C, a more limited temperature range tested (Turnbull et al., 2002), or each parameter mathematically standardized for comparison. It could also be complemented by a determination of rice Rubisco activase activity in response to temperature.

Shifts in VPD can affect stomatal behavior and lead to assimilation values that are not reflective of the actual photosynthetic rate (Lin et al., 2012). This was accounted for in the measurement by using the same VPD at each temperature measuring point, though it was not uniform across all temperatures, as it increased with the measurement temperature. It is not possible to adequately balance the constraints of dew point and the technical limitations of the IRGA to provide sufficient moisture control at temperatures above 30 °C. The observed trend of improved range and maxima in the treatments with higher NT to DT could be partially explained by the difference between the VPD in the growth chamber, grown at 75 % relative humidity in PSP2 (D28 °C/N22 °C), which was also the relative humidity for all temperature treatments in PSP1, to that found in the cuvette of the IRGA. As a result, the plants grown at higher DT would be pre-conditioned to the higher VPD during the temperature measurements, and more readily close their stomata to reduce transpiration, reducing assimilation, shown by the lower observed conductance values (Kawamitsu et al., 1993). In contrast, the plants grown at lower DTs, maintained conductance rates more consistently across the tested temperature range. The higher NT than DT treatments have lower DTs, and the plants would have been acclimatized to a lower VPD in comparison to the plants, for example grown at 30 °C during the day.

Another factor was the measurement conditions. In the TRs with DTs > 25 °C the plants were measured outside of the growth chamber so that the leaf temperature could be lowered to 18 °C. The temporary change in ambient conditions could have resulted in changes on a plant level that could have affected leaf behavior. However, the meristem and roots were in nutrient solution, which would delay any response to a change in ambient air temperature. The thermocouple was carefully placed underneath the leaf and placed to make contact with the leaf, but throughout the course of measurements dislodgement was possible, and the temperature of the cuvette measured rather than the leaf.

5.6 Sucrose and Monosaccharides

The product of the Calvin-Benson cycle is triose phosphates that are converted through a series of enzymatic steps into sucrose or starch in the mesophyll cytoplasm (Taiz & Zeiger, 2002). The sucrose concentrations in the leaves, sampled at the end of day were not linked to the assimilation measurements recorded the following day, or to temperature. However, sucrose is the predominant form of carbohydrate for storage in rice, particularly in the flag leaf, as well as the form in which photosynthates are transported throughout the plant (Ishimaru et al., 2007). Sucrose generated from photosynthetic activity is rapidly moved from the cytosol to the vacuole where it is stored (Kaiser & Heber, 1984), until being exported to sinks during the night. Therefore at the end of day, the sucrose levels in the leaf should correspond to photosynthetic activity. This is contradicted by the marginal means by TR (Table 11), in which the TRs with the lowest DTs and as result lower assimilation rates had the highest leaf sucrose concentrations, such as in TR D20 °C/N30 °C.

Sucrose could have been used in processes such as respiration, for maintenance or growth (Gordon et al., 1980), but the respiration rate, representing R_d , was insignificantly related to sucrose concentrations both at the end of day and end of night. Export is also a possible pathway to explain shifts in sucrose in the leaf. It has been shown in soybean plants that daytime rates of carbohydrate export were linked to the net assimilation rate (Mullen & Koller, 1988). Considering there were not significant differences in terms of biomass related to DT or NT, utilization of sucrose by sink tissues could be opportunistically responding to temperature, shifting growth to the period within the diurnal cycle with the most favorable temperature, as indicated in the literature by the positive response of leaf expansion rates (LER) in rice to HNT (Cutler et al., 1980). The sucrose levels in the leaves at the end of day significantly and negatively corresponded with RSR values, which can be used to represent the export of photoassimilates from the leaf (J. Farrar, 1996), and suggests greater sucrose export to the sinks during HNT. This indicates that in the scenario of higher NT to DT, growth would have shifted to the nighttime.

The degree of depletion in the sucrose concentration in the leaf at the end of night significantly increased with NT, provided sucrose concentrations at the end of day were taken into account, which complemented the results of Glaubitz et al. (2014) and Peraudeau et al. (2015), who linked this change to increased respiration rates. However, R_d in this study did not reflect this. The measured respiration rates, although aimed to reflect respiration during the day, were measured without light, and should also reflect respiration rates during the night (Griffin & Turnbull, 2012). Respiration encompasses several processes, and is also shaped by the surrounding processes and environment occurring during the day, such as the presence of byproducts from N assimilation, and would not serve as an accurate representation of respiration at night (Nunes-Nesi et al., 2011). Respiration rates at night could not be estimated by the comparison of sucrose levels before and after end of night due to sucrose's dual role in export and storage.

The mechanism controlling the exponential depletion of sucrose in source tissues during the night is the vacuolar sucrose transporter 2 (SUT2) (Mueller et al., 2018), and not by the genes governing the circadian clock, as observed for starch turnover in arabidopsis (Smith & Stitt, 2007). Further measurements of growth parameters, such as LER, should be made in future studies to achieve greater insight into the relationship between carbohydrate levels, growth, and diurnal shifts in temperature. This should be accompanied by knockout studies of sucrose transporters to understand the dynamics of sucrose transport within the diurnal cycle. The extent to which the power of the sink is related to assimilation rate remains unclear in literature, and may be linked to the photosynthate type, starch or sucrose. For example, little is known about the role of sucrose signaling (Horacio & Martinez-Noel, 2013). The results of the shading treatment in this study suggest depletion in sucrose levels in the leaf had no effect on assimilation rates, and neither did HNT, which also lowered sucrose levels at the end of the night. Not only is there a lack of literature on plants that rely primarily on sucrose rather than starch for energy storage, but the inherent nature of sucrose in rice physiology makes it difficult to measure, as it reflects both transport and storage. Although less significant, but considering its link in literature to assimilation (Turnbull et al., 2002), the role of starch should also be further investigated. In this study, the stored leaf segments from sucrose and chlorophyll analysis should also be analyzed for starch, even if starch concentrations in the leaf are considered negligible by comparison (Glaubitz et al., 2014).

The variation in sucrose concentration could be a result of the leaf sampling method. Before the end of day and end of night, 20:00 and 8:00 respectively, the plants were sampled one after another, so that within the constraints of the time needed for the samples to be taken, both theoretical maximum and minimum sucrose concentrations in the leaves could be achieved. However, only the last plants sampled are truly representative of either maximum or minimum sucrose concentrations. Errors could also be attributed to pipetting during the extraction process or filling the wells of the microplate, including the preparation of standards and the anthrone reagent solution. There was slight variability in the timing between runs, which may have affected the intensity of the color, reducing absorbance values, and could lead to underestimation of concentration. The same 96-well microplate was used within the same temperature treatment, may have led to skewed readings from scratches or fingerprints on the bottom of the plate or lid.

Monosaccharide concentrations in the leaf, a fraction composed of fructose and sucrose, were lower than sucrose concentrations (Table 12). Their levels at the end of the day increased significantly with HNT, and were significantly reduced at the end of the night. Glaubitz et al. (2013) found a link between monosaccharide levels and rice cultivar tolerance to HNT. It is not clear from the literature what benefits they potentially confer, or the mechanisms that could underly them. Due to their reactivity, they can not be transported or stored and are immediately converted either to sucrose or starch (Taiz & Zeiger, 2002). Therefore, their presence within the

leaf is not in itself important, but rather the processes they may indicate, such as the rate of sucrose synthesis, glycolysis, and polysaccharide formation, or overall physiological activity. This was supported by their concentrations in the leaf corresponding with temperature. TR D30 $^{\circ}$ C/N20 $^{\circ}$ C and D25 $^{\circ}$ C/N20 $^{\circ}$ C had the lowest differences between concentrations at the end of day and end of night.

Similar to the sucrose measurements, error may have resulted from sampling, pipetting, preparation of the PAHBAH reagent and standards, the integrity of the microplate, or variable timing between runs, which could affect the intensity of color, and therefore absorbance.

5.7 Chlorophylls and Carotenoids

Chlorophylls are photoreceptors essential to photosynthesis (Taiz & Zeiger, 2002). Chlorophyll a (Ca) and b (Cb) differ structurally, and as a consequence also by the wavelength of light they absorb (Taiz & Zeiger, 2002). Ca is the primary photosynthetic pigment and generally present at higher concentrations than Cb (ibid). This was also apparent from their marginal means by TR in Table 14. Chlorophylls a and b were found to significantly vary between temperature treatments, and significantly increased with DT and NT. TRs with higher chlorophyll and carotenoid content, such as 30 °C/25 °C and 30 °C/20 °C, mirrored the TRs with the highest ETRs (Figure 5). As such, increased chlorophyll concentration could be an acclimation to higher assimilation rates in response to increased DT, and increase photosynthetic efficiency by ensuring faster RuBP regeneration under ambient conditions. Whereas the relationship between chlorophyll content and assimilation rate is not clear in literature, other components of the photosystems have been linked to photosynthetic performance, such as the cytochrome bf complex concentration to J_{max} (von Caemmerer, 2000). This should be measured in a following study for further insight into the plant's acclimation to temperature.

Changes in chlorophyll content is often used as an indicator of plant stress, morphology (age and position in leaves), physiological, or a response to abiotic factors, such as nutrition, light quality, relative humidity, and light quality (Pavlovic et al., 2015). Glaubitz et al. (2014) found in rice cultivars more susceptible to NT had depleted carbohydrate levels that led to stress, and resulted in chlorosis and necrosis of the leaves. She determined that IR64 was intermediately ranked in its sensitivity to HNT. However, in this study neither necrosis or chlorosis was observed across temperature treatments. This could be due to the short length of the treatment, 12 days, whereas the length of the study of Glaubitz et al. (2014) was 23 days.

Carotenoids, organic pigments that serve both as photoreceptors alongside chlorophylls and protectors against photo-damage, include a wide range of compounds, divided into two classes, xanthophylls (containing O_2) and carotenes (do not contain O_2) (Taiz & Zeiger, 2002). In this study we did not discriminate between carotenoids, and are simply represented as a fraction representing absorbance at 470 nm. The leaves were the approx. the same age and position on

the main tiller, and were sampled at the same point. Although the light conditions were not homogenous in the growth chambers, they were effectively homogenized by consistently cycling the rice plants before and during the temperature treatments. Variability in the quality of the nutrient solution is possible, but unlikely to be consistent enough to have an effect. Nutrient dynamics, in particular N and P, could also have been affected by the dynamics of nutrient uptake according to the temperature of the roots.

An acclimation of photosynthesis to higher temperature is increased carotenoid content, specifically zeaxanthin, in the cell membrane to reduce liquidity and increase the robustness of the electron transport chain (Havaux, 1998). The rudimentary analysis used in this study is not able to discriminate between and identify carotenoids, or determine if they are embedded in the cell membrane. The differences in the carotenoid concentrations mirror those in chlorophylls, and could be attributed to the interaction between temperature and nutrient dynamics. They are also involved in quenching singlet O_2 , though this is mostly related to photo-oxidative stress, rather than temperature (Ramel et al., 2012).

Possible errors in their measurement include higher concentrations from evaporation of the 96% ethanol used as a solvent during the double extraction process, pipetting error, and the integrity of the 96-well microplate. The concentrations of chlorophylls and carotenoids were determined via the coefficients and equations from Lichtenthaler et al. (1983), which considering its age, may not accurately represent the capabilities of the spectrometer used in this study.

5.8 Hypotheses

The central claim of the hypothesis was that assimilation rates during the day would increase after HNT, as observed for example by Turnbull et al. (2002) in cottonwood trees and Kanno et al. (2009) in rice. In this study, according to the point measurements taken from the unshaded leaves on the final day of the temperature treatments, this was not observed. Of course, these were point measurements taken throughout the day, and as a result could misrepresent by virtue of timing of measurement the true photosynthetic behavior of the rice leaves. However, photosynthesis in plants grown in growth chambers has been shown to be relatively constant throughout the day (Hennessey & Field, 1991).

The proposed mechanism for higher assimilation following HNT was the coupling between assimilation and carbohydrate levels. The depleted carbohydrate reserves from increased NT would increase assimilation during the following day. Using a mixed model to determine if assimilation rates significantly corresponded with sucrose levels at the end of day or end of night, there was no significant interaction. This was further supported by the assimilation rates of the shaded leaves, which after around 40 hours of shading, had depleted sucrose levels, though did not have higher assimilation rates after steady state photosynthesis had been established on exposure to light than the unshaded leaves. The respiration rates did not shift according to

changes in DT, NT or the TRs. The increased differences between end of day and end of night sucrose concentrations in the leaf to NT could indicate not only increased respiration, but export. Photorespiration and mesophyll conductance, while significantly linked to assimilation, and in the case of photorespiration, DT, were not influenced by NT, and in fact based on their marginal means a decrease in rate to NT was suggested.

6 Conclusion

HNT did not have a significant effect on assimilation as a whole, or on the individual components of photosynthesis or associated processes, such as g_m , photorespiration, or R_d . However, the measured temperature curves suggest HNT led to increased photosynthetic tolerance to higher temperatures. There was also no significant effect observed in the morphology of the rice plants in response to shifts in DT and NT, other than to the ratios representing plant carbon allocation, RSR and SLA. The decrease in sucrose levels in the leaves decreased as NT increased, either due to export, as indicated by the significant relationship between sucrose levels and RSR, or nighttime respiration. Consequently, the rice plant may be shifting growth towards the nighttime. Whereas, the assimilation rate as well as photorespiration increased with DT.

As observed in this study, the assimilation rate and carbohydrate levels in the leaves were not coupled. This was the case in relation to carbohydrate levels at the end of the day to assimilation rates, as well as those at the end of night. Rice leaves depleted of carbohydrates by the shading treatment, did not show any increase in assimilation rate after re-exposure to light. R_d and assimilation were also not significantly linked.

The absence of significant morphological change, despite observed changes in assimilation rate in response to DT, and increases in utilization or export of sucrose in relation to NT, indicates a series of adjustments being made in the generation and utilization of photoassimilates. However, based on the results of this study, it is remains unclear what they are. It is possible the photosynthetic behavior of one leaf conflated to the whole plant may ignore shifts in changing dynamics in the entire plant physiology. The lack of coordination in the leaf between carbohydrate levels and assimilation rate should be further investigated with greater attention on not only starch levels within the leaf, but also the reserves stored in the leaf sheath. More research is also needed on the diurnal dynamics of sucrose in plants that use it as the primary form of storage for the products of photosynthesis.

References

- Alexander, L., Zhang, X., Peterson, T., Caesar, J., Gleason, B., Tank, A. K., ... others (2006). Global observed changes in daily climate extremes of temperature and precipitation. *Journal of Geophysical Research: Atmospheres*, 111(D5).
- Alward, R. D., Detling, J. K., & Milchunas, D. G. (1999). Grassland vegetation changes and nocturnal global warming. *Science*, 283(5399), 229–231.
- Archontoulis, S., Yin, X., Vos, J., Danalatos, N., & Struik, P. (2011). Leaf photosynthesis and respiration of three bioenergy crops in relation to temperature and leaf nitrogen: how conserved are biochemical model parameters among crop species? *Journal of Experimental Botany*, 63(2), 895–911.
- Asao, S., & Ryan, M. G. (2015). Carbohydrate regulation of photosynthesis and respiration from branch girdling in four species of wet tropical rain forest trees. *Tree physiology*, 35(6), 608–620.
- Aselmann, I., & Crutzen, P. (1989). Global distribution of natural freshwater wetlands and rice paddies, their net primary productivity, seasonality and possible methane emissions. *Journal of Atmospheric chemistry*, 8(4), 307–358.
- Atkin, O., Scheurwater, I., & Pons, T. (2006). High thermal acclimation potential of both photosynthesis and respiration in two lowland plantago species in contrast to an alpine congeneric. *Global Change Biology*, 12(3), 500–515.
- Baldry, C., Bucke, C., & Walker, D. (1966). Temperature and photosynthesis. i. some effects of temperature on carbon dioxide fixation by isolated chloroplasts. *Biochimica et biophysica acta*, 126(2), 207–213.
- Bauerle, W. L., Weston, D. J., Bowden, J. D., Dudley, J. B., & Toler, J. E. (2004). Leaf absorptance of photosynthetically active radiation in relation to chlorophyll meter estimates among woody plant species. *Scientia Horticulturae*, 101(1-2), 169–178.
- Bauwe, H., Hagemann, M., & Fernie, A. R. (2010). Photorespiration: players, partners and origin. *Trends in plant science*, 15(6), 330–336.
- Bellasio, C., Beerling, D. J., & Griffiths, H. (2016). An excel tool for deriving key photosynthetic parameters from combined gas exchange and chlorophyll fluorescence: theory and practice. *Plant, cell & environment*, 39(6), 1180–1197.
- Bernacchi, C., Pimentel, C., & Long, S. (2003). In vivo temperature response functions of parameters required to model rubp-limited photosynthesis. *Plant, Cell & Environment*, 26(9), 1419–1430
- Bernacchi, C. J., Portis, A. R., Nakano, H., von Caemmerer, S., & Long, S. P. (2002). Temperature response of mesophyll conductance. implications for the determination of rubisco enzyme kinetics and for limitations to photosynthesis in vivo. *Plant physiology*, 130(4), 1992–1998.
- Berry, J., & Björkman, O. (1980). Photosynthetic response and adaptation to temperature in higher plants. *Annual Review of Plant Physiology*, 31(1), 491–543.
- Biosciences, L.-C. (n.d.). Measuring photorespiration with the li-6400/xt system. Retrieved 2/9/2011, from http://www.licor.com/env/newsline/2011/02/measuring-photorespiration-with-the-li-6400xt-system/
- Brooks, A., & Farquhar, G. (1985). Effect of temperature on the co 2/o 2 specificity of ribulose-1, 5-bisphosphate carboxylase/oxygenase and the rate of respiration in the light. *Planta*, 165(3), 397–406.
- Bunce, J. A. (2007). Direct and acclimatory responses of dark respiration and translocation to temperature. *Annals of botany*, 100(1), 67–73.
- Busch, F. (2013). Current methods for estimating the rate of photorespiration in leaves. *Plant Biology*, 15(4), 648–655.

- Chen, J.-L., Reynolds, J. F., Harley, P. C., & Tenhunen, J. D. (1993). Coordination theory of leaf nitrogen distribution in a canopy. *Oecologia*, *93*(1), 63–69.
- Chen, T.-W., Kahlen, K., & Stützel, H. (2015). Disentangling the contributions of osmotic and ionic effects of salinity on stomatal, mesophyll, biochemical and light limitations to photosynthesis. *Plant, cell & environment*, 38(8), 1528–1542.
- Cheng, W., Sakai, H., Yagi, K., & Hasegawa, T. (2009). Interactions of elevated [co2] and night temperature on rice growth and yield. *Agricultural and forest meteorology*, 149(1), 51–58.
- Coast, O., Murdoch, A. J., Ellis, R. H., Hay, F. R., & Jagadish, K. S. (2016). Resilience of rice (o ryza spp.) pollen germination and tube growth to temperature stress. *Plant, cell & environment*, 39(1), 26–37.
- Cock, J., Yoshida, S., & Forno, D. A. (1976). *Laboratory manual for physiological studies of rice*. Int. Rice Res. Inst.
- Cutler, J. M., Steponkus, P. L., Wach, M. J., & Shahan, K. W. (1980). Dynamic aspects and enhancement of leaf elongation in rice. *Plant Physiology*, 66(1), 147–152.
- Davy, R., Esau, I., Chernokulsky, A., Outten, S., & Zilitinkevich, S. (2017). Diurnal asymmetry to the observed global warming. *International Journal of Climatology*, *37*(1), 79–93.
- De Datta, S. K. (1981). Principles and practices of rice production. Int. Rice Res. Inst.
- De Vries, F. P., Brunsting, A., & Van Laar, H. (1974). Products, requirements and efficiency of biosynthesis a quantitative approach. *Journal of theoretical Biology*, 45(2), 339–377.
- De Vries, M. E., Leffelaar, P. A., Sakane, N., Bado, B. V., & Giller, K. E. (2011). Adaptability of irrigated rice to temperature change in sahelian environments. *Experimental Agriculture*, 47(1), 69–87.
- Dewar, R., Medlyn, B., & McMurtrie, R. (1998). A mechanistic analysis of light and carbon use efficiencies. *Plant, Cell & Environment*, 21(6), 573–588.
- Dubois, J.-J. B., Fiscus, E. L., Booker, F. L., Flowers, M. D., & Reid, C. D. (2007). Optimizing the statistical estimation of the parameters of the farquhar–von caemmerer–berry model of photosynthesis. *New Phytologist*, 176(2), 402–414.
- Eichelmann, H., Talts, E., Oja, V., Padu, E., & Laisk, A. (2009). Rubisco in planta k cat is regulated in balance with photosynthetic electron transport. *Journal of experimental botany*, 60(14), 4077–4088.
- Ethier, G., & Livingston, N. (2004). On the need to incorporate sensitivity to co2 transfer conductance into the farquhar–von caemmerer–berry leaf photosynthesis model. *Plant, Cell & Environment*, 27(2), 137–153.
- FAO. (2013). Fao statistical yearbook part 3: Feeding the world. *Food and Agriculture Organization of the United Nations*.
- Farquhar, G., von Caemmerer, S., & Berry, J. (1980). A biochemical model of photosynthetic co2 assimilation in leaves of c3 species. *Planta*, 149(1), 78–90.
- Farquhar, G. D., & Busch, F. A. (2017). Changes in the chloroplastic co2 concentration explain much of the observed kok effect: a model. *New Phytologist*, 214(2), 570–584.
- Farrar, J. (1996). Regulation of root weight ratio is mediated by sucrose: opinion. *Plant and Soil*, *185*(1), 13–19.
- Farrar, S., & Farrar, J. (1985). Carbon fluxes in leaf blades of barley. *New Phytologist*, 100(3), 271–283.
- Flexas, J., Díaz-Espejo, A., Berry, J., Cifre, J., Galmés, J., Kaldenhoff, R., ... Ribas-Carbó, M. (2007). Analysis of leakage in irga's leaf chambers of open gas exchange systems: quantification and its effects in photosynthesis parameterization. *Journal of Experimental Botany*, 58(6), 1533–1543.
- Flexas, J., Ribas-Carbo, M., DIAZ-ESPEJO, A., GalmES, J., & Medrano, H. (2008). Mesophyll conductance to co2: current knowledge and future prospects. *Plant, Cell & Environment*,

- 31(5), 602-621.
- Folland, C. K., Rayner, N. A., Brown, S., Smith, T., Shen, S., Parker, D., ... others (2001). Global temperature change and its uncertainties since 1861. *Geophysical Research Letters*, 28(13), 2621–2624.
- Frantz, J. M., Cometti, N. N., & Bugbee, B. (2004). Night temperature has a minimal effect on respiration and growth in rapidly growing plants. *Annals of Botany*, 94(1), 155–166.
- Genty, B., Briantais, J.-M., & Baker, N. R. (1989). The relationship between the quantum yield of photosynthetic electron transport and quenching of chlorophyll fluorescence. *Biochimica et Biophysica Acta (BBA)-General Subjects*, 990(1), 87–92.
- Gevantman, L. (2000). Solubility of selected gases in water. Nitric oxide (NO), 308(3.348), 10-4.
- Glaubitz, U., Li, X., Köhl, K. I., van Dongen, J. T., Hincha, D. K., & Zuther, E. (2014). Differential physiological responses of different rice (oryza sativa) cultivars to elevated night temperature during vegetative growth. *Functional Plant Biology*, 41(4), 437–448.
- Gordon, A., Ryle, G., Powell, C., & Mitchell, D. (1980). Export, mobilization, and respiration of assimilates in uniculm barley during light and darkness. *Journal of Experimental Botany*, 31(2), 461–473.
- Griffin, K. L., Turnbull, M., & Murthy, R. (2002). Canopy position affects the temperature response of leaf respiration in populus deltoides. *New Phytologist*, 154(3), 609–619.
- Griffin, K. L., & Turnbull, M. H. (2012). Out of the light and into the dark: post-illumination respiratory metabolism. *New Phytologist*, 195(1), 4–7.
- Gu, J., Yin, X., STOMPH, T.-J., & Struik, P. C. (2014). Can exploiting natural genetic variation in leaf photosynthesis contribute to increasing rice productivity? a simulation analysis. *Plant, cell & environment*, 37(1), 22–34.
- Gunn, S., & Farrar, J. (1999). Effects of a 4 c increase in temperature on partitioning of leaf area and dry mass, root respiration and carbohydrates. *Functional Ecology*, 13, 12–20.
- Hall, N. P., & Keys, A. J. (1983). Temperature dependence of the enzymic carboxylation and oxygenation of ribulose 1, 5-bisphosphate in relation to effects of temperature on photosynthesis. *Plant Physiology*, 72(4), 945–948.
- Harley, P. C., Loreto, F., Di Marco, G., & Sharkey, T. D. (1992). Theoretical considerations when estimating the mesophyll conductance to co2 flux by analysis of the response of photosynthesis to co2. *Plant Physiology*, *98*(4), 1429–1436.
- Havaux, M. (1998). Carotenoids as membrane stabilizers in chloroplasts. *Trends in Plant Science*, 3(4), 147–151.
- Hennessey, T. L., & Field, C. B. (1991). Circadian rhythms in photosynthesis: oscillations in carbon assimilation and stomatal conductance under constant conditions. *Plant Physiology*, 96(3), 831–836.
- Henry, A., Gowda, V. R., Torres, R. O., McNally, K. L., & Serraj, R. (2011). Variation in root system architecture and drought response in rice (oryza sativa): phenotyping of the oryzasnp panel in rainfed lowland fields. *Field Crops Research*, 120(2), 205–214.
- Hirai, G.-i., Okumura, T., Takeuchi, S., Tanaka, O., & Chujo, H. (2000). Studies on the effect of the relative humidity of the atmosphere on the growth and physiology of rice plants: effects of relative humidity during the light and dark periods on the growth. *Plant production science*, 3(2), 129–133.
- Horacio, P., & Martinez-Noel, G. (2013). Sucrose signaling in plants: a world yet to be explored. *Plant signaling & behavior*, 8(3), e23316.
- Husic, D. W., Husic, H. D., Tolbert, N. E., & Black Jr, C. C. (1987). The oxidative photosynthetic carbon cycle or c2 cycle. *Critical Reviews in Plant Sciences*, *5*(1), 45–100.
- IPCC. (2014). Contribution of working groups i, ii, and iii to the fifth assessment report of the intergovernmental panel on climate change. In R. Pachauri & L. M. (eds.) (Eds.), *Climate*

- change 2014: Synthesis report (p. 151).
- Ishimaru, K., Hirotsu, N., Madoka, Y., & Kashiwagi, T. (2007). Quantitative trait loci for sucrose, starch, and hexose accumulation before heading in rice. *Plant Physiology and Biochemistry*, 45(10-11), 799–804.
- Jing, P., Wang, D., Zhu, C., & Chen, J. (2016). Plant physiological, morphological and yield-related responses to night temperature changes across different species and plant functional types. *Frontiers in plant science*, 7, 1774.
- Jones, P. D., & Moberg, A. (2003, Jan). Hemispheric and large-scale surface air temperature variations: An extensive revision and an update to 2001. *Journal of Climate*, 16(2), 206–223.
- Jones, P. D., New, M., Parker, D. E., Martin, S., & Rigor, I. G. (1999). Surface air temperature and its changes over the past 150 years. *Reviews of Geophysics*, 37(2), 173–199.
- Kaiser, G., & Heber, U. (1984). Sucrose transport into vacuoles isolated from barley mesophyll protoplasts. *Planta*, 161(6), 562–568.
- Kanno, K., Mae, T., & Makino, A. (2009). High night temperature stimulates photosynthesis, biomass production and growth during the vegetative stage of rice plants. *Soil Science and Plant Nutrition*, 55(1), 124–131.
- Kanno, K., & Makino, A. (2010). Increased grain yield and biomass allocation in rice under cool night temperature. *Soil Science & Plant Nutrition*, *56*(3), 412–417.
- Kawamitsu, Y., Yoda, S., & Agata, W. (1993). Humidity pretreatment affects the responses of stomata and co2 assimilation to vapor pressure difference in c3 and c4 plants. *Plant and Cell Physiology*, 34(1), 113–119.
- Khush, G. S. (2005). Ir varieties and their impact. Int. Rice Res. Inst.
- Kok, B. (1948). A critical consideration of the quantum yield of chlorella-photosynthesis. *Enzymologia*, 13, 1-56.
- Kozaki, A., & Takeba, G. (1996). Photorespiration protects c3 plants from photooxidation. *Nature*, 384(6609), 557.
- Krause, G. H., Winter, K., Matsubara, S., Krause, B., Jahns, P., Virgo, A., ... García, M. (2012). Photosynthesis, photoprotection, and growth of shade-tolerant tropical tree seedlings under full sunlight. *Photosynthesis research*, 113(1-3), 273–285.
- Krishnan, P., Ramakrishnan, B., Reddy, K. R., & Reddy, V. (2011). High-temperature effects on rice growth, yield, and grain quality. In *Advances in agronomy* (Vol. 111, pp. 87–206). Elsevier.
- Kruse, J., Rennenberg, H., & Adams, M. A. (2011). Steps towards a mechanistic understanding of respiratory temperature responses. *New Phytologist*, 189(3), 659–677.
- Ku, S.-B., & Edwards, G. E. (1978). Oxygen inhibition of photosynthesis. Planta, 140(1), 1-6.
- Laisk, A., & Loreto, F. (1996). Determining photosynthetic parameters from leaf co2 exchange and chlorophyll fluorescence (ribulose-1, 5-bisphosphate carboxylase/oxygenase specificity factor, dark respiration in the light, excitation distribution between photosystems, alternative electron transport rate, and mesophyll diffusion resistance). *Plant Physiology*, 110(3), 903–912.
- Laisk, A. K. (1977). Kinetics of photosynthesis and photorespiration of c3 in plants. Nauka, Mosco, Russia.
- Lambers, H. (1985). Respiration in intact plants and tissues: its regulation and dependence on environmental factors, metabolism and invaded organisms. In *Higher plant cell respiration* (pp. 418–473). Springer.
- Lambers, H., Chapin, F. S., & Pons, T. L. (2008). Long-distance transport of assimilates. In *Plant physiological ecology* (pp. 151–162). Springer.
- Lee, C. P., Eubel, H., & Millar, A. H. (2010). Diurnal changes in mitochondrial function reveal daily optimisation of light and dark respiratory metabolism in arabidopsis. *Molecular &*

- Cellular Proteomics, mcp-M110.
- Lee, K.-h., & Akita, S. (2000). Factors causing the variation in the temperature coefficient of dark respiration in rice (oryza sativa l.). *Plant production science*, *3*(1), 38–42.
- Lemoine, R., La Camera, S., Atanassova, R., Dédaldéchamp, F., Allario, T., Pourtau, N., ... others (2013). Source-to-sink transport of sugar and regulation by environmental factors. *Frontiers in plant science*, *4*, 272.
- Leuning, R. (1997). Scaling to a common temperature improves the correlation between the photosynthesis parameters j max and v cmax. *Journal of Experimental Botany*, 48(2), 345–347.
- Leuning, R. (2002). Temperature dependence of two parameters in a photosynthesis model. *Plant, Cell & Environment*, 25(9), 1205–1210.
- Lever, M. (1972). A new reaction for colorimetric determination of carbohydrates. *Analytical biochemistry*, 47(1), 273–279.
- Li, H., Chen, Z., Hu, M., Wang, Z., Hua, H., Yin, C., & Zeng, H. (2011). Different effects of night versus day high temperature on rice quality and accumulation profiling of rice grain proteins during grain filling. *Plant Cell Reports*, 30(9), 1641–1659.
- Lichtenthaler, H. K., & Wellburn, A. R. (1983). Determinations of total carotenoids and chlorophylls a and b of leaf extracts in different solvents. *Biochemical Society Transactions*, 11, 591-592.
- LICOR. (2018, 11). Estimating light absorptance in the leaf chamber fluorometer using an external quantum sensor. Retrieved from https://www.licor.com/env/support/LI-6400/topics/pps264-light-absorbance.html
- Lin, Y.-S., Medlyn, B. E., & Ellsworth, D. S. (2012). Temperature responses of leaf net photosynthesis: the role of component processes. *Tree Physiology*, 32(2), 219–231.
- Long, S., & Bernacchi, C. (2003). Gas exchange measurements, what can they tell us about the underlying limitations to photosynthesis? procedures and sources of error. *Journal of experimental botany*, 54(392), 2393–2401.
- Loriaux, S., Avenson, T., Welles, J., McDermitt, D., Eckles, R., Riensche, B., & Genty, B. (2013). Closing in on maximum yield of chlorophyll fluorescence using a single multiphase flash of sub-saturating intensity. *Plant, cell & environment*, 36(10), 1755–1770.
- Ludwig, L., & Canvin, D. (1971). The rate of photorespiration during photosynthesis and the relationship of the substrate of light respiration to the products of photosynthesis in sunflower leaves. *Plant Physiology*, 48(6), 712–719.
- Mackill, D. J., & Khush, G. S. (2018). Ir64: a high-quality and high-yielding mega variety. *Rice*, 11(1), 18.
- Makino, A., Mae, T., & Ohira, K. (1988). Differences between wheat and rice in the enzymic properties of ribulose-1, 5-bisphosphate carboxylase/oxygenase and the relationship to photosynthetic gas exchange. *Planta*, 174(1), 30–38.
- Makino, A., Nakano, H., & Mae, T. (1994). Effects of growth temperature on the responses of ribulose-1, 5-biphosphate carboxylase, electron transport components, and sucrose synthesis enzymes to leaf nitrogen in rice, and their relationships to photosynthesis. *Plant Physiology*, 105(4), 1231–1238.
- Maruyama, A., Nemoto, M., Hamasaki, T., Ishida, S., & Kuwagata, T. (2017). A water temperature simulation model for rice paddies with variable water depths. *Water Resources Research*, 53(12), 10065–10084.
- Maxwell, K., & Johnson, G. N. (2000). Chlorophyll fluorescence—a practical guide. *Journal of experimental botany*, 51(345), 659–668.
- McCree, K. (1974). Equations for the rate of dark respiration of white clover and grain sorghum, as functions of dry weight, photosynthetic rate, and temperature 1. *Crop science*, 14(4), 509–514.

- McCutchan, C. L., & Monson, R. K. (2001). Night-time respiration rate and leaf carbohydrate concentrations are not coupled in two alpine perennial species. *New Phytologist*, 149(3), 419–430.
- Medlyn, B., Dreyer, E., Ellsworth, D., Forstreuter, M., Harley, P., Kirschbaum, M., . . . others (2002). Temperature response of parameters of a biochemically based model of photosynthesis. ii. a review of experimental data. *Plant, Cell & Environment*, 25(9), 1167–1179.
- Mohammed, A., & Tarpley, L. (2009). High nighttime temperatures affect rice productivity through altered pollen germination and spikelet fertility. *Agricultural and Forest Meteorology*, 149(6-7), 999–1008.
- Moualeu-Ngangue, D. P., Chen, T.-W., & Stützel, H. (2016, Oct). *New Phytologist*, 213(3), 1543–1554. doi: 10.1111/nph.14260
- Mueller, L. M., Gol, L., Jeon, J.-S., Weber, A. P., Davis, S. J., & von Korff, M. (2018). Temperature but not the circadian clock determines nocturnal carbohydrate availability for growth in cereals. *bioRxiv*, 363218.
- Mullen, J. A., & Koller, H. R. (1988). Trends in carbohydrate depletion, respiratory carbon loss, and assimilate export from soybean leaves at night. *Plant Physiology*, 86(2), 517–521.
- Niinemets, Ü., Díaz-Espejo, A., Flexas, J., Galmés, J., & Warren, C. R. (2009). Role of mesophyll diffusion conductance in constraining potential photosynthetic productivity in the field. *Journal of Experimental Botany*, 60(8), 2249–2270.
- Niinemets, Ü., Oja, V., & Kull, O. (1999). Shape of leaf photosynthetic electron transport versus temperature response curve is not constant along canopy light gradients in temperate deciduous trees. *Plant, Cell & Environment*, 22(12), 1497–1513.
- Nunes-Nesi, A., Araújo, W. L., & Fernie, A. R. (2011). Targeting mitochondrial metabolism and machinery as a means to enhance photosynthesis. *Plant Physiology*, 155(1), 101–107.
- Okami, M., Kato, Y., Kobayashi, N., & Yamagishi, J. (2015). Morphological traits associated with vegetative growth of rice (oryza sativa l.) during the recovery phase after early-season drought. *European Journal of Agronomy*, 64, 58–66.
- O'Leary, B. M., Lee, C. P., Atkin, O. K., Cheng, R., Brown, T. B., & Millar, A. H. (2017). Variation in leaf respiration rates at night correlate with carbohydrate and amino acid supply. *Plant physiology*, pp–00610.
- Ouyang, W., Struik, P. C., Yin, X., & Yang, J. (2017). Stomatal conductance, mesophyll conductance, and transpiration efficiency in relation to leaf anatomy in rice and wheat genotypes under drought. *Journal of experimental botany*, 68(18), 5191–5205.
- Ow, L. F., Griffin, K. L., Whitehead, D., Walcroft, A. S., & Turnbull, M. H. (2008). Thermal acclimation of leaf respiration but not photosynthesis in populus deltoides× nigra. *New Phytologist*, 178(1), 123–134.
- Pallas, J. E., Michel, B. E., & Harris, D. G. (1967). Photosynthesis, transpiration, leaf temperature, and stomatal activity of cotton plants under varying water potentials. *Plant Physiology*, 42(1), 76–88.
- Pavlovic, D., Nikolic, B., Djurovic, S., Waisi, H., Andjelkovic, A., & Marisavljevic, D. (2015). Chlorophyll as a measure of plant health: Agroecological aspects. *Pesticide Phytomedicine* (*Belgrade*), 29(1), 21-34.
- Peng, S., Huang, J., Sheehy, J. E., Laza, R. C., Visperas, R. M., Zhong, X., ... Cassman, K. G. (2004). Rice yields decline with higher night temperature from global warming. *Proceedings of the National Academy of Sciences*, 101(27), 9971–9975.
- Peng, S., Laza, R., Visperas, R., Sanico, A., Cassman, K. G., & Khush, G. (2000). Grain yield of rice cultivars and lines developed in the philippines since 1966. *Agronomy & Horticulture-Faculty Publications*, 98.
- Peraudeau, S., Roques, S., Quiñones, C. O., Fabre, D., Van Rie, J., Ouwerkerk, P. B., ... Lafarge, T.

- (2015). Increase in night temperature in rice enhances respiration rate without significant impact on biomass accumulation. *Field Crops Research*, 171, 67–78.
- Perdomo, J. A., Carmo-Silva, E., Hermida-Carrera, C., Flexas, J., & Galmés, J. (2016). Acclimation of biochemical and diffusive components of photosynthesis in rice, wheat, and maize to heat and water deficit: implications for modeling photosynthesis. *Frontiers in plant science*, 7, 1719.
- Perdomo, J. A., Cavanagh, A. P., Kubien, D. S., & Galmés, J. (2015). Temperature dependence of in vitro rubisco kinetics in species of flaveria with different photosynthetic mechanisms. *Photosynthesis research*, 124(1), 67–75.
- Peterhansel, C., Horst, I., Niessen, M., Blume, C., Kebeish, R., Kürkcüoglu, S., & Kreuzaler, F. (2010). Photorespiration. *The Arabidopsis book/American Society of Plant Biologists*, 8.
- Peterhänsel, C., & Maurino, V. G. (2010). Photorespiration redesigned. *Plant physiology*, pp–110.
- Peterson, R. B., & Zelitch, I. (1982). Relationship between net co2 assimilation and dry weight accumulation in field-grown tobacco. *Plant physiology*, 70(3), 677–685.
- Poire, R., Wiese-Klinkenberg, A., Parent, B., Mielewczik, M., Schurr, U., Tardieu, F., & Walter, A. (2010). Diel time-courses of leaf growth in monocot and dicot species: endogenous rhythms and temperature effects. *Journal of Experimental Botany*, 61(6), 1751–1759.
- Pollock, C., & Lloyd, E. (1987). The effect of low temperature upon starch, sucrose and fructan synthesis in leaves. *Annals of Botany*, 60(2), 231–235.
- Pons, T. L., Flexas, J., von Caemmerer, S., Evans, J. R., Genty, B., Ribas-Carbo, M., & Brugnoli, E. (2009). Estimating mesophyll conductance to co2: methodology, potential errors, and recommendations. *Journal of Experimental Botany*, 60(8), 2217–2234.
- Portis, A. R. (2003). Rubisco activase–rubisco's catalytic chaperone. *Photosynthesis research*, 75(1), 11–27.
- Prins, A., Orr, D. J., Andralojc, P. J., Reynolds, M. P., Carmo-Silva, E., & Parry, M. A. (2016). Rubisco catalytic properties of wild and domesticated relatives provide scope for improving wheat photosynthesis. *Journal of Experimental Botany*, 67(6), 1827–1838.
- Ramel, F., Birtic, S., Cuiné, S., Triantaphylidès, C., Ravanat, J.-L., & Havaux, M. (2012). Chemical quenching of singlet oxygen by carotenoids in plants. *Plant Physiology*, pp–111.
- Raschke, K. (1970). Temperature dependence of co2 assimilation and stomatal aperture in leaf sections of zea mays. *Planta*, 91(4), 336–363.
- Rawyler, A., Arpagaus, S., & Braendle, R. (2002). Impact of oxygen stress and energy availability on membrane stability of plant cells. *Annals of Botany*, 90(4), 499–507.
- Ray, D. K., Mueller, N. D., West, P. C., & Foley, J. A. (2013). Yield trends are insufficient to double global crop production by 2050. *PloS one*, 8(6), e66428.
- Rosbakh, S., Römermann, C., & Poschlod, P. (2015). Specific leaf area correlates with temperature: new evidence of trait variation at the population, species and community levels. *Alpine botany*, 125(2), 79–86.
- Sage, R. F., & Kubien, D. S. (2007). The temperature response of c3 and c4 photosynthesis. *Plant, cell & environment*, 30(9), 1086–1106.
- Sage, R. F., Pearcy, R. W., & Seemann, J. R. (1987). The nitrogen use efficiency of c3 and c4 plants: Iii. leaf nitrogen effects on the activity of carboxylating enzymes in chenopodium album (l.) and amaranthus retroflexus (l.). *Plant physiology*, 85(2), 355–359.
- Sage, R. F., Way, D. A., & Kubien, D. S. (2008). Rubisco, rubisco activase, and global climate change. *Journal of experimental botany*, 59(7), 1581–1595.
- Scafaro, A. P., von Caemmerer, S., Evans, J. R., & Atwell, B. J. (2011). Temperature response of mesophyll conductance in cultivated and wild oryza species with contrasting mesophyll cell wall thickness. *Plant, Cell & Environment*, 34(11), 1999–2008.

- Schneider, C. A., Rasband, W. S., & Eliceiri, K. W. (2012). Nih image to imagej: 25 years of image analysis. *Nature methods*, *9*(7), 671.
- Seck, P. A., Diagne, A., Mohanty, S., & Wopereis, M. C. (2012). Crops that feed the world 7: Rice. *Food security*, 4(1), 7–24.
- Sharkey, T. (1986). Theoretical and experimental observations on o2 sensitivity of c3 photosynthesis. In *Biological control of photosynthesis* (pp. 115–125). Springer.
- Sharkey, T. D. (1985). O2-insensitive photosynthesis in *C*3 plants: its occurrence and a possible explanation. *Plant Physiology*, *78*(1), 71–75.
- Sharkey, T. D. (1988). Estimating the rate of photorespiration in leaves. *Physiologia Plantarum*, 73(1), 147–152.
- Sharkey, T. D., Bernacchi, C. J., Farquhar, G. D., & Singsaas, E. L. (2007). Fitting photosynthetic carbon dioxide response curves for c3 leaves. *Plant, cell & environment*, 30(9), 1035–1040.
- Sicher, R. C., Kremer, D. F., & Harris, W. G. (1984). Diurnal carbohydrate metabolism of barley primary leaves. *Plant Physiology*, *76*(1), 165–169.
- Sillmann, J., Kharin, V., Zwiers, F., Zhang, X., & Bronaugh, D. (2013). Climate extremes indices in the cmip5 multimodel ensemble: Part 2. future climate projections. *Journal of Geophysical Research: Atmospheres*, 118(6), 2473–2493.
- Smith, A. M., & Stitt, M. (2007). Coordination of carbon supply and plant growth. *Plant, cell & environment*, 30(9), 1126–1149.
- Stocker, T. F., Qin, D., Plattner, G., Tignor, M., Allen, S., Boschung, J., ... Midgley, P. (2013). Climate change 2013: the physical science basis. intergovernmental panel on climate change, working group i contribution to the ipcc fifth assessment report (ar5). *New York*.
- Sun, Y., Gu, L., Dickinson, R. E., Pallardy, S. G., Baker, J., Cao, Y., . . . others (2014). Asymmetrical effects of mesophyll conductance on fundamental photosynthetic parameters and their relationships estimated from leaf gas exchange measurements. *Plant, Cell & Environment*, 37(4), 978–994.
- Taiz, L., & Zeiger, E. (2002). Plant physiology (3rd. ed.). Sunderland: Sinauer Associates.
- Takahashi, S., & Badger, M. R. (2011). Photoprotection in plants: a new light on photosystem ii damage. *Trends in plant science*, *16*(1), 53–60.
- Tamimi, A., Rinker, E. B., & Sandall, O. C. (1994). Diffusion coefficients for hydrogen sulfide, carbon dioxide, and nitrous oxide in water over the temperature range 293-368 k. *Journal of Chemical and Engineering data*, 39(2), 330–332.
- Tao, F., Hayashi, Y., Zhang, Z., Sakamoto, T., & Yokozawa, M. (2008). Global warming, rice production, and water use in china: developing a probabilistic assessment. *Agricultural and forest meteorology*, 148(1), 94–110.
- Tcherkez, G., Gauthier, P., Buckley, T. N., Busch, F. A., Barbour, M. M., Bruhn, D., ... others (2017). Leaf day respiration: low co2 flux but high significance for metabolism and carbon balance. *New Phytologist*, 216(4), 986–1001.
- Tcherkez, G. G., Farquhar, G. D., & Andrews, T. J. (2006). Despite slow catalysis and confused substrate specificity, all ribulose bisphosphate carboxylases may be nearly perfectly optimized. *Proceedings of the National Academy of Sciences*, 103(19), 7246–7251.
- Tjoelker, M. G., Oleksyn, J., & Reich, P. B. (2001). Modelling respiration of vegetation: evidence for a general temperature-dependent q10. *Global Change Biology*, 7(2), 223–230.
- Tjoelker, M. G., Oleksyn, J., Reich, P. B., & ŻYTKOWIAK, R. (2008). Coupling of respiration, nitrogen, and sugars underlies convergent temperature acclimation in pinus banksiana across wide-ranging sites and populations. *Global Change Biology*, 14(4), 782–797.
- Tomás, M., Flexas, J., Copolovici, L., Galmés, J., Hallik, L., Medrano, H., ... Niinemets, Ü. (2013). Importance of leaf anatomy in determining mesophyll diffusion conductance to co2 across

- species: quantitative limitations and scaling up by models. *Journal of experimental botany*, 64(8), 2269–2281.
- Turnbull, M., Murthy, R., & Griffin, K. (2002). The relative impacts of daytime and night-time warming on photosynthetic capacity in populus deltoides. *Plant, Cell & Environment*, 25(12), 1729–1737.
- Venkateswarlu, B., & Visperas, R. M. (1987). Source-sink relationships in crop plants. *International Rice Research Institute Paper*, 125, 1-19.
- von Caemmerer, S. (2000). Biochemical models of leaf photosynthesis. CSIRO publishing.
- von Caemmerer, S., & Evans, J. R. (2015). Temperature responses of mesophyll conductance differ greatly between species. *Plant, Cell & Environment*, 38(4), 629–637.
- von Caemmerer, S., & Farquhar, G. D. (1981). Some relationships between the biochemistry of photosynthesis and the gas exchange of leaves. *Planta*, 153(4), 376–387.
- von Caemmerer, S., & Quick, W. P. (2000). Rubisco: physiology in vivo. In *Photosynthesis* (pp. 85–113). Springer.
- Vrabl, D., Vaskova, M., Hronkova, M., Flexas, J., & Santrucek, J. (2009). Mesophyll conductance to co2 transport estimated by two independent methods: effect of variable co2 concentration and abscisic acid. *Journal of Experimental Botany*, 60(8), 2315–2323.
- Walker, A. P., Beckerman, A. P., Gu, L., Kattge, J., Cernusak, L. A., Domingues, T. F., ... Woodward, F. I. (2014). The relationship of leaf photosynthetic traits–vcmax and jmax–to leaf nitrogen, leaf phosphorus, and specific leaf area: a meta-analysis and modeling study. *Ecology and evolution*, 4(16), 3218–3235.
- Walker, B., Ariza, L. S., Kaines, S., Badger, M. R., & Cousins, A. B. (2013). Temperature response of in vivo rubisco kinetics and mesophyll conductance in arabidopsis thaliana: comparisons to nicotiana tabacum. *Plant, Cell & Environment*, 36(12), 2108–2119.
- Went, F. (1953). The effect of temperature on plant growth. *Annual Review of Plant Physiology*, 4(1), 347–362.
- Will, R. (2000). Effect of different daytime and night-time temperature regimes on the foliar respiration of pinus taeda: predicting the effect of variable temperature on acclimation. *Journal of Experimental Botany*, 51(351), 1733–1739.
- Wilson, J. B. (1988). A review of evidence on the control of shoot: root ratio, in relation to models. *Annals of botany*, *61*(4), 433–449.
- Wilson, P. J., Thompson, K., & Hodgson, J. G. (1999). Specific leaf area and leaf dry matter content as alternative predictors of plant strategies. *New phytologist*, 143(1), 155–162.
- Wullschleger, S. D. (1993). Biochemical limitations to carbon assimilation in c3 plants: a retrospective analysis of the a/ci curves from 109 species. *Journal of Experimental Botany*, 44(5), 907–920.
- Xiong, D., Chen, J., Yu, T., Gao, W., Ling, X., Li, Y., ... Huang, J. (2015). Spad-based leaf nitrogen estimation is impacted by environmental factors and crop leaf characteristics. *Scientific reports*, *5*, 13389.
- Yamasaki, T., Yamakawa, T., Yamane, Y., Koike, H., Satoh, K., & Katoh, S. (2002). Temperature acclimation of photosynthesis and related changes in photosystem ii electron transport in winter wheat. *Plant Physiology*, 128(3), 1087–1097.
- Yamori, W., Noguchi, K., & Terashima, I. (2005). Temperature acclimation of photosynthesis in spinach leaves: analyses of photosynthetic components and temperature dependencies of photosynthetic partial reactions. *Plant, Cell & Environment*, 28(4), 536–547.
- Yemm, E., & Willis, A. (1954). The estimation of carbohydrates in plant extracts by anthrone. *Biochemical journal*, *57*(3), 508.
- Yin, X., Sun, Z., Struik, P. C., & Gu, J. (2011). Evaluating a new method to estimate the rate of leaf respiration in the light by analysis of combined gas exchange and chlorophyll fluorescence

measurements. Journal of Experimental Botany, 62(10), 3489–3499.

Yin, X., Van Oijen, M., & Schapendonk, A. (2004). Extension of a biochemical model for the generalized stoichiometry of electron transport limited c3 photosynthesis. *Plant, Cell & Environment*, 27(10), 1211–1222.

Yoshida, S. (1981). Fundamentals of rice crop science. Int. Rice Res. Inst.

Zhang, W., Huang, W., Yang, Q.-Y., Zhang, S.-B., & Hu, H. (2013). Effect of growth temperature on the electron flow for photorespiration in leaves of tobacco grown in the field. *Physiologia plantarum*, 149(1), 141–150.

Zou, D., Gao, K., & Xia, J. (2011). Dark respiration in the light and in darkness of three marine macroalgal species grown under ambient and elevated co2 concentrations. *Acta Oceanologica Sinica*, 30(1), 106–112.

7 Appendices

7.1 Appendix 1

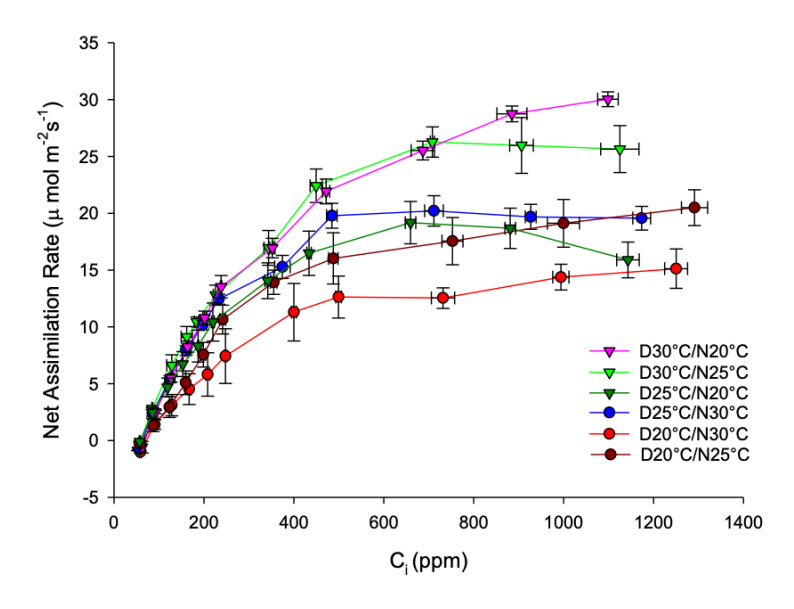


Figure 11: Mean A-C_i Curves of Leaf 2 (n=4) by Temperature Treatment, the error bars represent the standard error of the mean

Table 16: Mean and S.E. of of Unshaded and A- C_i Curve Assimilation Rates of L2 (n=5) by Temperature Treatment

| Treatment | Assimilation | A-C _i |
|-----------------|---|---|
| (Day°C/Night°C) | MeanS.E. (μmol m ⁻² s ⁻¹ | MeanS.E. $^{-1}$)(µmol m ⁻² s ⁻¹) |
| 20/25 | 15.154.19 | 15.47 1.24 |
| 20/30 | 13.254.19 | 14.14 1.24 |
| 25/20 | 16.132.96 | 17.190.88 |
| 25/30 | 16.434.19 | 18.92 1.24 |
| 30/20 | 19.444.19 | 20.49 1.44 |
| 30/25 | 20.744.19 | 21.181.24 |

7.2 Appendix 2

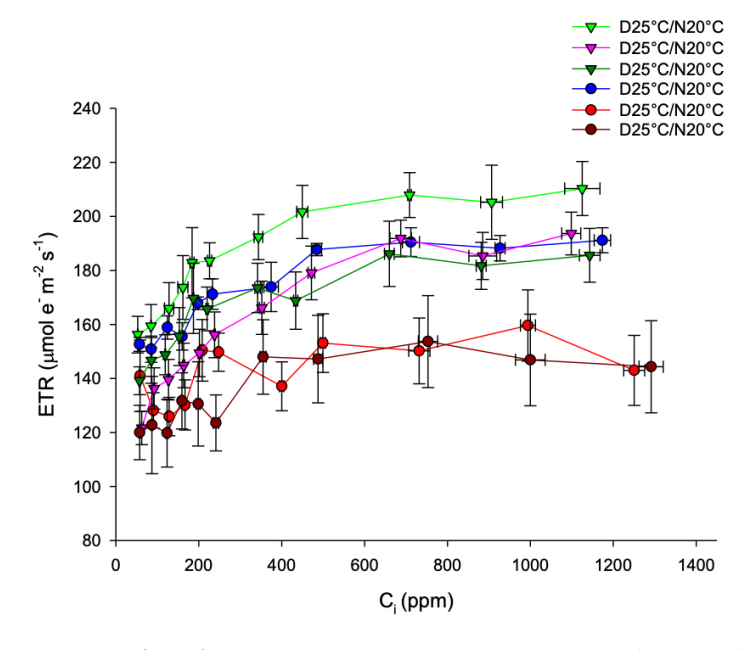


Figure 12: Mean ETR- C_i of Leaf 2 (n=4) by Temperature Treatment, the error bars represent the standard error of the mean

7.3 Appendix 3

Table 17: Appendix 3: Mean and S.E. of J_{max} and V_{cmax} of L2 (n=4) by Temperature Treatment

| Treatment | J_{max} | | V _{cmax} | |
|-----------------|---|-------|--------------------------------|-------|
| | Mean | S.E. | Mean | S.E. |
| (Day°C/Night°C) | $(\mu \text{mol } e^- \text{m}^{-2} \text{s}^{-1})$ | | $(\mu mol CO_2 m^{-2} s^{-1})$ | |
| 20/25 | 150.73 | 37.24 | 148.00 | 29.74 |
| 20/30 | 151.99 | 37.24 | 146.23 | 29.73 |
| 25/20 | 174.94 | 26.33 | 130.99 | 21.03 |
| 25/30 | 196.21 | 37.24 | 137.49 | 29.74 |
| 30/20 | 210.73 | 37.24 | 137.18 | 29.74 |
| 30/25 | 188.49 | 37.24 | 147.63 | 29.74 |

7.4 Appendix 4

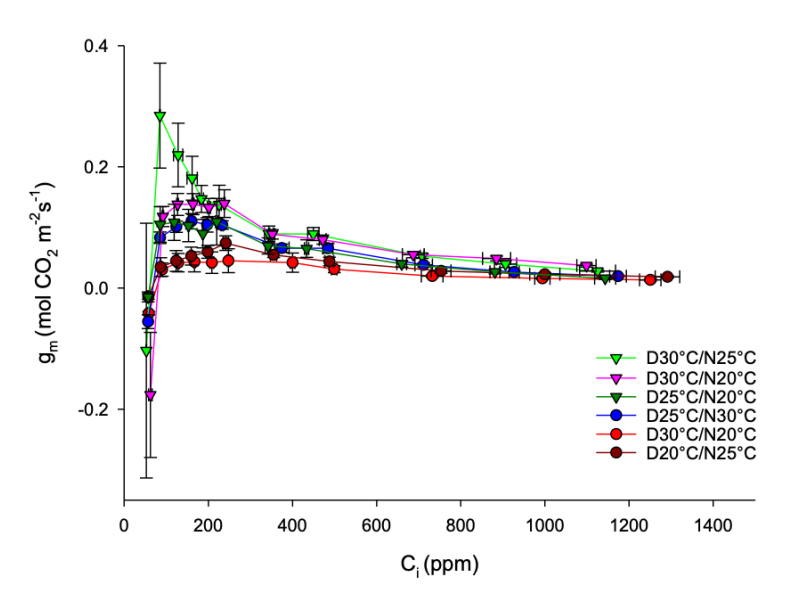


Figure 13: Mean g_m - C_i of L2 (n=4) by Temperature Treatment, the error bars represent the standard error of the mean

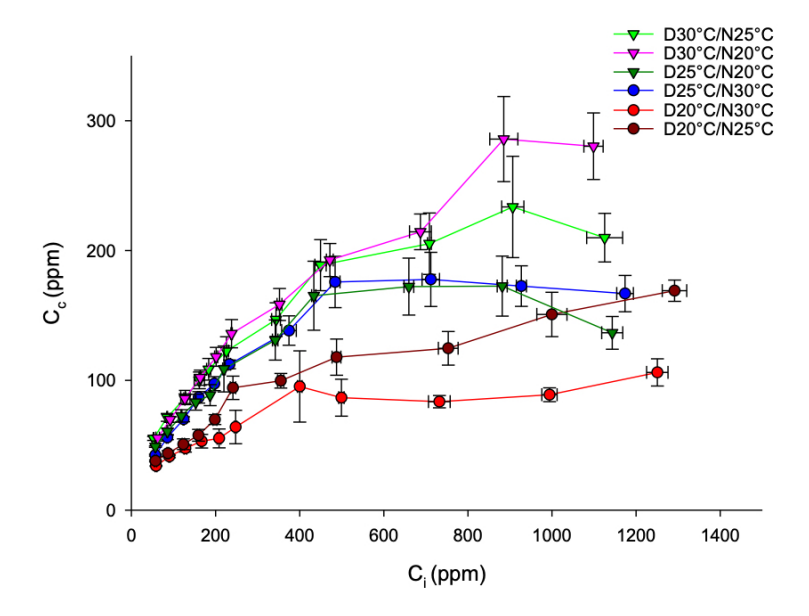


Figure 14: Mean C_c - C_i of L2 (n=4) by Temperature Treatment, the error bars represent the standard error of the mean

7.5 Appendix 5

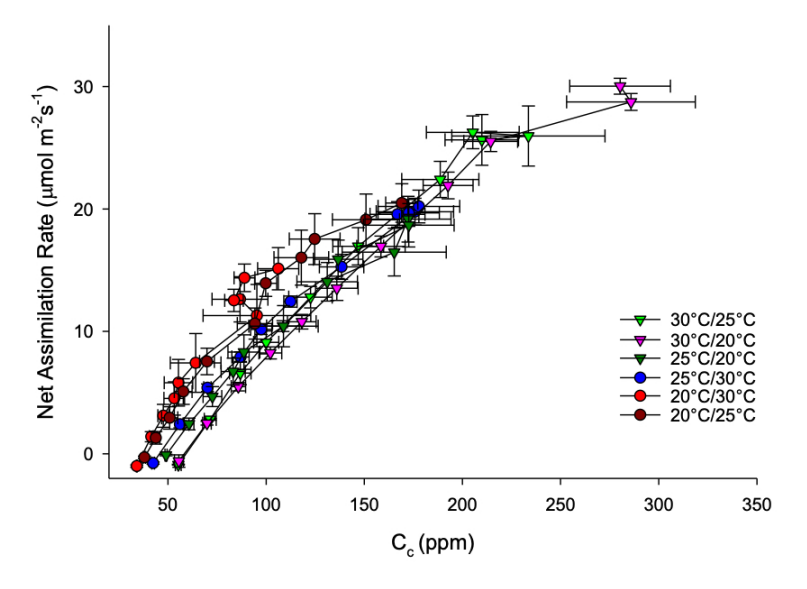


Figure 15: Mean A - C_c of L2 (n=4) by Temperature Treatment, the error bars represent the standard error of the mean

7.6 Appendix 6

Table 18: Appendix 6: Mean and S.E. of g_m and C_c at 450 ppm of L2 (n=4) by Temperature Treatment

| Treatment | gm | | | C_c |
|-----------------|---|------|--------|-------|
| | Mean | S.E. | Mean | S.E. |
| (Day°C/Night°C) | $(\text{mol CO}_2 \text{m}^{-2} \text{s}^{-1})$ | | (ppm) | |
| 20/25 | 0.05 | 0.03 | 99.75 | 22.75 |
| 20/30 | 0.04 | 0.03 | 95.31 | 22.75 |
| 25/20 | 0.09 | 0.02 | 147.16 | 16.08 |
| 25/30 | 0.07 | 0.03 | 138.39 | 22.75 |
| 30/20 | 0.09 | 0.03 | 158.47 | 22.75 |
| 30/25 | 0.09 | 0.03 | 146.87 | 22.75 |

7.7 Appendix 7

Table 19: Appendix 7: Mean and S.E. C_{tr} of L2 (n=4) by Temperature Treatment

| Treatment | C_{t} | r |
|-----------------|--|-------|
| (Day°C/Night°C) | Mean (μ mol m ⁻² s ⁻¹) | S.E. |
| 20/25 | 21.76 | 11.62 |
| 20/30 | 22.61 | 11.62 |
| 25/20 | 103.37 | 8.21 |
| 25/30 | 106.88 | 11.62 |
| 30/20 | 201.21 | 11.62 |
| 30/25 | 136.02 | 11.62 |

7.8 Appendix 8

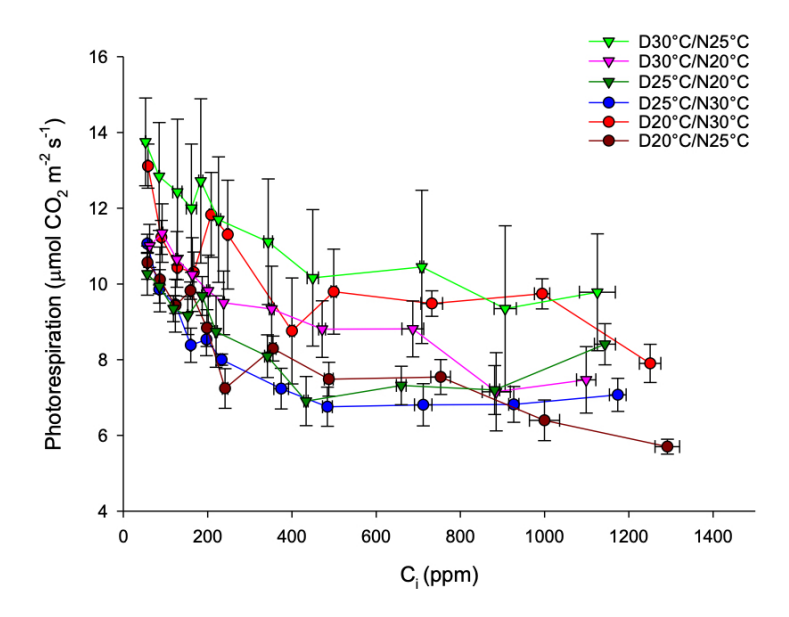


Figure 16: Mean Photorespiration - $C_{\rm i}$ of L2 (n=4) by Temperature Treatment, the error bars represent the standard error of the mean

Table 20: Mean and S.E. of Photorespiration according to M1 of L2 (n=4) by Temperature Treatment

| Treatment | Photorespiration | |
|-----------------|------------------|--------------------------|
| | Mean | |
| (Day°C/Night°C) | (µmol | $(CO_2 m^{-2} s^{-1})$ |
| 20/25 | 4.47 | 0.93 |
| 20/30 | 3.97 | 0.93 |
| 25/20 | 6.78 | 0.66 |
| 25/30 | 7.18 | 0.93 |
| 30/20 | 9.65 | 0.93 |
| 30/25 | 8.06 | 0.93 |

Table 21: Mean and S.E. of Photorespiration according to M2 of L2 (n=4) by Temperature Treatment

| Treatment | Photorespiration at 300 ppm | | Photorespiration | at 450 ppm |
|-----------------|---|------|--|------------|
| | Mean | S.E. | Mean | S.E. |
| (Day°C/Night°C) | μ mol CO ₂ m ⁻² s ⁻¹) | | $(\mu \text{mol m}^{-2}\text{s}^{-1})$ | |
| 20/25 | 7.24 | 0.98 | 8.29 | 0.98 |
| 20/30 | 11.30 | 0.98 | 8.75 | 0.98 |
| 25/20 | 8.16 | 0.69 | 7.46 | 0.69 |
| 25/30 | 7.90 | 0.98 | 7.23 | 0.98 |
| 30/20 | 9.50 | 0.98 | 9.34 | 0.98 |
| 30/25 | 11.70 | 0.98 | 11.11 | 0.98 |

7.9 Appendix 9

Table 22: Mean and S.E. of Respiration of L2 (n=4) by Temperature Treatment

| Treatment | Respiration Rate | | |
|-----------------|---------------------------------|---|--|
| (Day°C/Night°C) | Mean (µmol CO ₂ n | S.E. n ⁻² s ⁻¹) | |
| 20/25 | 1.01 | 0.33 | |
| 20/30 | 0.84 | 0.33 | |
| 25/20 | 0.94 | 0.23 | |
| 25/30 | 0.77 | 0.33 | |
| 30/20 | 1.2 | 0.33 | |
| 30/25 | 1.08 | 0.33 | |

7.10 Appendix 10

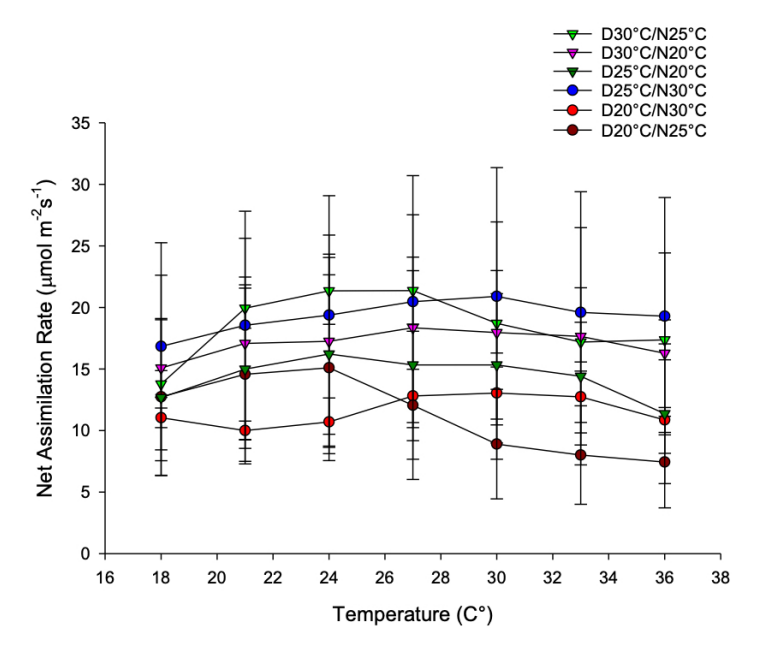


Figure 17: Mean Temperature Curves of Leaf 2 (n=4) by Temperature Treatment, the error bars represent the standard error of the mean

7.11 Appendix 11

Table 23: Mean and S.E. of Sucrose Concentrations at End of Day and Night of Leaf 2 (n=5) by Temperature Treatment

| Treatment | End of Day | | End of Night | |
|-----------------|----------------------------------|------|----------------------------------|------|
| (Day°C/Night°C) | Mean (mmol cm ⁻²) | S.E. | Mean (mmol cm ⁻²) | S.E. |
| | (IIIIIIOI CIII) | | (IIIIIOI CIII) | |
| 20/25 | 3.93 | 0.45 | 1.69 | 0.41 |
| 20/30 | 4.86 | 0.45 | 1.25 | 0.44 |
| 25/20 | 3.32 | 0.32 | 2.21 | 0.29 |
| 25/30 | 3.46 | 0.45 | 0.90 | 0.41 |
| 30/20 | 2.86 | 0.45 | 2.07 | 0.42 |
| 30/25 | 3.75 | 0.45 | 2.22 | 0.41 |

7.12 Appendix 12

Table 24: Mean and S.E. of Monosaccharide Concentrations at End of Day and Night of Leaf 2 (n=5) by Temperature Treatment

| Treatment | End of Day | | End of Night | |
|-----------------|----------------------------------|------|----------------------------------|------|
| (Day°C/Night°C) | Mean (mmol cm ⁻²) | S.E. | Mean (mmol cm ⁻²) | S.E. |
| 20/25 | 1.24 | 0.07 | 0.88 | 0.06 |
| 20/30 | 0.76 | 0.07 | 0.63 | 0.06 |
| 25/20 | 0.98 | 0.05 | 0.84 | 0.04 |
| 25/30 | 0.73 | 0.07 | 0.62 | 0.06 |
| 30/20 | 0.85 | 0.07 | 0.83 | 0.06 |
| 30/25 | 1.26 | 0.07 | 0.97 | 0.06 |

7.13 Appendix 13

Table 25: Mean and S.E. Ca, Cb, and Total Chlorophyll Concentrations of Leaf 1 (n=10) by Temperature Treatment

| Treatment | Ca | ! | Ch | • | Total Chlo | rophylls |
|-----------------|--------------------------------|------|--------------------------------|------|--------------------------------|----------|
| (Day°C/Night°C) | Mean (μg cm ⁻²) | S.E. | Mean (μg cm ⁻²) | S.E. | Mean (μg cm ⁻²) | S.E. |
| 20/25 | 12.31 | 0.81 | 4.50 | 0.28 | 16.81 | 1.08 |
| 20/30 | 13.25 | 0.81 | 5.02 | 0.28 | 18.28 | 1.08 |
| 25/20 | 15.88 | 0.57 | 5.52 | 0.20 | 21.39 | 0.76 |
| 25/30 | 13.43 | 0.81 | 5.22 | 0.28 | 18.65 | 1.08 |
| 30/20 | 26.60 | 0.81 | 9.84 | 0.28 | 36.44 | 1.08 |
| 30/25 | 17.74 | 0.81 | 6.50 | 0.28 | 24.24 | 1.08 |

7.14 Appendix 14

Table 26: Mean and S.E. Carotenoid Concentrations of Leaf 1 (n=10) by Temperature Treatment

| Treatment | Carotenoids | | |
|-----------------|------------------------|------|--|
| | Mean | S.E. | |
| (Day°C/Night°C) | (μg cm ⁻²) | | |
| 20/25 | 2.23 | 0.14 | |
| 20/30 | 2.34 | 0.14 | |
| 25/20 | 2.82 | 0.10 | |
| 25/30 | 1.85 | 0.14 | |
| 30/20 | 3.94 | 0.14 | |
| 30/25 | 2.72 | 0.14 | |